

# Jordan Journal of Mechanical and Industrial Engineering (JJMIE)

JJMIE is a high-quality scientific journal devoted to fields of Mechanical and Industrial Engineering. It is published by Hashemite University in corporation with the Jordanian Scientific Research Support Fund.

## EDITORIAL BOARD

---

### Editor-in-Chief

Prof. Ahmed M. Al-Ghandoor

### Editorial board

Prof. **Mohammad Ahmad Hamdan**  
University of Jordan

Prof. **Naseem Sawaqed**  
Mutah University

Prof. **Amin Al Robaidi**  
Al Balqa Applied University

Prof. **Naser Al-Huniti**  
University of Jordan

Prof. **Mohammad Hayajneh**  
Jordan University of Science and Technology

Prof. **Suhil Kiwan**  
Jordan University of Science and Technology

## THE INTERNATIONAL ADVISORY BOARD

---

**Abu-Qudais, Mohammad**  
Jordan University of Science & Technology, Jordan

**Abu-Mulaweh, Hosni**  
Purdue University at Fort Wayne, USA

**Afaneh Abdul-Hafiz**  
Robert Bosch Corporation, USA

**Afonso, Maria Dina**  
Institute Superior Tecnico, Portugal

**Badiru, Adedji B.**  
The University of Tennessee, USA

**Bejan, Adrian**  
Duke University, USA

**Chalhoub, Nabil G.**  
Wayne State University, USA

**Cho, Kyu-Kab**  
Pusan National University, South Korea

**Dincer, Ibrahim**  
University of Ontario Institute of Technology,  
Canada

**Douglas, Roy**  
Queen's University, U. K

**El Bassam, Nasir**  
International Research Center for Renewable  
Energy, Germany

**Haik, Yousef**  
United Arab Emirates University, UAE

**Jaber, Jamal**  
Al- Balqa Applied University, Jordan

**Jubran, Bassam**  
Ryerson University, Canada

**Kakac, Sadik**  
University of Miami, USA

**Khalil, Essam-Eddin**  
Cairo University, Egypt

**Mutoh, Yoshiharu**  
Nagaoka University of Technology, Japan

**Pant, Durbin**  
Iowa State University, USA

**Riffat, Saffa**  
The University of Nottingham, U. K

**Saghir, Ziad**  
Ryerson University, Canada

**Sarkar, MD. Abdur Rashid**  
Bangladesh University of Engineering &  
Technology, Bangladesh

**Signer, Dennis**  
Wichita State University, USA

**Sopian, Kamaruzzaman**  
University Kebangsaan Malaysia, Malaysia

**Tzou, Gow-Yi**  
Yung-Ta Institute of Technology and Commerce,  
Taiwan

## EDITORIAL BOARD SUPPORT TEAM

---

### Language Editor

Dr. Qusai Al-Debyan

### Publishing Layout

Eng. Ali Abu Salimeh

## SUBMISSION ADDRESS:

---

Prof. Ahmed Al-Ghandoor, Editor-in-Chief  
Jordan Journal of Mechanical & Industrial Engineering,  
Hashemite University,  
PO Box 330127, Zarqa, 13133 , Jordan  
E-mail: jjmie@hu.edu.jo



Hashemite Kingdom of Jordan



Hashemite University

Jordan Journal of  
Mechanical and Industrial Engineering

JJMIE

*An International Peer-Reviewed Scientific Journal*  
*Financed by Scientific Research Support Fund*

<http://jjmie.hu.edu.jo/>

ISSN 1995-6665

# Jordan Journal of Mechanical and Industrial Engineering (JJMIE)

JJMIE is a high-quality scientific journal devoted to fields of Mechanical and Industrial Engineering. It is published by The Jordanian Ministry of Higher Education and Scientific Research in corporation with Hashemite University.

**Introduction:** The Editorial Board is very committed to build the Journal as one of the leading international journals in mechanical and industrial engineering sciences in the next few years. With the support of the Ministry of Higher Education and Scientific Research and Jordanian Universities, it is expected that a heavy resource to be channeled into the Journal to establish its international reputation. The Journal's reputation will be enhanced from arrangements with several organizers of international conferences in publishing selected best papers of the conference proceedings.

**Aims and Scope:** *Jordan Journal of Mechanical and Industrial Engineering* (JJMIE) is a refereed international journal to be of interest and use to all those concerned with research in various fields of, or closely related to, mechanical and industrial engineering disciplines. *Jordan Journal of Mechanical and Industrial Engineering* aims to provide a highly readable and valuable addition to the literature which will serve as an indispensable reference tool for years to come. The coverage of the journal includes all new theoretical and experimental findings in the fields of mechanical and industrial engineering or any closely related fields (Materials, Manufacturing, Management, Design, Thermal and Fluid, Energy, Control, Mechatronics, and Biomedical). The journal also encourages the submission of critical review articles covering advances in recent research of such fields as well as technical notes.

## Guide for Authors

---

### **Manuscript Submission:**

High-quality submissions to this new journal are welcome now and manuscripts may be either submitted online or email.

**Online:** For online and email submission upload one copy of the full paper including graphics and all figures at the online submission site, accessed via <http://jjmie.hu.edu.jo>. The manuscript must be written in MS Word 2010 Format. All correspondence, including notification of the Editor's decision and requests for revision, takes place by e-mail and via the Author's homepage, removing the need for a hard-copy paper trail.

### **Submission address and contact:**

Prof. Ahmed Al-Ghandoor  
Editor-in-Chief  
*Jordan Journal of Mechanical & Industrial Engineering*,  
Hashemite University,  
PO Box 330127, Zarqa, 13115, Jordan  
E-mail: [jjmie@hu.edu.jo](mailto:jjmie@hu.edu.jo)

**Types of contributions:** Original research papers and Technical reports

**Corresponding author:** Clearly indicate who is responsible for correspondence at all stages of refereeing and publication, including post-publication. Ensure that telephone and fax numbers (with country and area code) are provided in addition to the e-mail address and the complete postal address. Full postal addresses must be given for all co-authors.

**Original material:** Submission of an article implies that the work described has not been published previously (except in the form of an abstract or as part of a published lecture or academic thesis), that it is not under consideration for publication elsewhere, that its publication is approved by all authors and that, if accepted, it will not be published elsewhere in the same form, in English or in any other language, without the written consent of the Publisher. Authors found to be deliberately contravening the submission guidelines on originality and exclusivity shall not be considered for future publication in this journal.

**Withdrawing:** If the author chooses to withdraw his article after it has been assessed, he shall reimburse JJMIE with the cost of reviewing the paper.

### **Manuscript Preparation:**

---

**General:** Editors reserve the right to adjust style to certain standards of uniformity. Original manuscripts are discarded after publication unless the Publisher is asked to return original material after use. Please use MS Word 2010 for the text of your manuscript.

**Structure:** Follow this order when typing manuscripts: Title, Authors, Authors title, Affiliations, Abstract, Keywords, Introduction, Main text, Conclusions, Acknowledgements, Appendix, References, Figure Captions, Figures and then Tables. Please supply figures imported into the text AND also separately as original graphics files. Collate acknowledgements in a separate section at the end of the article and do not include them on the title page, as a footnote to the title or otherwise.

**Text Layout:** Use 1.5 line spacing and wide (3 cm) margins. Ensure that each new paragraph is clearly indicated. Present tables and figure legends on separate pages at the end of the manuscript. If possible, consult a recent issue of the journal to become familiar with layout and conventions. All footnotes (except for table and corresponding author footnotes) should be identified with superscript Arabic numbers. To conserve space, authors are requested to mark the less important parts of the paper (such as records of experimental results) for printing in smaller type. For long papers (more than 4000 words) sections which could be deleted without destroying either the sense or the continuity of the paper should be indicated as a guide for the editor. Nomenclature should conform to that most frequently used in the scientific field concerned. Number all pages consecutively; use 12 or 10 pt font size and standard fonts.

**Corresponding author:** Clearly indicate who is responsible for correspondence at all stages of refereeing and publication, including post-publication. The corresponding author should be identified with an asterisk and footnote. Ensure that telephone and fax numbers (with country and area code) are provided in addition to the e-mail address and the complete postal address. Full postal addresses must be given for all co-authors. Please consult a recent journal paper for style if possible.

**Abstract:** A self-contained abstract outlining in a single paragraph the aims, scope and conclusions of the paper must be supplied.

**Keywords:** Immediately after the abstract, provide a maximum of six keywords (avoid, for example, 'and', 'of'). Be sparing with abbreviations: only abbreviations firmly established in the field may be eligible.

**Symbols:** All Greek letters and unusual symbols should be identified by name in the margin, the first time they are used.

**Units:** Follow internationally accepted rules and conventions: use the international system of units (SI). If other quantities are mentioned, give their equivalent in SI.

**Maths:** Number consecutively any equations that have to be displayed separately from the text (if referred to explicitly in the text).

**References:** All publications cited in the text should be presented in a list of references following the text of the manuscript.

*Text:* Indicate references by number(s) in square brackets in line with the text. The actual authors can be referred to, but the reference number(s) must always be given.

*List:* Number the references (numbers in square brackets) in the list in the order in which they appear in the text.

**Examples:**

**Reference to a journal publication:**

[1] M.S. Mohsen, B.A. Akash, "Evaluation of domestic solar water heating system in Jordan using analytic hierarchy process". Energy Conversion & Management, Vol. 38 (1997) No. 9, 1815-1822.

**Reference to a book:**

[2] Strunk Jr W, White EB. The elements of style. 3rd ed. New York: Macmillan; 1979.

**Reference to a conference proceeding:**

[3] B. Akash, S. Odeh, S. Nijmeh, "Modeling of solar-assisted double-tube evaporator heat pump system under local climate conditions". 5th Jordanian International Mechanical Engineering Conference, Amman, Jordan, 2004.

**Reference to a chapter in an edited book:**

[4] Mettam GR, Adams LB. How to prepare an electronic version of your article. In: Jones BS, Smith RZ, editors. Introduction to the electronic age, New York: E-Publishing Inc; 1999, p. 281-304

**Free Online Color :** If, together with your accepted article, you submit usable color and black/white figures then the journal will ensure that these figures will appear in color on the journal website electronic version.

**Tables:** Tables should be numbered consecutively and given suitable captions and each table should begin on a new page. No vertical rules should be used. Tables should not unnecessarily duplicate results presented elsewhere in the manuscript (for example, in graphs). Footnotes to tables should be typed below the table and should be referred to by superscript lowercase letters.

**Notification:** Authors will be notified of the acceptance of their paper by the editor. The Publisher will also send a notification of receipt of the paper in production.

**Copyright:** All authors must sign the Transfer of Copyright agreement before the article can be published. This transfer agreement enables Jordan Journal of Mechanical and Industrial Engineering to protect the copyrighted material for the authors, but does not relinquish the authors' proprietary rights. The copyright transfer covers the exclusive rights to reproduce and distribute the article, including reprints, photographic reproductions, microfilm or any other reproductions of similar nature and translations.

**Proof Reading:** One set of page proofs in MS Word 2010 format will be sent by e-mail to the corresponding author, to be checked for typesetting/editing. The corrections should be returned within **48 hours**. No changes in, or additions to, the accepted (and subsequently edited) manuscript will be allowed at this stage. Proofreading is solely the author's responsibility. Any queries should be answered in full. Please correct factual errors only, or errors introduced by typesetting. Please note that once your paper has been proofed we publish the identical paper online as in print.

**Author Benefits:**

*No page charges:* Publication in this journal is free of charge.

*Free offprints:* One journal issues of which the article appears will be supplied free of charge to the corresponding author and additional offprint for each co-author. Corresponding authors will be given the choice to buy extra offprints before printing of the article.



**PAGES****PAPERS**

---

- 141 - 145     **Potentials and Barriers of Energy Saving in Jordan's Residential Sector through Thermal Insulation**  
*I. Al-Hinti, H. Al-Sallami*
- 147 - 154     **Reduced Filtered Dynamic Model for Joint Friction Estimation of Walking Biped.**  
*Iyad Hashlamon , Kemalettin Erbatur*
- 155– 164     **Fire Extinguisher Training: Subjective Assessment of a Newly Developed Method by Expert and Novice Firefighters**  
*Awwad J. Dababneh , Manar M. Ajlouni*
- 165– 171     **Nonlinear Natural Frequencies and Frequency Veering of a Beam with an Arbitrary Initial Rise Supported by Flexible Ends and Resting on Elastic Foundation.**  
*Mutasim S. Abdeljaber*
- 173– 180     **Experimental Studies the Effect of Flap Peening Process on Aluminum Alloys**  
*K. N. Abushgair*
- 181– 184     **Solar Thermal Hybrid Heating System**  
*Ahmad Al aboushi.*
- 185– 194     **A Comparative Study of Single Phase Grid Connected Phase Looked Loop Algorithms.**  
*Ashraf Samarah*
- 195– 200     **Optimal Batch Size Considering Partial Outsourcing Plan and Rework**  
*Yuan-Shyi Peter Chiu , Chen-Ju Liu , Ming-Hon Hwang*
-



# Potentials and Barriers of Energy Saving in Jordan's Residential Sector through Thermal Insulation

I. Al-Hinti <sup>a\*</sup>, H. Al-Sallami

<sup>a</sup>Mechanical and Maintenance Engineering Department, School of Applied Technical Sciences, German Jordanian University, Madaba, Jordan

Received Dec 16, 2016

Accepted July 20, 2017

## Abstract

The residential sector in Jordan accounts for 21% of final energy consumption and 43% of total electricity consumption. More than 60 % of energy consumed in households is used for space heating and cooling. Thermal insulation of building is a decisive factor in reducing residential heating and cooling energy needs. Although thermal insulation codes have been adopted since the early eighties, enforcement of these codes has been limited. This resulted in sporadic implementation of thermal insulation in residential buildings that varies according to the ownership type, income and education levels. This paper presents an analysis of potential energy savings that can be achieved through retrofitting Jordanian households to comply with the existing thermal insulation codes. In addition, the legal, social, economic, and technical barriers of the use of thermal insulation are discussed in an attempt to bring a better understanding of how the projected savings can be assured.

© 2017 Jordan Journal of Mechanical and Industrial Engineering. All rights reserved

**Keywords:** Thermal insulation, building codes, residential buildings, energy saving.

## 1. Introduction

Jordan is a non-oil producing country which suffers from inadequate supplies of natural resources including water, natural gas and crude oil. Consequently, 97% of total national energy needs are imported from neighbour Arab countries; which costs 17% of Jordanian gross domestic product [1]. The residential sector accounts for 21% of final energy consumption and 43% of total electricity consumptions [2]. Zarei and Zare [3] stated that urbanisation, the increasing of population, and the improvement of living standards are all contributors to increasing the residential energy requirements. On the other hand, Al-Ghandoor et. al. [4] found that population is the key factor on energy consumption while electricity and fuel prices have no effect on electricity and fuel consumptions. The urban subsector represents about 80% of households and responsible for 84% of the residential energy consumption in Jordan [5]. Jaber et. al. [6] revealed that space heating presents 61% of total consumption in households, which accounts for about 14% of total national energy demand. Further, they reported that traditional un-vented kerosene and LPG heating systems are the most common to provide space heating in urban areas.

Since more than 60 % of energy consumed in household is used for space heating, improvement of the physical building envelope or using more efficient space heating systems are two options that should be adopted. Jaber et. al. [7] recommended that a careful selection of

boilers, air-conditioning systems, and lighting as well as thermal insulation, all could contribute in increasing the energy efficiency in this sector. While, Mohsen and Akash [8] stated that it is more convenient to focus on building fabric instead of the heating systems. In addition, Yang et. al. [9] found that thermal insulation of envelope plays the key role in the assessment of space heating and cooling especially in cold winter regions, while in mild regions orientation of building is the most important indicator in building energy efficiency assessment followed by outdoor and indoor shading and insulation; which both have the same weight. Further, through a research conducted by Tommerup and Svendsen [10] on energy saving measures in households in Denmark, it was found that well insulated external walls reduce the heat loss by 50% which in turn reduces the heating requirement by 46%.

Al Zyood et. al. [11] revealed that if building envelope is provided with 5.7 cm of thermal insulation and of trombe wall, this could reduce heating needs by about 82% and such system has less than 2 years payback period. While, Chvatal et. al. [12] stated that thermal insulation is important in heating season and any increase in insulation thickness will reduce the total U-value of envelope which directly reduces heating requirements. However, he showed that in summer; when the gains (internal or solar) are not well controlled, a highly insulated envelope may cause an increase in the indoor temperature, which could reach unacceptable comfort limits. This could possibly offset any savings obtained from increased insulation during the heating season. High indoor temperatures could enhance fungi which is one of serious sick building

syndrome. Moreover, poor building insulation could enhance Fungi appearance in internal building corners because of thermal losses near the corners [13]. Suliman and Beithou [14] stated that improper insulated envelope is a significant factor that cause the indoor environment during the cold season to be uncomfortable, damp and unhealthy.

## 2. Current Status of Thermal Insulation in Jordan

Jordan was one of the first countries in the region to specify a thermal insulation code (since the mid-1980s). The Jordanian Thermal Insulation Code specifies the following:

- Design requirements concerning the U value for walls, roofs, and floors.
- Insulation materials types properties and standards.
- Principles of thermal design and dampness in buildings.

A summary of the maximum allowed U-values required by the code is presented in Table 1 [15]. It can be noticed that such code requirements for external walls and roofs cannot be achieved without the use of a minimum layer of 5 cm of insulating material such polystyrene or polyurethane.

**Table 1.** Thermal insulation code U-value requirements for different types of walls

Type of wall	Maximum U-value (W/m <sup>2</sup> °C)
External opaque walls (without openings)	0.57
External walls (with openings)	1.6
External roofs	0.55
Divider wall between two independent spaces	2.0
Divider roof section between two independent spaces	1.2

More recently, another code “Energy Efficient Building Code” has been adopted to face the increasing energy challenges. The code contains seven chapters covering: general considerations, architectural aspects, mechanical ventilation, heating and air conditioning, hot water supply, lighting, and electrical power. This combination of architectural, mechanical and electrical topics makes it one of the most comprehensive sustainable building-related code in the region.

Although compliance with all building codes is compulsory and is mandated by the national building law, enforcement mechanisms are either absent or ineffective. Design documents and drawings of all new buildings are inspected for compliance with the code by the Jordan Engineers Association before a building permit is granted. However, on-site inspection is rarely carried out to ensure that the construction follows the design requirements, and therefore the code requirements. This resulted in limited and sporadic compliance with the thermal insulation code, as well as other building codes. In a recent survey conducted in 2015 by Al-Sallami [16], it was found that only 23% of Jordanian dwellings are insulated either with polystyrene, polyurethane, or rock wool. Although this percentage reveals the scale of the problem, it represents a significant improvement in comparison with the reported

percentage of only 6% in 1998 [8]. However, only 38% of the owners of insulated dwellings reported the use of insulation layer of 5cm thickness or more, which is required to meet the code specifications. This indicates that the use of thermal insulation is still a matter of choice for contractors and owners, and although the level of awareness is increasing, code compliance is still far from being widespread.

## 3. Barriers of Implementing Thermal Insulation in Jordan

In order to better understand the drivers and barriers that affect the decision of using thermal insulation in buildings and conforming to the existing thermal insulation code in Jordan, the data from the survey mentioned in the previous section [16] was used. It is worth mentioning that the survey was designed to gather information about a large number of indicators that can affect the energy use in local buildings. Households were selected randomly. The 375 surveys were distributed in different districts, but the number of completed surveys was 235. Out of the completed surveys, only 86% were considered and the rest excluded from calculations due to statistical considerations. The following factors have been identified: Ownership, income level, and education level.

Regarding the correlation between ownership and the use of thermal insulation, it can be seen from figure 1 that while 48% of owned dwellings are insulated, in one way or another, only 19% of dwellings that are rented are insulated. Such contrasting result indicates that owners are more likely to insulate their buildings if they actually live in them and tenants are very unlikely to pay extra costs to insulate dwellings they do not own. Further analysis of the data revealed that 70% of the owned but uninsulated dwellings are apartments that were built by construction companies and not by their current owners. It can be concluded that implementing thermal insulation in residential buildings is strongly driven by its economic feasibility to the party who is constructing the building rather than the willingness to comply with existing codes. This on one hand confirms the weakness of supervision and enforcement mechanisms, and on the other reflects the lack of incentives for construction companies and contractors to voluntarily comply with the insulation code. The provision of a voluntary certification or rating system that can distinguish properly insulated dwellings can be an incentive for contractors who can directly benefit from such certification system in promoting their code-compliant properties to owners and tenants.

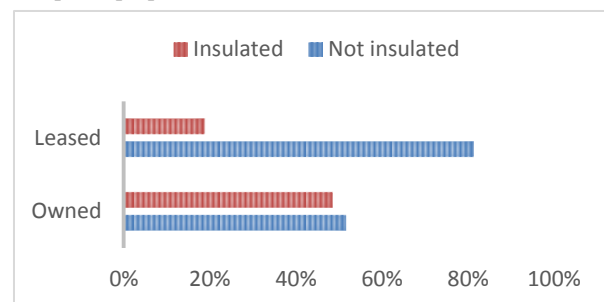


**Figure 1.** Percentages of insulated and uninsulated dwellings based on the type of ownership

Regarding the correlation of income level with the use of thermal insulation, Figure 2 indicates that a clear gap between low income and high income households when it comes to the use of thermal insulation. The initial cost of investment is most likely the reason behind this gap. While high income households are willing to invest in an energy conservation measure that pays back in several years, low income households find it difficult to source such investment. This in turn results in poor comfort conditions and in increased energy costs for low income households. The provision of eased, long term, low-interest financing schemes that target low income households can be very helpful in assisting them in overcoming the initial cost obstacle and implement thermal insulation in their dwellings without increasing their financial burdens.

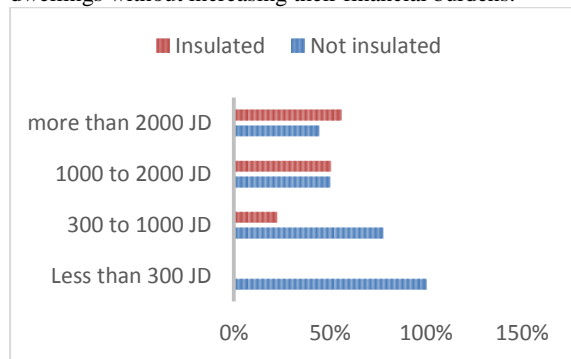


**Figure 2.** Percentages of insulated and uninsulated dwellings based on the monthly income level

Figure 3 shows the correlation between the education level of the head of the household and the existence of thermal insulation. It is interesting to note that while less than 10% of the dwellings headed by a person with relatively low education level are insulated, this percentage rises to nearly 60% in dwellings headed by a person with relatively high education level. Such gap can be attributed to the correlation between income level and the level of education in part, but clearly points to an awareness gap. Highly educated households are clearly more aware of the benefits and potential savings that can result from the implementation of thermal insulation in their dwellings. This highlights the need for awareness campaigns and program that can simplify the potential benefits of thermal insulation to all sectors of the society regardless of their level of education.

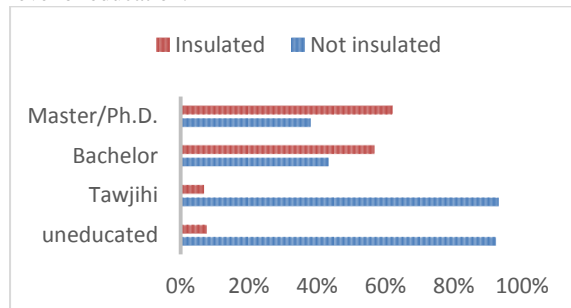


**Figure 3:** Percentages of insulated and uninsulated dwellings based on the education level

#### 4. Potential Savings of Enforcing Thermal Insulation Codes

An essential element in raising awareness on the importance of thermal insulation and compliance to the thermal insulation code is evaluating the potential energy and economic savings that can be achieved. In order to do so, a simplified model has been developed. The model is based on the degree.day approach and allows for varying simple house/apartment layout, weather data, wall construction, window/wall ratios, glazing and shading properties,...etc. The degree.day approach is simple and is very useful in establishing energy models, baselines, comparative analysis of energy consumption, despite the fact that it only takes the dry bulb temperature into consideration and that it is based on average temperatures. Internal loads were also ignored for simplicity. The following is a description of the equations used in the model:

$$Q_t = Q_c + Q_i + Q_s \quad (1)$$

Where,

$Q_t$  : Total heat gain/loss (kWh)

$Q_c$  : heat gain/loss due to conduction through walls, windows, and roof (kWh)

$Q_i$  : Heat gain/loss due to infiltration (kWh)

$Q_s$  : Heat gain due to direct solar radiation (kWh)

$$Q_c = \frac{24}{1000} U A DD \quad (2)$$

Where,

U: Overall heat transfer coefficient ( $W/m^2 \cdot ^\circ C$ )

A: Area of wall, window, or roof ( $m^2$ )

DD: Heating/cooling degree day ( $^\circ C \cdot day$ )

$$U = \frac{1}{R_i + R_o + \sum R_l} \quad (3)$$

Where,

$R_i$ : Inside surface convection resistance ( $m^2 \cdot ^\circ C/W$ )

$R_o$ : Outside surface convection resistance ( $m^2 \cdot ^\circ C/W$ )

$R_l$ : Conduction resistance in each layer of the wall or roof ( $m^2 \cdot ^\circ C/W$ )

$$R_l = \frac{t}{k} \quad (4)$$

Where,

t: Layer thickness (m)

k: Layer conductivity ( $W/m \cdot ^\circ C$ )

$$Q_i = \frac{24}{1000} \frac{\rho c_p V}{3600} DD \quad (5)$$

Where,

$\rho$ : Density of air ( $kg/m^3$ )

$c_p$ : Specific heat of air ( $J/kg \cdot ^\circ C$ )

V: Volume changed per hour based on the Air Change Method ( $m^3/h$ )

$$Q_s = I A_w (SC) \quad (6)$$

Where,

I: Incident solar radiation on the surface at a given orientation ( $kWh/m^2 \cdot month$ )

$A_w$ : Window area ( $m^2$ )

SC: Shading coefficient

This calculation model was used with a modular house/apartment in order to calculate the effect of thermal insulation on the overall heating and cooling energy demand under the typical climatic conditions in Jordan. The model house was rectangular shape one story 20 m x 10 m, with a total floor area of 200 m<sup>2</sup>. The climatic data used for the calculation are shown in Table 2 [17]. The reference for the degree.day calculation was 21.°C for all months. The resulting monthly degree.days are also shown in Table 2. It should be noted that the degree.days shown for the months of June till September are cooling degree.days (CDD) while they are heating degree.days (HDD) for the remaining months. The total HDDs are 1726 and the total CDDs are 441. The model was run twice: The first time with typical building constructing and in accordance with the specifications shown in Table 3. These specifications represent the typical construction and materials and methods normally used by contractors in Jordan. In the second time, the model was run with the same specifications but with adding a 5 cm layer of extruded polystyrene ( $k = 0.029$  W/m.°C) within the wall

and roof sections in order to achieve compliance with the thermal insulation code.

The resulting U value decreased from 2.63 to 0.48 W/m<sup>2</sup>.°C for the wall section and from 2.24 to 0.46 W/m<sup>2</sup>.°C for the roof section when the insulation layer was added. The resulting annual heating load went down from 50,716 kWh to 22,270 kWh and the annual cooling load went down from 15,838 kWh to 8,572 kWh. Therefore, the total heating/cooling load can be reduced by nearly 52% by simply adding the insulation layer to the walls and roofs. The details of the heating and cooling loads monthly variations before and after the insulation are shown in Figure 4 and Figure 5, respectively.

Assuming that such saving percentage can be implemented across the residential sector for uninsulated dwellings, and considering that this sector is responsible for 21% of the final energy consumption, of which 60% is consumed in space heating and cooling, a total of around 6% of the total national energy bill can be saved through enforcing code-compliant insulation to all new and existing buildings.

**Table 2.** Climatic data of Amman used for the model calculations

Month	Jan	Feb	Mar	Apr	May	Jun	Jul	Aug	Sep	Oct	Nov	Dec
Average Temp (°C)	8.0	9.0	11.8	16.1	20.7	23.8	25.3	25.6	23.7	20.5	14.9	9.8
Daily Solar irradiance (kWh/m <sup>2</sup> )	2.7	3.7	5.0	6.8	7.8	8.4	8.2	7.5	6.4	4.8	3.6	2.7
Degree.days	403	336	285	147	9	84	133	143	81	16	183	347

**Table 3.** Building construction specifications

	Material	Conductivity (W/m.°C)	Thickness (cm)
Wall Section	Ajloun stone	2.46	7
	Concrete	1.17	5
	Hollow blocks	0.63	7
	Plaster	0.72	2
Roof Section	Concrete tile	1.2	2
	Gravel	0.28	3
	Concrete ribs	0.95	10
	Reinforced concrete	1.44	7
	Plaster	0.72	2
Windows	Aluminium single glazed ( $U = 5.7$ W/m <sup>2</sup> .°C)		
Window/Wall ratio	0.15		
Windows shading coefficient	0.8		
Windows on North side	13.5 m <sup>2</sup>		
Windows on South side	8.5 m <sup>2</sup>		
Windows on East/West sides	5.4 m <sup>2</sup>		

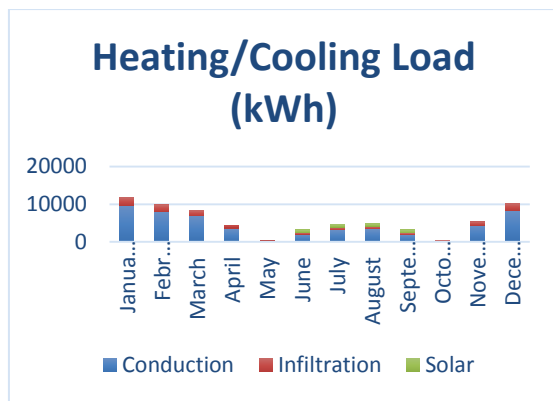


Figure 4. Heating and cooling load results for the model building without insulation

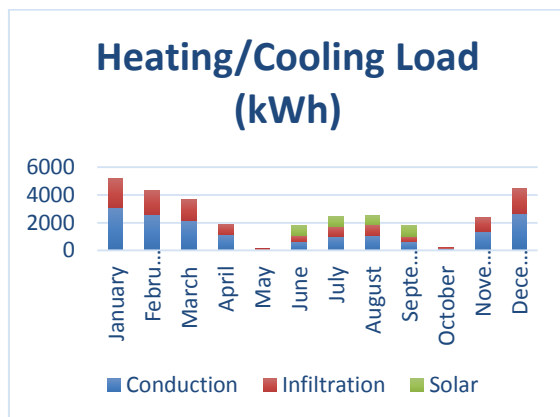


Figure 5. Heating and cooling load results for the model building with insulation

## 5. Conclusions

In this paper, it was demonstrated that although compliance with the thermal insulation code is compulsory, 77% of Jordanian dwellings lack any type of insulation and less than 9% comply with the code. This indicates that the use of thermal insulation is still a matter of choice for contractors and owners and code compliance is still far from being widespread.

Three factors that affect the decision of implementing thermal insulation in residential buildings were analysed: Ownership, income level, and education level. The findings indicate a strong relationship between each of these factors and the use of thermal insulation. The provision of a voluntary certification or rating system that can distinguish insulated dwellings can provide sufficient incentive for contractors and landlords to comply with the code. The cost of the initial investment and the lack of awareness are clear barriers to the implementation of thermal insulation. The income gap can be bridged through the introduction of eased, long term, low-interest financing schemes that target low income households. The education gap highlights the need for awareness campaigns and program that can simplify the potential benefits of thermal insulation to all sectors of the society regardless of their level of education.

A simplified model was developed and implemented to calculate the potential savings that can result from compliance with the thermal insulation code. Results indicated that the cooling and heating loads can be reduced by 52%. Considering such potential savings, the total national energy bill can be reduced by 6% if a national retrofitting program is implemented to all uninsulated residential buildings to bring them to comply with the thermal insulation code.

## References

- [1] Ministry of Energy and Mineral Resources (MEMR) "Annual report 2015". Amman, Jordan, 2016.
- [2] Ministry of Energy and Mineral Resources (MEMR) "Energy 2015 - Facts & Figures". Amman, Jordan, 2016.
- [3] Zarei M., Zare H. "Energy Consumption Modeling in Residential Buildings". *International Journal of Architecture and Urban Development*, 3, pp. 35-38, 2013.
- [4] Al-Ghandour A., Jaber J., Al-Hinti L., Mansour I. "Residential Past and Future Energy Consumption: Potential Savings and Environmental Impact". *Renewable and Sustainable Energy Reviews*, 13, pp. 1262-1274, 2009.
- [5] Akash B., Mohsen M. "Energy Analysis of Jordan's Urban Residential Sector". *Energy*, 24, pp. 823-831, 1999.
- [6] Jaber J., Jaber Q., Swalha S., Mohsen M. "Evaluation of Conventional and Renewable Energy Sources for Space Heating in the Household Sector". *Renewable and Sustainable Energy Reviews*, 12, pp. 278-289, 2008.
- [7] Jaber J., Mohsen M., Al-Sarkhi A., Akash B. "Energy Analysis of Jordan's Commercial Sector". *Energy Policy*, 31, pp. 887-894, 2003.
- [8] Mohsen M., Akash B. "Some Prospects of Energy Savings in Buildings". *Energy Conversion and Management*, 42, pp. 1307-1315, 2001.
- [9] Yang Y., Li B., Yao R. "A Method of Weighting Indicators of Energy Efficiency Assessment in Residential Building in China". *PLEA 2008 - 25th Conference on Passive and Low Energy Architecture*, Dublin, 2008.
- [10] Tommerup H., Svendsen S. "Energy Saving in Danish Residential Building Stocks". *Energy and Buildings*, 38, pp. 618-626, 2006.
- [11] AlZyood M., Harahsheh H., Hammad M. "Thermal Economical Analysis of Renewable Energy Buildings, Towards Low Energy House in Jordan". *International Renewable Energy Congress*, Tunisia, 2010.
- [12] Chvatal K., Soares M., Corvacho H. "The impact of increasing the building envelope insulation upon the risk of overheating in summer and an increased energy consumption". *Journal of Building Performance Simulation*, 2, pp. 267-282, 2009.
- [13] Al Momani H., Ali H. "Sick Building Syndrome in Apartment Buildings in Jordan". *Jordan Journal of Civil Engineering*, 2, 2008.
- [14] Suliman S., Beithou N. "Residential Building Walls and Environment in Amman, Jordan". *International Journal of Thermal & Environmental Engineering*, 3, pp. 101-107, 2011.
- [15] Jordan National Building Council, Thermal insulation code, Ministry of Housing & Public Works, Amman, 2008.
- [16] Al-Sallami H. "Analysis of energy use intensity in residential buildings in Jordan". Master thesis, German Jordanian University, 2015.
- [17] Jordan National Building Council, Energy saving buildings code, Ministry of Housing & Public Works, Amman, 2010.



# Reduced Filtered Dynamic Model for Joint Friction Estimation of Walking Biped

Iyad Hashlamon<sup>\* a</sup>, Kemalettin Erbatur<sup>b</sup>

<sup>a</sup> Palestine Polytechnic University, Hebron, Palestine

<sup>b</sup> Faculty of Engineering and Natural Sciences, Sabanci University, Tuzla, Istanbul, Turkey

Received 27 Jan, 2017

Accepted April 5, 2017

## Abstract

The present paper presents a novel method for estimating the joint friction of walking bipeds. It combines a measurement-based method with an adaptive model-based method to estimate the joint friction. The former is used when the feet is in contact, while the latter is used when the leg is swinging. The measurements are the feet forces and the readings of an inertial measure unit located at the biped body. The measurement-based method utilizes these measurements into a reduced filtered dynamic model of the biped to obtain an online estimated filtered version of the joint friction. Once the foot swings, a friction model is adopted to represent the joint friction behavior. The model parameters are adaptively identified using the online estimated filtered friction whenever the foot is in contact. The results are validated using full-dynamics of 12-DOF biped model and show a dramatic tracking of the estimated friction to the true one.

© 2017 Jordan Journal of Mechanical and Industrial Engineering. All rights reserved

**Keywords:** Humanoid robot, joint friction, CoM states, biped model.

## 1. Introduction

The interest in the humanoid adaptive, efficient, and robust motion control is dramatically increased [1-7, 8]. However, the biped structure makes its dynamics highly nonlinear and hard to be stabilized. Another difficulty rises from the robot mechanical structure which makes the control challenge harder. Robots contain transmissions or drive mechanisms to transfer the power from the actuator to the robot link through the joint [9]. Therefore, friction is observed at the joints. Friction has a considerable effect on the robot behavior. It may deteriorate the robot walking performance. Typical consequences of joint friction are steady state errors, limit cycles and poor dynamic response [10, 11]. Therefore, joint friction compensation attracted the researchers' attention and interest [12, 13].

### 1.1. Related Work

Friction model-based method is intensively used for friction compensation. The friction behavior is represented using a mathematical model [14-17] and the model parameters are identified using offline identification methods [18-21]. However, the friction is environment and load dependant phenomenon [12, 22]. Therefore, adaptive identification methods were developed to identify the friction model parameters [23-27]. However, the friction is a complex phenomenon and representing it using a mathematical model is a challenge.

Friction modeling challenge was a strong motivation for the researchers to look for model-free methods. The friction is considered a disturbance along with external disturbances, system model uncertainty and so on. Then, a disturbance observer [28, 29] is used to reduce the effect of this disturbance [30-33]. Other studies used friction approximators based on soft computing techniques, such as Neural Networks (NN) and Fuzzy systems [24, 34-44]. However, approximation errors exist [45]. Model-free and measurement base method is reported too. Here the difficulty of friction modeling is avoided by mounting extra torque/force sensors on the robot. In [46, 47], the manipulator link torque is measured using a torque sensor and used in the feedback of the control loop. However, the sensors should be added in the design process. For fixed base robots, the base is equipped by a force/torque sensor to form the Base Sensor Control (BSC) method [22]. The sensor readings are mapped to the manipulator's link to calculate the link torque which is used in the feedback torque control loop. However, the humanoid robot is mobile and not fixed in the ground.

### 1.2. Problem Importance and Definition

Joint friction is the major disturbance of the actuator and transmission unit at the joint. As a demonstration of joint friction effect for legged robots, refer to the video of some experiments conducted in the control system laboratory in Toyota technological institute [48].

Beyond the aforementioned consequences of joint friction, the compensation of joint friction is crucial for

\* Corresponding author e-mail: iyad@ppu.edu.

some control techniques and locomotion in legged robots. In the absence of joint torque sensors, the joint torque is estimated using the transpose of the Jacobian for each leg. However, the accuracy of this method is not sufficient when joint friction is observed and not compensated [49, 50, 51].

To this end, joint friction for legged robots is either neglected [52-55], regarded as a disturbance and tried to be eliminated by a disturbance observer [30], or estimated using a friction model with offline identified parameters [56, 57]. Here, if the model parameters are known or identified with very small uncertainty then model-based method of joint friction estimation has better precision compensation [58]. On the other hand, high accuracy requires adaptive parameter tuning and, hence, information about the friction is required. The measurement-based method avoids friction modeling and approximation problems. However, it requires joint torque sensors. Furthermore, it is inapplicable directly to bipedal applications because, while walking, the biped switches its legs from the Double Support phase (DS) to the Single Support phase (SS), and so forth. Other challenges rise from the structure of the bipeds; its model includes the hard to measure body position and its derivatives in addition to the joint angles and their derivatives.

Therefore, a method is required to estimate the joint friction for walking biped. This method would have the advantages of the measurement-based and the adaptive model-based methods. It must be able to overcome the unmeasured variables limitations.

### 1.3. Proposed Method

The present paper proposes a new method for biped joint friction estimation. It combines the measurement-based method with the adaptive model-based method.

Measurement-based method is a method that works only when the foot is in contact with the ground and employs the biped model without friction models to estimate the joint friction. To accomplish this estimation, the joints angular accelerations, which are not measured directly, are required. The robot body (called base later on) velocity and orientation are estimated as in [59-61]. The explicit calculation of the joint angular accelerations is avoided by adopting the filtered dynamics model method [62]. Here, the biped model is reduced then filtered using a stable first order low pass filter to form the reduced filtered dynamical model of the biped. Then, the measured Ground Reaction Forces (GRF), the readings of Inertial Measurement Unit (IMU), and the estimated base velocity are utilized in the obtained reduced filtered dynamical model to estimate a filtered version of the joint friction online. However, when the GRF are no longer available (the foot is not in contact with the ground), the former estimation method is inapplicable. Therefore, a friction model is adopted to overcome this problem. The friction model is used only when the foot is not in contact with the ground and its parameters are adaptively identified whenever the foot is in contact with the ground.

The rest of the paper is organized as follows: Section **Error! Reference source not found.** describes the biped model. Friction estimation is derived in section **Error! Reference source not found.** Section **Error! Reference**

**source not found.** presents the results. The paper conclusion is in Section (5).

## 2. Biped Model

For a biped with  $N$  number of joints, the robot model is:

$$\begin{pmatrix} H_{11} & H_{12} & H_{13} & H_{14} \\ H_{21} & H_{22} & H_{23} & H_{24} \\ H_{31} & H_{32} & H_{33} & 0 \\ H_{41} & H_{42} & 0 & H_{44} \end{pmatrix} \begin{pmatrix} \dot{\mathbf{v}}_b \\ \dot{\boldsymbol{\omega}}_b \\ \ddot{\boldsymbol{\theta}}_L \\ \ddot{\boldsymbol{\theta}}_R \end{pmatrix} + \begin{pmatrix} \mathbf{b}_1 \\ \mathbf{b}_2 \\ \mathbf{b}_L \\ \mathbf{b}_R \end{pmatrix} + \begin{pmatrix} \mathbf{u}_{F_1} \\ \mathbf{u}_{F_2} \\ \mathbf{u}_{F_L} \\ \mathbf{u}_{F_R} \end{pmatrix} = \begin{pmatrix} \mathbf{f}_b \\ \mathbf{n}_b \\ \boldsymbol{\tau}_L \\ \boldsymbol{\tau}_R \end{pmatrix} + \begin{pmatrix} \mathbf{u}_{E_1} \\ \mathbf{u}_{E_2} \\ \mathbf{u}_{E_L} \\ \mathbf{u}_{E_R} \end{pmatrix} \quad (1)$$

where  $\boldsymbol{\theta} \in R^N$  and  $\dot{\boldsymbol{\theta}} = \boldsymbol{\omega} \in R^N$  are the joint displacements and angular velocity vectors, respectively,  $\boldsymbol{\theta}$  is measured using joint encoders attached to the joint actuators.  $\mathbf{p}_b$  and  $\dot{\mathbf{p}}_b = \mathbf{v}_b$  are the position and linear velocity of the robot base-link.  $\dot{\mathbf{v}}_b$  and  $\boldsymbol{\omega}_b$  are the acceleration and angular velocity of the robot body, respectively, they are measured using an IMU.  $\mathbf{f}_b$  and  $\mathbf{n}_b$  are the force and torque vectors at the base-link, and  $\boldsymbol{\tau}$  is the generalized joint control vector.  $\mathbf{b}$  is the bias term which contains the coriolis and gravity effects.  $H_{ij}$  for  $(i, j) \in \{1, 2, 3, 4\}$  are sub-matrices of the robot inertia matrix.  $\mathbf{u}_{E_1}$  and  $\mathbf{u}_{E_2}$  are the net force and torque effects of the reaction forces on the robot body,  $\mathbf{u}_{E_L}$  and  $\mathbf{u}_{E_R}$  stand for the effect of reaction forces on the robot joints for the left and right legs, respectively. They are calculated by utilizing the measured external forces  $\mathbf{F}_{E_L}$  and  $\mathbf{F}_{E_R}$ , respectively, from the contact force sensors assembled at the feet soles as:

$$\mathbf{u}_{E_m} = \mathbf{J}_m^T(\mathbf{x}) \mathbf{F}_{E_m}, \quad (2)$$

where  $\mathbf{J}_m$  is the Jacobian of the leg  $\mathbf{m}$  with:

$$\mathbf{m} = \begin{cases} \mathbf{L} & \text{left} \\ \mathbf{R} & \text{right} \end{cases}. \quad (3)$$

The subscripts  $(\ )_L$  and  $(\ )_R$  stand for the left and right leg, respectively.

Referring to the last two rows in (1) and (2), the unknowns are  $\ddot{\boldsymbol{\theta}}_m$  and  $\mathbf{u}_{F_m}$  which is the required vector to be calculated or estimated. Here, the other variables are either measured or estimated using known methods [59-61]. Therefore, the biped model is reduced and filtered to avoid the explicit calculation of  $\ddot{\boldsymbol{\theta}}_m$ . The obtained reduced filtered dynamic is used to calculate the filtered version of required vector  $\mathbf{u}_{F_m}$ .

## 3. Friction Estimation

In the proposed approach, the joint friction estimation depends on the knowledge of the applied control torque at the joint and the transmitted torque to the link which can be sensed by the reaction forces. The transmission and frictional forces are internal forces. Then, (1) can be reduced to represent the active joints dynamics and reshaped in terms of friction as:

$$\begin{pmatrix} \mathbf{u}_{F_L} \\ \mathbf{u}_{F_R} \end{pmatrix} = \begin{pmatrix} \boldsymbol{\tau}_L \\ \boldsymbol{\tau}_R \end{pmatrix} + \begin{pmatrix} \mathbf{u}_{E_L} \\ \mathbf{u}_{E_R} \end{pmatrix} - \bar{\mathbf{H}} \begin{pmatrix} \dot{\boldsymbol{\omega}}_b \\ \ddot{\boldsymbol{\theta}}_L \\ \ddot{\boldsymbol{\theta}}_R \end{pmatrix} - \begin{pmatrix} H_{31} \\ H_{41} \end{pmatrix} \dot{\mathbf{v}}_b - \begin{pmatrix} \mathbf{b}_L \\ \mathbf{b}_R \end{pmatrix} \quad (4)$$

with:

$$\bar{\mathbf{H}} = \begin{pmatrix} H_{32} & H_{33} & 0 \\ H_{42} & 0 & H_{44} \end{pmatrix}. \quad (5)$$

From(4), one can see that the right hand-side is the response due to the torque transmitted to the manipulator's links from the total applied joint control torque  $\boldsymbol{\tau}_m$ .

The basic idea is to compute the right hand-side of (4), however, the existence of the angular acceleration terms which are in most cases unmeasured directly imposes a challenge. The solution to this problem is reported in the literature. The use of the band limited periodic excitation trajectories is reported in [63] which is not always possible. The offline numerical differentiation [9] is used too; however, it is inapplicable in the real time applications. Another method depends on the filtered dynamic model [62, 64] which is adopted here. By using this method, the explicit calculation of the angular acceleration terms is avoided by filtering both sides of (4) using a proper stable filter. The first order filter transfer function  $Z(s)$  with the constant  $\sigma$  is adopted here. It is expressed as:

$$Z(s) = \sigma \frac{1}{s + \sigma}, \quad (6)$$

with its impulse response:

$$z(t) = \ell^{-1}(Z(s)) = \sigma e^{-\sigma t}, \quad (7)$$

where  $\ell^{-1}(\cdot)$  is the Laplace inverse transform. The multiplication in the frequency domain is equivalent to the convolution in time domain, and since there are  $N$  joint equations in (4), each of them can be filtered by (6). Therefore, there will be  $N$  filters with impulse responses as:

$$\mathbf{z}(t) = \begin{bmatrix} \sigma_1 e^{-\sigma_1 t} & & 0 \\ & \ddots & \\ 0 & & \sigma_N e^{-\sigma_N t} \end{bmatrix}, \quad (8)$$

where  $\sigma_i$ ,  $i=1,2,\dots,N$  are the  $i^{th}$  joint filter constants. Then the filtered version of (4) is:

$$\begin{aligned} \int_0^t \mathbf{z}(t-\tau) \begin{pmatrix} \mathbf{u}_{F_L} \\ \mathbf{u}_{F_R} \end{pmatrix} d\tau &= \int_0^t \mathbf{z}(t-\tau) \left( \begin{pmatrix} \boldsymbol{\tau}_L \\ \boldsymbol{\tau}_R \end{pmatrix} + \begin{pmatrix} \mathbf{u}_{E_L} \\ \mathbf{u}_{E_R} \end{pmatrix} \right) d\tau + \\ &\quad - \int_0^t \mathbf{z}(t-\tau) \left( \bar{\mathbf{H}} \begin{pmatrix} \dot{\boldsymbol{\omega}}_b \\ \ddot{\boldsymbol{\theta}}_L \\ \ddot{\boldsymbol{\theta}}_R \end{pmatrix} \right) d\tau \\ &\quad - \int_0^t \mathbf{z}(t-\tau) \left( \begin{pmatrix} H_{31} \\ H_{41} \end{pmatrix} \dot{\mathbf{v}}_b + \begin{pmatrix} \mathbf{b}_L \\ \mathbf{b}_R \end{pmatrix} \right) d\tau \end{aligned} \quad (9)$$

The term  $\int_0^t \mathbf{z}(t-\tau) \left( \bar{\mathbf{H}} \begin{pmatrix} \dot{\boldsymbol{\omega}}_b \\ \ddot{\boldsymbol{\theta}}_L \\ \ddot{\boldsymbol{\theta}}_R \end{pmatrix} \right) d\tau$  can be integrated

by parts with  $\dot{\boldsymbol{\theta}}_L(0) = \dot{\boldsymbol{\theta}}_R(0) = \dot{\boldsymbol{\omega}}_b(0) = 0$

and:  $\mathbf{z}(0) = \boldsymbol{\sigma} = \begin{bmatrix} \sigma_1 & & 0 \\ & \ddots & \\ 0 & & \sigma_N \end{bmatrix}$  as:

$$\begin{aligned} \int_0^t \mathbf{z}(t-\tau) \left( \bar{\mathbf{H}} \begin{pmatrix} \dot{\boldsymbol{\omega}}_b \\ \ddot{\boldsymbol{\theta}}_L \\ \ddot{\boldsymbol{\theta}}_R \end{pmatrix} \right) d\tau &= \boldsymbol{\sigma} \bar{\mathbf{H}} \begin{pmatrix} \boldsymbol{\omega}_b \\ \dot{\boldsymbol{\theta}}_L \\ \dot{\boldsymbol{\theta}}_R \end{pmatrix} - \\ \int_0^t \mathbf{z}(t-\tau) \dot{\bar{\mathbf{H}}} \begin{pmatrix} \boldsymbol{\omega}_b \\ \dot{\boldsymbol{\theta}}_L \\ \dot{\boldsymbol{\theta}}_R \end{pmatrix} - \dot{\mathbf{z}}(t-\tau) \bar{\mathbf{H}} \begin{pmatrix} \boldsymbol{\omega}_b \\ \dot{\boldsymbol{\theta}}_L \\ \dot{\boldsymbol{\theta}}_R \end{pmatrix} d\tau \end{aligned} \quad (10)$$

then (9) is modified accordingly as:

$$\begin{aligned} \int_0^t \mathbf{z}(t-\tau) \begin{pmatrix} \mathbf{u}_{F_L} \\ \mathbf{u}_{F_R} \end{pmatrix} d\tau &= -\boldsymbol{\sigma} \bar{\mathbf{H}} \begin{pmatrix} \boldsymbol{\omega}_b \\ \dot{\boldsymbol{\theta}}_L \\ \dot{\boldsymbol{\theta}}_R \end{pmatrix} \\ + \int_0^t \mathbf{z}(t-\tau) \left( \begin{pmatrix} \boldsymbol{\tau}_L \\ \boldsymbol{\tau}_R \end{pmatrix} + \begin{pmatrix} \mathbf{u}_{E_L} \\ \mathbf{u}_{E_R} \end{pmatrix} + \dot{\bar{\mathbf{H}}} \begin{pmatrix} \boldsymbol{\omega}_b \\ \dot{\boldsymbol{\theta}}_L \\ \dot{\boldsymbol{\theta}}_R \end{pmatrix} - \begin{pmatrix} H_{31} \\ H_{41} \end{pmatrix} \dot{\mathbf{v}}_b - \begin{pmatrix} \mathbf{b}_L \\ \mathbf{b}_R \end{pmatrix} \right) d\tau \\ + \int_0^t \dot{\mathbf{z}}(t-\tau) \bar{\mathbf{H}} \begin{pmatrix} \boldsymbol{\omega}_b \\ \dot{\boldsymbol{\theta}}_L \\ \dot{\boldsymbol{\theta}}_R \end{pmatrix} d\tau \end{aligned} \quad (11)$$

All the terms are filtered using (6), except for the last term  $\int_0^t \dot{\mathbf{z}}(t-\tau) \bar{\mathbf{H}} \begin{pmatrix} \boldsymbol{\omega}_b \\ \dot{\boldsymbol{\theta}}_L \\ \dot{\boldsymbol{\theta}}_R \end{pmatrix} d\tau$  which is filtered using:

$$Z_2(s) = \ell\{\dot{\mathbf{z}}(t)\} = \ell\{-\sigma^2 e^{-\sigma t}\} = -\sigma^2 \frac{1}{s + \sigma}, \quad (12)$$

or in matrix form:

$$\mathbf{z}_2(t) = - \begin{bmatrix} \sigma_1^2 e^{-\sigma_1 t} & & 0 \\ & \ddots & \\ 0 & & \sigma_N^2 e^{-\sigma_N t} \end{bmatrix} \quad (13)$$

By introducing the notation  $\langle \boldsymbol{\eta} \rangle_\lambda$  to indicate that the term  $\boldsymbol{\eta}$  is filtered using the filter  $\lambda$ , the filtered dynamic equation is:

$$\left\langle \begin{pmatrix} \mathbf{u}_{F_L} \\ \mathbf{u}_{F_R} \end{pmatrix} \right\rangle_{Z(s)} = \boldsymbol{\sigma} \xi_1 + \langle \xi_2 \rangle_{Z(s)} + \langle -\xi_1 \rangle_{Z_2(s)}, \quad (14)$$

where:

$$\xi_1 = -\bar{H} \begin{pmatrix} \omega_b \\ \dot{\theta}_L \\ \dot{\theta}_R \end{pmatrix}, \quad (15)$$

and:

$$\xi_2 = \begin{pmatrix} \tau_L \\ \tau_R \end{pmatrix} + \begin{pmatrix} u_{E_L} \\ u_{E_R} \end{pmatrix} + \dot{\bar{H}} \begin{pmatrix} \omega_b \\ \dot{\theta}_L \\ \dot{\theta}_R \end{pmatrix} - \begin{pmatrix} H_{31} \\ H_{41} \end{pmatrix} \dot{v}_b - \begin{pmatrix} b_L \\ b_R \end{pmatrix}, \quad (16)$$

The cut-off frequency of the first order filter affect the results. Its value depends on the highest meaningful frequency in the measurements ( $F_E$  and  $\dot{v}_b$ ). The cut-off frequency value should be higher than the highest meaningful frequency, at the same time, it should be able to smooth the measurements and reject the other higher frequencies. Therefore, the cut-off frequency value must not be too high.

All of the right hand terms of (14) are known and can be computed. Then the estimated filtered joint friction is used for two purposes: friction compensation when the foot is in contact with the ground and friction model parameter identification. The identification process takes place whenever the foot is in the contact with the ground and thus the identification is adaptive. When the leg is swinging, the friction model with the identified parameters is used to the represent the friction behavior. Friction models differ in their characteristics [12, 65]; however, the model parameters can be identified using identification tools, like the Recursive Least Squares method (RLS) [66]. For the identification process, the joint angular velocity is measured and  $\langle u_{F_m} \rangle_{Z(s)}$  is estimated from (14) when the foot is in contact.

#### 4. Results

The simulations are carried on 12 Degrees of Freedom (DOF) biped model. It consists of a trunk which connects a two 6-DOF legs. Three joint axes are positioned at the hip, two joints are at the ankle and one at the knee (Figure 1). MATLAB simulink contains a-three -axes IMU which consists of three -axes accelerometer and three -axes gyroscope with contaminated noise. The force sensors are fixed at the feet soles. It is assumed to have four three-axes

force sensors located at known positions with respect to the foot link frame [67].

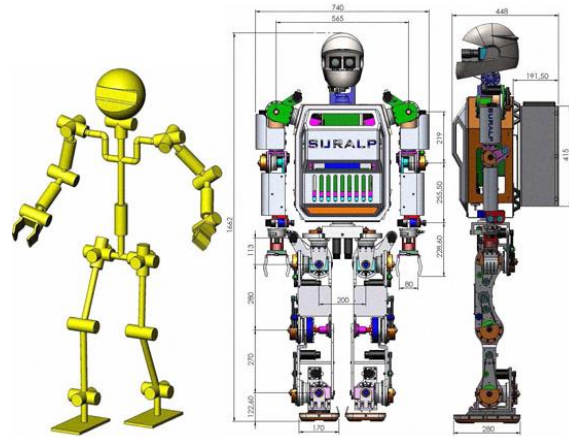


Figure 1. The kinematic arrangement and dimensional drawing of SURALP

To compare the true friction with the estimated one, the true friction values at the joints of the real biped have to be measured while walking. Therefore, only simulations are carried on the biped model and the true friction at the joint is generated using the nonlinear model [17]:

$$u_F = \gamma_1 \underbrace{\left( \tanh(\gamma_2 \dot{\theta}) - \tanh(\gamma_3 \dot{\theta}) \right)}_{\text{Stribeck effect}} + \underbrace{\gamma_4 \tanh(\gamma_5 \dot{\theta})}_{\text{coulomb friction}} + \underbrace{\gamma_6 \dot{\theta}}_{\text{viscous dissipation}} \quad (17)$$

where  $\gamma_i, i=1, \dots, 6$  are positive constants and the static coefficient of friction can be approximated by  $\gamma_1 + \gamma_4$ . **Note: This model is used solely as a joint friction generator.** The values of the parameters  $\gamma_i, i=1, \dots, 6$  for each joint of the leg are listed in Table 1 and generated true friction is the red line in Figure 3.

Figure 2 shows the walking trajectories, the walking starts after 0.5 sec, then the biped is in the left single support LS, DS then right single support RS and so forth.

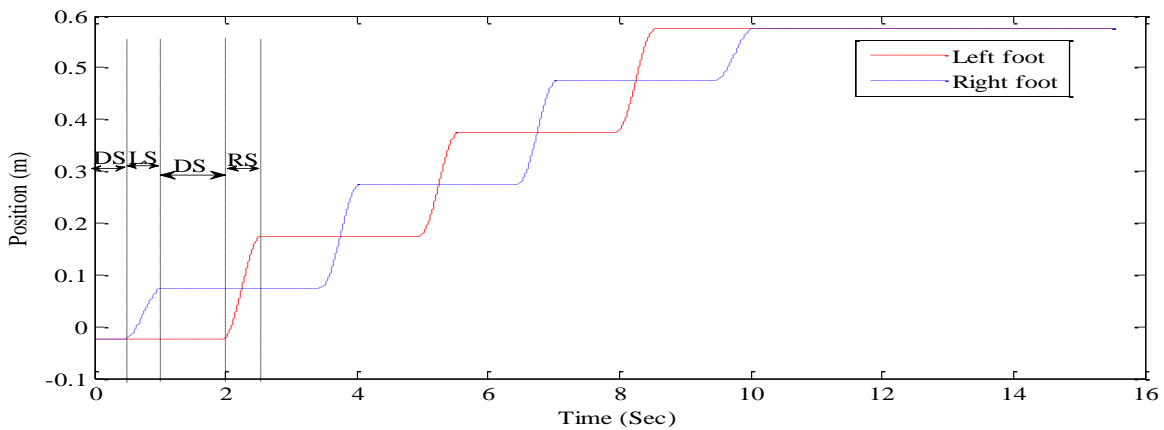


Figure 2. Feet walking trajectories, DS stands for the double support phase, LS stands for the left leg single support phase, and RS stands for the right leg single support phase

**Table 1:** True friction model parameters for each joint

	$\theta_1$	$\theta_2$	$\theta_3$	$\theta_4$	$\theta_5$	$\theta_6$
$\gamma_1$	0.7	0.6	0.5	0.4	0.2	0.05
$\gamma_2$	100	100	100	100	100	100
$\gamma_3$	10	10	10	10	10	10
$\gamma_4$	0.6	0.5	0.4	0.3	0.02	0.01
$\gamma_5$	100	100	100	100	100	100
$\gamma_6$	0.9	0.9	0.9	0.9	0.9	0.9

4.1. Model-Based Joint Friction Estimation

To be more realistic, the model-based friction estimation adopts another model differs from (17). For the joint  $n, |n = 1, \dots, 6$ , the model is written as:

$$\langle \mathbf{u}_{F_m} \rangle_{Z(s)} = F_c^n \text{sgn}(\dot{\theta}_n) + F_v^n \dot{\theta}_n, \tag{18}$$

Or for the joints of the leg  $m$  :

$$\langle \mathbf{u}_{F_m} \rangle_{Z(s)} = \begin{bmatrix} \text{sgn}(\dot{\theta}_1) & 0 & 0 & \dot{\theta}_1 & 0 & 0 \\ 0 & \ddots & 0 & 0 & \ddots & 0 \\ 0 & 0 & \text{sgn}(\dot{\theta}_6) & 0 & 0 & \dot{\theta}_6 \end{bmatrix}_{6 \times 12} \begin{bmatrix} F_c^1 \\ \vdots \\ F_c^6 \\ F_v^1 \\ \vdots \\ F_v^6 \end{bmatrix} \tag{19}$$

where  $F_v$  and  $F_c$  are the viscous friction coefficient the coulomb friction, respectively. The estimated  $\langle \mathbf{u}_{F_m} \rangle_{Z(s)}$  from (14) is utilized in to estimate  $F_c^n$  and  $F_v^n$  when the leg is in contact based on the RLS algorithm. On the other hand, the friction behavior is represent by the estimated parameters  $\hat{F}_v^n$  and  $\hat{F}_c^n$  for each joint when the leg is swinging.

4.2. Measurement-Based Joint Friction Estimation

The estimation process of the joint friction is carried out simultaneously. Each joint of the two lgs has the same adopted friction model. The used filter constants are listed in

Table 2 and the estimated filtered friction is based on (14). The biped starts with the DS phase for 0.5 sec, during this period the friction estimation is measurement-based using (14). The resulted estimated filtered friction is used for the parameter identification process of the friction model parameters  $F_v^n$  and  $F_c^n$ . Once the biped switches to the LS phase, the friction behavior for the right leg joints is represented by the friction models with the identified

parameters  $\hat{F}_v^n$  and  $\hat{F}_c^n$ . Meanwhile, for the left leg joints, the estimation method is measurement-based and the corresponding friction models parameters are being identified. Later at the time instant  $t=1.1$  sec, the estimation method is measurement-based and the friction model parameters are identified for both legs since the biped switches to the DS phase. Hence the identified parameters  $\hat{F}_v^n$  and  $\hat{F}_c^n$  for the right leg are re-identified and corrected. The biped switched to the RS phase at the time instant  $t=2$  sec. Accordingly, the estimation process is measurement-based for the right leg joints and the parameter  $F_v^n$  and  $F_c^n$  are being identified. On the other hand, the identified parameters  $\hat{F}_v^n$  and  $\hat{F}_c^n$  of the left leg joints are used to represent the friction through the adopted friction models, and so forth.

Figure 3 shows both the true friction trajectory (dashed red line) and the estimated filtered friction (solid blue line) for the left leg. The true friction trajectory is generated using (17) with the parameters listed in Table 1. When the leg is swinging, the estimated friction uses the model (19) with the identified parameters. In these simulations, small and large frictional forces are used to test the ability of the proposed method. As depicted in Figure 3, the estimated filtered friction tracks the true friction. The present work differs from the work which is proposed by the authors in [60]. The differences lie in the facts that the present work does not assume the non-slipping case of the walking biped (therefore, it avoids the numerical errors of the pseudo inverse) and that the estimated filtered friction estimation is smoother in the present work.

**Table 2.** Filter constants

	$\theta_1$	$\theta_2$	$\theta_3$	$\theta_4$	$\theta_5$	$\theta_6$
$\sigma$	1	1	1	2	4	2

5. Conclusion

The joint friction of walking bipeds is estimated by combining the measurement-based method with the adaptive model-based method. The measurement-based estimation employs the biped reduced filtered dynamical model to compute the online filtered friction when the foot is in contact. It is based on readings of IMU and GRF. The dynamical model is filtered to avoid the explicit calculation of the joint angular accelerations. On the other hand, the adaptive model-based friction employs a friction model to represent the friction behavior when the leg is swinging. The model parameters are identified whenever the foot is in contact with the ground.

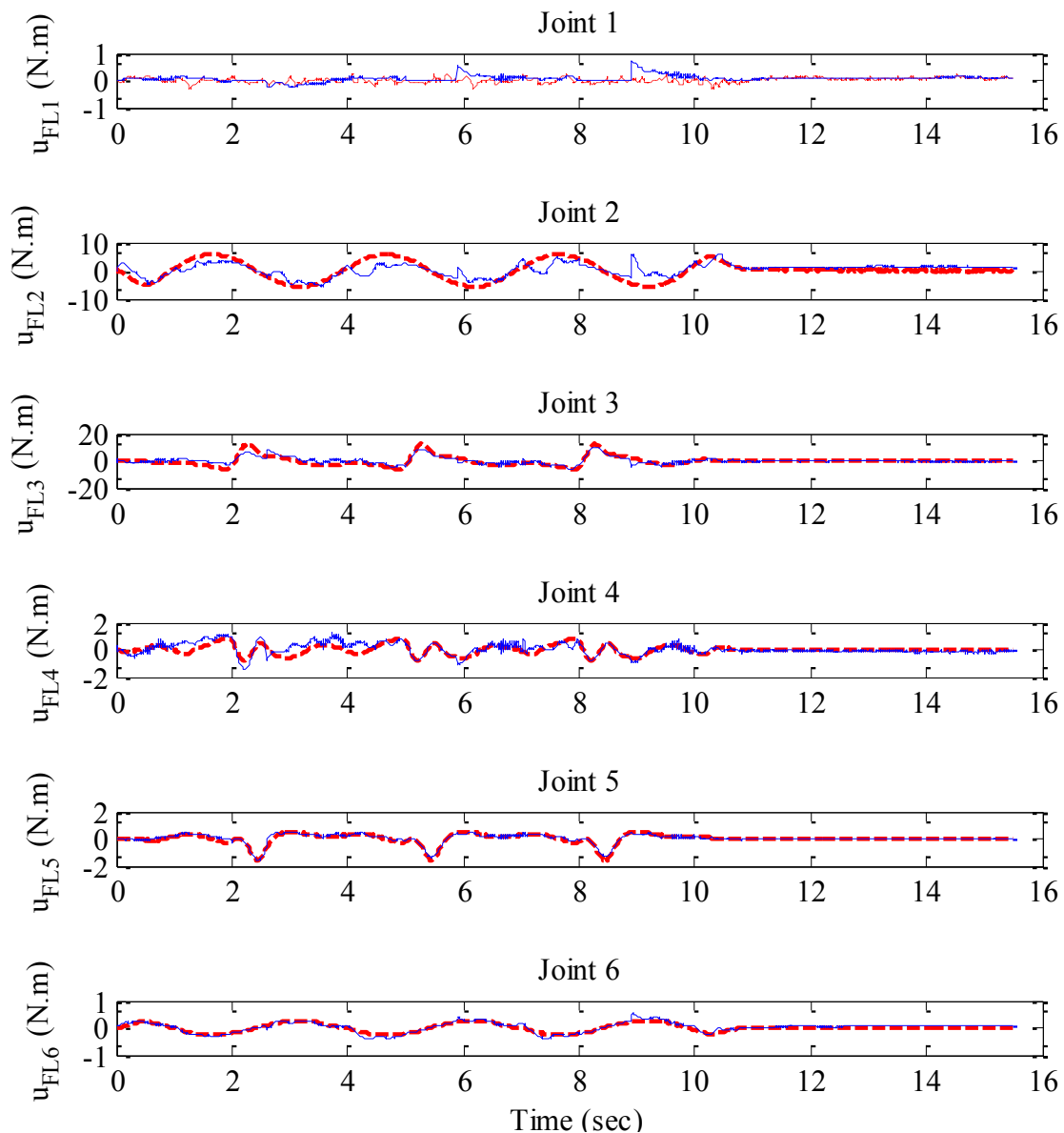


**Figure 3:** The estimated friction (solid blue line) and the true generated friction (dashed red line) for the left leg joints

## References

- [1] M. Koeda, Y. Uda, S. Sugiyama, T. Yoshikawa, "Shuffle turn and translation of humanoid robots". IEEE International Conference on Robotics and Automation (ICRA), Shanghai, 2011.
- [2] K. Miura, S. Nakaoka, M. Morisawa, F. Kanehiro, K. Harada, S. Kajita, "Analysis on a friction based "Twirl" for biped robots". IEEE International Conference on Robotics and Automation (ICRA), Alaska, USA, 2010.
- [3] S. Kajita, M. Morisawa, K. Miura, S. Nakaoka, K. Harada, K. Kaneo, F. Kanehiro, K. Yokoi, "Biped walking stabilization based on linear inverted pendulum tracking". IEEE/RSJ International Conference on Intelligent Robots and Systems (IROS), Taipei, Taiwan, 2010.
- [4] T. Liu, Y. Inoue, K. Shibata, "A wearable ground reaction force sensor system and its application to the measurement of extrinsic gait variability". Sensors, Vol. 10, No. 11, 2010, 10240-10255.
- [5] U. Seven, T. Akbas, K. Fidan, K. Erbatur, "Bipedal robot walking control on inclined planes by fuzzy reference trajectory modification". Soft Computing, Vol. 16, No. 11, 2012, 1959-1976.
- [6] S. J. Yi, B. T. Zhang, D. Hong, D. D. Lee, "Practical bipedal walking control on uneven terrain using surface learning and push recovery". IEEE/RSJ International Conference on Intelligent Robots and Systems (IROS), San Francisco, CA, USA, 2011.
- [7] K. Yeoun-Jae, L. Joon-Yong, L. Ju-Jang, "A balance control strategy of a walking biped robot in an externally applied force". International Conference on Information and Automation (ICIA), Shenyang, China, 2012.
- [8] J. P. Ferreira, M. M. Crisostomo, A. P. Coimbra, "Human Gait Acquisition and Characterization". IEEE Transactions on Instrumentation and Measurement, Vol. 58, No. 9, 2009, 2979-2988.
- [9] B. Siciliano, O. Khatib. Springer Handbook of Robotics. Springer-Verlag New York, Inc. 2007.

- [10] R. H. Hensen, M. Van de Molengraft, M. Steinbuch, "Friction induced hunting limit cycles: A comparison between the LuGre and switch friction model". *Automatica*, Vol. 39, No. 12, 2003, 2131-2137.
- [11] H. Olsson, K. J. Astrom, "Friction generated limit cycles". *IEEE Transactions on Control Systems Technology*, Vol. 9, No. 4, 2001, 629-636.
- [12] B. Bona, M. Indri, "Friction Compensation in Robotics: an Overview". *IEEE European Control Conference on Decision and Control*, Seville, Spain, 2005.
- [13] F. Jatta, R. Adamini, A. Visioli, G. Legnani, "Hybrid force/velocity robot contour tracking: an experimental analysis of friction compensation strategies". *IEEE International Conference on Robotics and Automation*, Washington DC, 2002.
- [14] B. Armstrong-Hélouvy, P. Dupont, C. C. De Wit, "A survey of models, analysis tools and compensation methods for the control of machines with friction". *Automatica*, Vol. 30, No. 7, 1994, 1083-1138.
- [15] R. H. A. Hellsen, G. Z. Angelis, M. J. G. van de Molengraft, A. G. de Jager, J. J. Kok, "Grey-box Modeling of Friction: An Experimental Case-study". *European Journal of Control*, Vol. 6, No. 3, 2000, 258-267.
- [16] V. Lampaert, J. Swevers, F. Al-Bender, "Modification of the Leuven integrated friction model structure". *IEEE Transactions on Automatic Control*, Vol. 47, No. 4, 2002, 683-687.
- [17] C. Makkar, W. E. Dixon, W. G. Sawyer, G. Hu, "A new continuously differentiable friction model for control systems design". *IEEE/ASME International Conference on Advanced Intelligent Mechatronics*. Proceedings, Monterey, CA, 2005.
- [18] R. H. A. Hensen, M. J. G. Van de Molengraft, M. Steinbuch, "Frequency domain identification of dynamic friction model parameters". *IEEE Transactions on Control Systems Technology*, Vol. 10, No. 2, 2002, 191-196.
- [19] J. Moreno, R. Kelly, "Manipulator velocity field control with dynamic friction compensation". *IEEE Conference on Decision and Control*, Maui Hawaii, USA, 2003.
- [20] J. Moreno, R. Kelly, R. Campa, "Manipulator velocity control using friction compensation". *IEEE Proceedings-Control Theory and Applications*, Vol. 150, No. 2, 2003, 119-126.
- [21] D. Kostic, B. de Jager, M. Steinbuch, R. Hensen, "Modeling and identification for high-performance robot control: an RRR-robotic arm case study". *IEEE Transactions on Control Systems Technology*, Vol. 12, No. 6, 2004, 904-919.
- [22] G. Morel, K. Iagnemma, S. Dubowsky, "The precise control of manipulators with high joint-friction using base force/torque sensing". *Automatica*, Vol. 36, No. 7, 2000, 931-941.
- [23] S. Grami, Y. Gharbia, "GMS friction compensation in robot manipulator". *IEEE conference on Industrial Electronics Society (IECON)*, Vienna, Austria, 2013.
- [24] Z. Dongdong, N. Jing, R. Xuemei, G. Herrmann, S. Longo, "Adaptive control of robotic servo system with friction compensation". *IEEE Conference on Robotics, Automation and Mechatronics (RAM)*, 2011.
- [25] L. R. Ray, A. Ramasubramanian, J. Townsend, "Adaptive friction compensation using extended Kalman-Bucy filter friction estimation". *Control Engineering Practice*, Vol. 9, No. 2, 2001, 169-179.
- [26] P. Vedagarbha, D. M. Dawson, M. Feemster, "Tracking control of mechanical systems in the presence of nonlinear dynamic friction effects". *IEEE Transactions on Control Systems Technology*, Vol. 7, No. 4, 1999, 446-456.
- [27] B. Friedland, Y. J. Park, "On adaptive friction compensation". *IEEE Transactions on Automatic Control*, Vol. 37, No. 10, 1992, 1609-1612.
- [28] A. Mohammadi, M. Tavakoli, H. J. Marquez, F. Hashemzadeh, "Nonlinear disturbance observer design for robotic manipulators". *Control Engineering Practice*, Vol. 21, No. 3, 2013, 253-267.
- [29] C. Wen-Hua, D. J. Ballance, P. J. Gawthrop, J. O'Reilly, "A nonlinear disturbance observer for robotic manipulators". *IEEE Transactions on Industrial Electronics*, Vol. 47, No. 4, 2000, 932-938.
- [30] D. Xing, J. Su, Y. Liu, J. Zhong, "Robust approach for humanoid joint control based on a disturbance observer". *Control Theory & Applications*, IET, Vol. 5, No. 14, 2011, 1630-1636.
- [31] J.-H. Ryu, J. Song, D.-S. Kwon, "A nonlinear friction compensation method using adaptive control and its practical application to an in-parallel actuated 6-DOF manipulator". *Control Engineering Practice*, Vol. 9, No. 2, 2001, 159-167.
- [32] B. Armstrong, D. Neevel, T. Kusik, "New results in NPID control: Tracking, integral control, friction compensation and experimental results". *IEEE Transactions on Control Systems Technology*, Vol. 9, No. 2, 2001, 399-406.
- [33] V. Lampaert, J. Swevers, F. Al-Bender, "Comparison of model and non-model based friction compensation techniques in the neighbourhood of pre-sliding friction". *Proceedings of the American Control Conference*, Boston, Massachusetts, 2004.
- [34] S. N. Huang, K. K. Tan, T. H. Lee, "Adaptive friction compensation using neural network approximations". *IEEE Transactions on Systems, Man, and Cybernetics, Part C: Applications and Reviews*, Vol. 30, No. 4, 2000, 551-557.
- [35] V. Vitiello, A. Tornambe, "Adaptive compensation of modeled friction using a RBF neural network approximation". *IEEE Conference on Decision and Control*, New Orleans, LA, 2007.
- [36] Y. H. Kim, F. L. Lewis, "Reinforcement adaptive learning neural network based friction compensation for high speed and precision". *Proceedings of the IEEE Conference on Decision and Control*, Tampa, Florida USA, 1998.
- [37] Y. F. Wang, D. H. Wang, T. Y. Chai, "Modeling and control compensation of nonlinear friction using adaptive fuzzy systems". *Mechanical Systems and Signal Processing*, Vol. 23, No. 8, 2009, 2445-2457.
- [38] L. Mostefai, M. Denai, S. Oh, Y. Hori, "Optimal Control Design for Robust Fuzzy Friction Compensation in a Robot Joint". *IEEE Transactions on Industrial Electronics*, Vol. 56, No. 10, 2009, 3832-3839.
- [39] W. Yongfu, W. Dianhui, C. Tianyou, "Extraction and Adaptation of Fuzzy Rules for Friction Modeling and Control Compensation". *IEEE Transactions on Fuzzy Systems*, Vol. 19, No. 4, 2011, 682-693.
- [40] D. Velez-Diaz, T. Yu, "Adaptive robust fuzzy control of nonlinear systems". *IEEE Transactions on Systems, Man, and Cybernetics, Part B: Cybernetics*, Vol. 34, No. 3, 2004, 1596-1601.
- [41] M. A. Llama, R. Kelly, V. Santibanez, "Stable computed-torque control of robot manipulators via fuzzy self-tuning". *IEEE Transactions on Systems, Man, and Cybernetics, Part B: Cybernetics*, Vol. 30, No. 1, 2000, 143-150.
- [42] K. Shiev, N. Shakev, A. V. Topalov, S. Ahmed, "Trajectory control of manipulators using type-2 fuzzy neural friction and disturbance compensator". *IEEE International Conference Intelligent Systems (IS)*, Sofia, 2012.
- [43] Y. Yousif, K. Daws, B. Kazem, "Prediction of friction stir Welding characteristic using neural network". *Jordan Journal of Mechanical and Industrial Engineering*, Vol. 2, No. 3, 2008,
- [44] B. S. Reddy, J. S. Kumar, K. V. K. Reddy, "Prediction of surface roughness in turning using adaptive neuro-fuzzy inference system". *Jordan Journal of Mechanical and Industrial Engineering*, Vol. 3, No. 4, 2009, 252-259.

- [45] G. L. Wang, Y. F. Li, D. X. Bi, "Support Vector Networks in Adaptive Friction Compensation". IEEE Transactions on Neural Networks, Vol. 18, No. 4, 2007, 1209-1219.
- [46] D. Vischer, O. Khatib, "Design and development of high-performance torque-controlled joints". IEEE Transactions on Robotics and Automation, Vol. 11, No. 4, 1995, 537-544.
- [47] L. E. Pfeiffer, O. Khatib, J. Hake, "Joint torque sensory feedback in the control of a PUMA manipulator". IEEE Transactions on Robotics and Automation, Vol. 5, No. 4, 1989, 418-425.
- [48] C. S. L. Y. C. Toyota Technological Institute, "ICM13 Kana Kotaka et al," 2012.
- [49] B. Ugurlu, T. Kawasaki, M. Kawanishi, T. Narikiyo, "Continuous and dynamically equilibrated one-legged running experiments: Motion generation and indirect force feedback control". International Conference on Intelligent Robots and Systems (IROS), Vilamoura, Algarve, Portugal, 2012.
- [50] B. Ugurlu, I. Havoutis, C. Semini, D. G. Caldwell, "Dynamic trot-walking with the hydraulic quadruped robot- HyQ: Analytical trajectory generation and active compliance control". International Conference on Intelligent Robots and Systems (IROS), Tokyo, Japan, 2013.
- [51] B. Ugurlu, K. Kotaka, T. Narikiyo, "Actively-compliant locomotion control on rough terrain: Cyclic jumping and trotting experiments on a stiff-by-nature quadruped". IEEE International Conference on Robotics and Automation (ICRA), Karlsruhe, Germany, 2013.
- [52] H. Yan, B. Vanderborght, R. Van Ham, W. Qining, M. Van Damme, X. Guangming, D. Lefeber, "Step Length and Velocity Control of a Dynamic Bipedal Walking Robot With Adaptable Compliant Joints". IEEE/ASME Transactions on Mechatronics, Vol. 18, No. 2, 2013, 598-611.
- [53] P. van Zutven, D. Kostic, H. Nijmeijer, "Foot placement for planar bipeds with point feet". IEEE International Conference on Robotics and Automation (ICRA), Saint Paul, Minnesota, USA, 2012.
- [54] T. Hase, H. Qingjiu, C. Xuedong, "Performance analysis of biped walking robot with circular feet using optimal trajectory planning method". IEEE International Conference on Robotics and Biomimetics, Bangkok, Thailand, 2009.
- [55] K. Miyahara, Y. Harada, D. N. Nenchev, D. Sato, "Three-dimensional Limit Cycle Walking with joint actuation". IEEE/RSJ International Conference on Intelligent Robots and Systems (IROS), Louis, USA, 2009.
- [56] K. Joohyung, K. Hoseong, L. Heekuk, S. Keehong, L. Bokman, L. Minhyung, L. Jusuk, R. Kyungsik, "Balancing control of a biped robot". IEEE International Conference on Systems, Man, and Cybernetics (SMC), Seoul, Korea, 2012.
- [57] T. Yoshikawa, O. Khatib, "Compliant humanoid robot control by the torque transformer". IEEE/RSJ International Conference on Intelligent Robots and Systems (IROS), Louis, USA, 2009.
- [58] S. I. Han, K. S. Lee, "Robust friction state observer and recurrent fuzzy neural network design for dynamic friction compensation with backstepping control". Mechatronics, Vol. 20, No. 3, 2010, 384-401.
- [59] I. Hashlamon, K. Erbatur, *Experimental verification of an orientation estimation technique for autonomous robotic platforms*, Master thesis, Sabanci University, 2010.
- [60] I. Hashlamon, K. Erbatur, "Joint friction estimation for walking bipeds". Robotica, Vol. 34, No. 7, 2014, 1610-1629.
- [61] I. Hashlamon, K. Erbatur, "Center of Mass States and Disturbance Estimation for a Walking Biped ". IEEE International Conference on Mechatronics (ICM 2013), Vicenza, Italy, 2013.
- [62] M. Van Damme, P. Beyl, B. Vanderborght, V. Grosu, R. Van Ham, I. Vanderniepen, A. Matthys, D. Lefeber, "Estimating robot end-effector force from noisy actuator torque measurements". IEEE International Conference on Robotics and Automation (ICRA), Shanghai, 2011.
- [63] J. Swevers, C. Ganseman, D. B. Tukel, J. De Schutter, H. Van Brussel, "Optimal robot excitation and identification". IEEE Transactions on Robotics and Automation, Vol. 13, No. 5, 1997, 730-740.
- [64] P. Hsu, M. Bodson, S. Sastry, B. Paden, "Adaptive identification and control for manipulators without using joint accelerations". Proceedings IEEE International Conference on Robotics and Automation, Raleigh, NC, USA, 1987.
- [65] H. Olsson, K. J. Åström, C. Canudas de Wit, M. Gäfvert, P. Lischinsky, "Friction models and friction compensation". European journal of control, Vol. 4, No. 1998, 176-195.
- [66] L. Ljung, *System Identification: Theory for the User*. 2nd. Upper Saddle River, NJ: Prentice-Hall PTR. 1999.
- [67] K. Erbatur, U. Seven, E. Taskiran, O. Koca, M. Yilmaz, M. Unel, G. Kiziltas, A. Sabanovic, A. Onat, "SURALP: A New Full-Body Humanoid Robot Platform". IEEE-Rsj International Conference on Intelligent Robots and Systems, New York, 2009.

# Fire Extinguisher Training: Subjective Assessment of a Newly Developed Method by Expert and Novice Firefighters

Awwad J. Dababneh <sup>a</sup>, Manar M. Ajlouni <sup>b\*</sup>

<sup>a</sup> Department of Industrial Engineering, Faculty of Engineering and Technology, The University of Jordan, Amman, 11942, Jordan.

<sup>b</sup> Department of Civil Defense, Amman, Jordan

Received Feb 20,2017

Accepted June 10,2017

## Abstract

The present article reports an evaluation study of a newly developed fire extinguisher training program that contained a video in Arabic, and a novel hands-on training apparatus. Fire extinguishers are an important part of the overall strategy for fire protection; however, its effectiveness depends on the availability of competent and willing users. Fire extinguisher training is important and should include both theoretical and hands-on training. Traditional hands-on training methods expensive and has adverse effects on the environment. New apparatus has been developed (the "Honeycomb" fire simulator); it uses a combination of propane clean fire, and inexpensive air-pressurized water extinguishers. Complementary to the new apparatus, a training video has been developed in Arabic that explains the fundamentals of fire extinguishers. Thirteen expert and fourteen Novice firefighters from the General directorate of Civil Defense in Jordan subjectively assessed the training video and apparatus. After watching the video and practicing/experimenting with the new hands-on apparatus they answered questionnaires, and indicated their likes, dislikes, and other comments in designated areas on the study forms. Expert and Novice firefighters indicated that the video contained important, comprehensive, and well-presented information, and they endorsed it for training employees and school students. The new apparatus were preferred by to the traditional fire-pan method by 13 firefighters, and only 5 preferred by 5 the traditional method. Also, with the advantages of low cost and low environmental impact, the new method is obviously superior to the traditional method. The findings of the present study endorse the newly developed training program for Arabic speaking countries. In addition, it can be projected that following the same structure program, effective programs may be established with different languages.

© 2017 Jordan Journal of Mechanical and Industrial Engineering. All rights reserved

Keywords: ...

## 1. Introduction

The use of portable fire extinguishers is an important part of the overall strategy for fire protection. It is designed and used to put out small fires before becoming too big. Handheld fire extinguishers are extremely common in public and work places worldwide, but for it to work a competent and willing person is needed. Improper use of fire extinguishers may cause more harm than good. Also, most extinguishers discharge its content in 10 to 30 seconds, which leaves no room for experimentation in an emergency situation. Advances have been made to the design of fire extinguishers, making it more easy and intuitive to use. However, training is still very important for developing the necessary Skills, Knowledge, and Understandings (SKUs). Classroom presentations, online classes, and videos have been used for developing the knowledge and understanding of employees and prospective users. Practice or hands-on training is essential

for developing and verifying the necessary skills for safe and effective use. This report presents a fire extinguisher training program that was developed in Arabic, and it included both theory and hands-on components. A video was produced to present and explain the necessary knowledge and understandings, and a novel design fire simulator was developed for hands-on training. The program was evaluated by expert and novice firefighters from the General Directorate of Civil Defense/Civil Defense Training Center in Jordan.

Many countries have regulations that mandate fire extinguishers training. In the United States, Occupational Health and Safety Administration (OSHA) regulations require "hands-on" fire extinguisher training for all workplace employees who have been designated to use fire extinguishers. These standards also require that employers provide educational programs (which may, or may not, include hands-on training) to familiarize employees with the general principles of fire extinguisher [13] (see OSHA 1910.157 (g) (1, 3)). Notably, firefighters and safety

\* Corresponding author e-mail: manaromhy@hotmail.com.

professionals associations (e.g., the National Safety Council (NSC) and the National Fire Protection Association (NFPA)) view hands-on training as the only viable option that can ensure all employees can use extinguishers safely and effectively [7,11].

The traditional method for hands-on extinguisher training includes the use of actual extinguishers and a fire pan. Typically, the fire pan is a metallic flat pan about 5-10 cm (2-4 inches) deep. The pan allows trainers to start, contain, and control a liquid fuel fire for training. The pan is usually half filled with water, and a small amount of a gasoline and diesel fuel mixture is poured over the water in the pan. The fuel mixture is lighter than water and floats on top. The water helps keep the overall temperature of the fuel low, and thus slows evaporation and keeps fire size under control. The resulting fire is a class B fire for which foam, powder, or CO<sub>2</sub> fire extinguishers maybe used to put it out. However, because of the mess and the difficulty in quickly re-igniting the fire, foam and powder extinguishers are rarely used. The CO<sub>2</sub> extinguishers, in contrast, leave no residue and allow for quick re-ignition, and are, thus, the preferred choice to use with the fire pan method. The major challenges for using the traditional fire pan method include cost and the negative impact on the environment. Although the pan itself is not expensive to construct, re-charging the fire extinguishers can be expensive and time-consuming, and, therefore, often limit the amount of practice a trainee receives. Furthermore, foam, powder, and CO<sub>2</sub> fire extinguishing agents have negative impacts on the environment, ranging from being "dirty and messy" to contributing to global warming by releasing CO<sub>2</sub> into the air.

Driven by the increased demand for hands-on training and by the shortcomings of the traditional fire pan method, several hands-on training apparatuses have been developed and commercialized in the past decade. Review of patents revealed clear design trends; protecting the environment, simplifying operations of apparatuses, and reducing cost of training. Design solutions included real and virtual simulation of fire. Real fire simulators used propane fuel to produce a clean fire [3, 4, 5, 9, 16], while virtual simulators used equipment similar to those used with electronic games [1, 2, 5, 6, 10]. Unfortunately, little viable research has been published investigating the effectiveness of these training methods.

A study [15] at Eastern Kentucky University investigated the effects of hands-on fire extinguisher training on the ability of ordinary people to put out small fires. The results demonstrated that subjects were able to operate a fire extinguisher without prior training. However, their conclusion might have been biased somewhat by the subject demographics: subjects were students recruited voluntarily from the campuses of Worcester Polytechnic Institute and Eastern Kentucky University, both of which have firefighting/safety educational programs and which raises a plausible concern that the subjects may have had higher average interest and knowledge regarding portable extinguishers than that of

the general public. Another possibility for bias is the fire simulator used in the study; participants did not actually putout flames, rather a fuel solenoid valve closed if sensors picked up that the participant was doing the right sweeping motion. Also, participants were required to keep a distance of 2.44 m (8 ft.) away from the fire at all times, which is unrealistic and counter to common professional practices and reliable standards. NFPA recommends starting the extinguisher at a safe distance of 2.44 m (8 ft.) and gradually closing on the fire until it is out [7,11]. On the upside, the apparatus in the Poole's study includes an air pressurized water extinguisher that can be charged easily on site using an ordinary air compressor. Regardless the shortcomings, the present study has important findings; it reports that participants showed improved performance and confidence as a result of hands-on training.

In a study [14] that used an electronic fire simulator, to assess the learning curve for fire extinguisher training; showed that subjects' performance improved with practice. On average it took participants five to six successful training attempts until there performance leveled, which implies that hands-on training must allow each trainee to practice 5 to 6 times to ensure full development of skills. Practically, it means that a trainee must empty 5 or 6 extinguishers, which may makes training costly and further limit access to hands-on training.

The use of virtual reality and electronic flame simulators are not widely spread; they may have low running cost, but the initial investment is considerable. Besides, they may require trainers with special skills in order to operate the equipment. Furthermore, trainees would not feel the fire heat even with the best designed virtual reality training apparatus.

Due to their very low environmental impact and low operational costs, propane gas fire simulators, and easily rechargeable water extinguishers, provide excellent solutions for hands-on training. However, propane gas fire does not normally extinguish with water. the fire simulator is designed in a specific way to produce flames that can be extinguished by the training extinguisher commercially available hands-on extinguisher training apparatus use either a simple propane burner with CO<sub>2</sub> extinguishers, or air pressurized water extinguisher with a complex burning system that has sensors and computer controlled valves to shut down the fuel line whenever the proper sweeping motion, are registered [3, 4]. In an unpublished study at the University of Minnesota-Duluth, done by the corresponding author of the present article, expert firefighters indicated that a commercially available computer controlled fire simulator had unrealistic and misleading flame-behavior.

The present study reports on a new fire simulator that was developed to address the aforementioned shortcomings of current fire simulators. It uses propane fire and air-pressurized water extinguishers. It is believed that the new design better simulates real fire, and is inexpensive to produce. The new design is called the "Honeycomb" fire simulator (Figure 1).

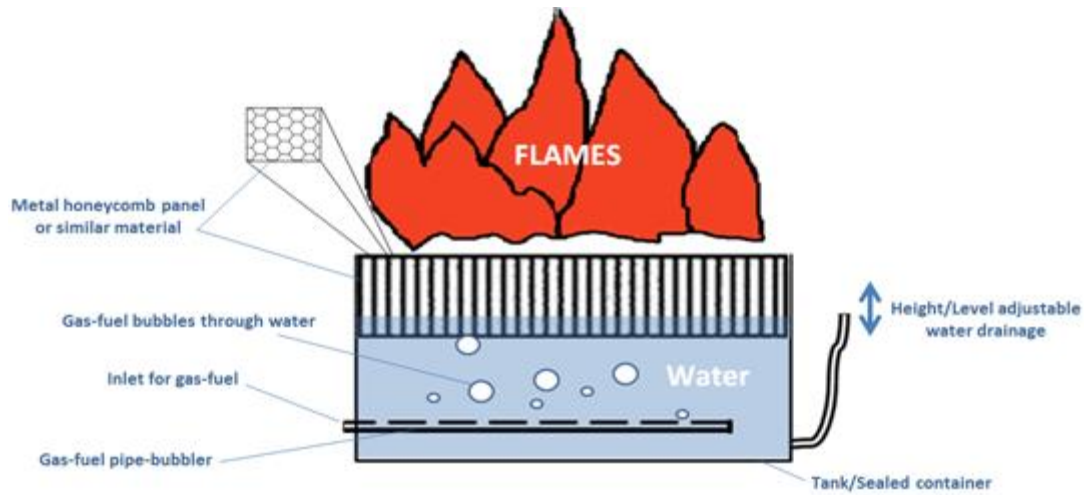


Figure 1. The "Honeycomb" fire simulator

Figure (1) illustrates the parts and construction of the honeycomb fire simulator. The largest part of the simulator is a leak-proof tank or container. The top side of the tank is open while the cross section of the tank may be any shape: circular, oval, rectangular, etc. The tank is partially filled with water, and a height adjustable drainage pipe is used to control the water level. Propane gas enters the simulator at the bottom of the tank through a dedicated pipe which is perforated to allow the gas to bubble up through the water. A metal honeycomb panel is installed at the top of the tank, completely covering the open side of the tank. The honeycomb panel is 5 cm (2-inch) thick, entirely comprised of vertical hexagonal 6 mm (1/4-inch) openings. The honeycomb grid is partially submersed in the water. As the propane bubbles up, it gets divided through the honeycomb panel into many smaller bubbles. Once the simulator is lit, the flames flicker vertically through and above the honeycomb grid. When using the air-pressurized water extinguisher with the honeycomb simulator, flames are extinguished by the combined actions of cooling the fire and blowing the flames off the top of the honeycomb panel. This creates a flame front that behaves like flames in an actual liquid fuel fire. As a result, the trainee has to direct the extinguishing stream at the flame front and use sweeping motions to chase the flames off their bases and extinguish it. The difficulty in extinguishing the flames can be controlled by adjusting the level of the water; as the level of water rises inside each of the honeycomb tubes, the base of the flames rise with it and become easier to blow off. A low water level will leave more space for flames to hide inside the honeycomb tubes and become harder to extinguish. For safety, the simulator is equipped with a dead man switch that is held by the trainer; it will close a solenoid valve that will block the flow of fuel to the simulator and, also, to reduce the burden of dealing with electrical hazard controls, an operating voltage of less than 50 volts maybe used; a 12 volt was used in the present study.

A video was produced to be used for theoretical training prior to having trainees practicing/experimenting with the new hands-on apparatus. The audience of the video was defined as the general public. The main objective of the video was to provide scientific and easy to

follow study material for employees and students. No specific educational rubric was found for extinguisher training, and, therefore, the contents of the video were set based on experience as described in Table (1).

Table 1. Detailed description for video's segments

#	Title	Content	Durati on (min)
1	Fire fundamentals	Brief outline of the whole movie. Fire triangle. Stages and spread of fire and smoke. Effects of fire on human.	6.5
2	Overall fire protection strategy	Fire prevention: Recognition and control of ignition sources. Proper storage and handling of combustibles. Automatic sprinkler systems. Role of potable fire extinguishers as a part of the overall protection strategy. Emergency and evacuation planning and exercises.	7.5
3	Fire extinguishers use	Types of fire and extinguisher classifications. Extinguishing agents and its suitability for use. Extinguisher components and structure Method of operation (PASS) Safe and effective fighting distances	11.5
4	Fight or evacuate decision	5-point list to help make the decision of fighting a fire or evacuating: warning others, small fire, availability of proper extinguisher, confident user, having an escape route if failing to extinguish the fire.	2
5	Introduction to the hands-on training	Description of the training apparatus, how to carry and operate a training fire extinguisher, what to do when fire goes out, and how to back up if fire is not extinguished.	2

As mentioned earlier, the objective of the present research effort is to evaluate the newly developed fire extinguisher training program; theoretical (video) and hands-on (training apparatus).

## 2. Methodology

The methodology depended on the subjective assessment of two groups of evaluators: expert trainers and novice firefighting students. Both groups watched the video, and practiced putting out fires using the newly developed apparatus, prior to providing their assessments. The assessment had two components: a structured feedback using a specially constructed questionnaire and a semi-structured feedback where participants wrote in designated blocks titled "likes", "dislikes", and "other comments".

### 2.1. Participants

The present study was carried out at civil defense training center. Thirteen expert trainers and fourteen firefighting students participated in this study; all were males. Students were in their first year of study to become firefighters or paramedics. Students' ages ranged from 20 to 23, with an average of 20.6 years. Although, they were chosen because they had not received fire extinguishers training yet, they reported having ample knowledge, but lesser experience. None of the novice participants had used the fire extinguisher to put out a fire in a real emergency situation. Also, none of the novice participants had trained anyone on the use of fire extinguishers.

All experts were firefighting trainers at the training center, and their years of experience ranged from 7 to 15

with an average of 10.6 years. Experts' age ranged from 29 to 35 with an average of 31.7 years. Eleven of the trainers reported they had trained more than 100 people on fire extinguishers, and the other two trained 50 to 100. Also, eleven out of the thirteen experts had used extinguishers in real emergency situation. All experts reported they were knowledgeable and had a practical experience with fire extinguishers. Table (2) shows the questions, and frequencies and averages of the participants' responses related to experience and knowledge.

### 2.2. Training Video Evaluation

The video was divided into five segments for evaluation, as shown in Table (1). All segments were evaluated the same way. After watching each of the segments, participants were asked to answer five questions on a five-point agreement scale, and to provide their semi-structured feedback by writing likes, dislikes, and other comments. The five questions are listed in the first column of Table (3). Researchers explained that although all were gathered in one room, that the study is interested in the opinion of each individual; therefore, participants were asked not to discuss their thoughts and opinions about the study, and only write them on the study form.

### 2.3. Apparatus Evaluation

After using the training extinguisher to put out the simulator fire, participants were asked to answer seven questions on a five-point agreement scale, and to provide their semi-structured feedback by writing likes, dislikes, and other comments. The seven questions are listed in the first column of Table (4).

**Table 2.** frequencies and averages of the participants' responses related to experience and knowledge

	Expert / Novice	Strongly Disagree	Disagree	Neither Agree nor Disagree	Agree	Strongly Agree	Average
I have comprehensive theoretical knowledge about how fire extinguishers work	E				7	6	<b>4.46</b>
	N		1	3	10		<b>3.64</b>
I have comprehensive practical experience about how fire extinguishers work	E				6	7	<b>4.54</b>
	N	1	1	2	7	3	<b>3.71</b>
Fire extinguishers theoretical training is important for employees and students	E				1	12	<b>4.92</b>
	N				7	7	<b>4.50</b>
Fire extinguishers hands-on training is important for employees and students	E					13	<b>5.00</b>
	N				7	7	<b>4.50</b>

Bold average numbers indicate statistically significant difference between Experts and Novice with  $P < 0.05$ .

2.4. Equipment and Study Protocol

A third generation prototype of the Honeycomb fire simulator and ten training extinguishers were used in the study (see Figure 2). First, all participants were gathered in one of the classrooms at the training center. Before starting to watch the training video, the objectives and procedure for the study were explained. After each of the five segments of the movie, the showing stopped and the participants were given enough time to complete the associated part of the study form.



Figure 2. Third generation prototype of the Honeycomb fire simulator, and training extinguishers

The segmental evaluation was followed by two questions. In the first one, participants were asked to rate the suitability of the whole movie for training employees and students. Secondly, to indicate what the youngest school grade was that would benefit from the training video.

Next, all participants moved to an outside open court where the fire simulator and training extinguishers were set. One by one, all participants practiced putting out the simulator fire. Each participant completed the study form directly after his practice.

2.5. Analyses

Basic descriptive statistics were calculated by using Minitab software for each of the questionnaire items, while analysis of variance and pairwise comparisons were used to investigate differences between experts and students. Correlation analyses were done between all items on the questionnaire. The participants' comments, criticisms and suggestions were also reviewed, categorized, and summarized.

3. Results

Frequencies and averages of responses to questionnaire items for all segments of the training video are shown in Table (3). Statistically significant differences between experts' and novices' responses are indicated by bold average numbers for  $P < 0.05$ , and by italic average numbers for  $P < 0.10$ . Overall assessment of the video was highly positive among both experts and novices. Frequencies and averages of participants' overall ratings are shown in Table (5).

Table 4. Frequencies and averages of responses to questionnaire items for evaluating the training apparatus

	Expert / Novice	Strongly Disagree	Disagree	Neither Agree nor Disagree	Agree	Strongly Agree	Average
Method to operate training extinguisher is the same as for real ones.	E		2	2	6	2	3.67
	N	1		2	9	2	4.00
Training fire reacts to extinguishment in the same way like in real situation.	E		4	2	6	1	3.31
	N	1	1	3	7	1	3.38
Using this hands on training method will develop the trainees' skills essential to put out a fire in a real emergency	E			3	7	3	4.00
	N		1	2	5	5	4.08
Using this hands on training method may lead to trainees having wrong impressions about fire and extinguishment.	E	2	4	4	3		2.62
	N	4	6	2		1	2.08
Using this hands on training method does not provide any additional benefits over classroom training.	E	4	4	3	2		2.23
	N	4	4	2	3		2.31
Hands on training cancel the need for classroom training.	E	7	4	2			1.62
	N	6	3	2	1		1.69
In general, the traditional method of burning a mixture of gasoline and diesel in a fire pan, and using real extinguishers is better than the method used for this study.	E	2	4	4	2	1	2.69
	N	3	4	4	1	1	2.46

Bold average numbers indicate statistically significant difference between Experts and Novice with  $P < 0.05$ .

Table 5. Frequencies and averages of the overall ratings for the training video

	Expert / Novice	Strongly Disagree	Disagree	Neither Agree nor Disagree	Agree	Strongly Agree	Average
Overall the movie is suitable for training employees and students.	E			2	6	5	4.23
	N				10	4	4.28

Twenty-five participants either strongly agreed or agreed that the video was suitable for training employees and school students, and only two experts neither agreed nor disagreed. Consistently, the ratings of the video by novices were more positive than those of experts. Significant differences at  $P < 0.05$  were found for the video segments number 4 and 5.

In reference to segment-4, fight or evacuate decision, the ratings for containing comprehensive information were significantly different between experts (average rating 3), and novices (average rating 4.5). Review of comments indicated that some experts were against including the "fight or evacuate decision"; they stated that it was the responsibility of firefighters to fight.

Segment-5 was relatively short (2 minutes) and introduced the hands-on training part; however, differences in ratings between experts and novices were significant; three out of the five questionnaire items were significantly different at  $P < 0.05$ , and two were significant at  $P < 0.10$ .

Segment-3 was the longest at 11.5 minutes (39% of the total time), and it explained the types of fire extinguishers and how to use it safely and effectively. Ratings of this segment were mainly positive and there were no significant differences between experts and novices. However, and in regards to that, segment-3 contained comprehensive information, the average ratings for novice and expert were 4.60, and 3.38, respectively.

Although the difference was not statically significant, it is large. Review of study forms revealed that experts who gave low rating for this item wrote comments about not including information on the "need to stand up wind from the fire", "use of personal protective equipment PPE", and the "need to shake the extinguisher before use".

Segment-2 was the second longest at 7.5 minutes (25.4% of total time), and it contained vast information on the general strategy for fire protection. Nevertheless, it was rated the least for containing comprehensive information. Also, the average rating for "containing important information" was 4.07 for novices and 4.00 for experts. There were no significant differences between experts and novices in the ratings for this segment.

Segment-1 was 6.5 minutes (22.0% of total time) and it contained fundamentals of fire. Overall, the ratings for this segment were positive. It had the highest scores for "containing important information", and for having "clear and acceptable presentation".

There was a significant difference at  $P < 0.10$ , between experts and novices in regards to "suitability of the segment for training employees and school students"; novices had higher ratings (4.36) than experts (3.85).

In response to the question of what was the youngest school grade that can benefit from the training video, novice participants reported younger school grade than of that reported by the experts ( $P = 0.08$ ). Novices' answers ranged from 3<sup>rd</sup> to 10<sup>th</sup> grade with an average of 5.75, and experts' answers ranged from 4<sup>th</sup> to 11<sup>th</sup> with an average of 7.8.

Frequencies and averages of responses to questionnaire items for evaluating the training apparatus are shown in Table (4). Novices' ratings of the apparatus were more positive than the ratings of experts; however, differences were not significant statistically. There was an overall agreement in regards to the following statements: "Method to operate training extinguisher is the same as for real ones", "Training fire reacts to extinguishment in the same way like in real situation", and "using this hands-on training method will develop the trainees' skills essential to put out a fire in a real emergency".

Also, there was an overall disagreement to the following statements: "Using this hands-on training method may lead to trainees having wrong impressions about fire and extinguishment", "using this hands-on training method does not provide any additional benefits over classroom training", and "Hands-on training cancels the need for classroom training".

Concerning the comparison between hands-on training using this apparatus and using the traditional method, ratings spread overall the five-point scale. The averages favored the new method. A closer look at the frequency of responses indicated that six experts favored the new method, three did not, and four were hung between the two methods. Also, novice participants had similar assessment.

Significant correlations were only found when combining the data of both experts and novices. Table (6) shows the person correlation factor and corresponding error probability value ( $P$ ) for questionnaire items that had at least one statistically significant correlation.

There was a positive strong correlation ( $r = 0.864$ ,  $P = 0.035$ ) between ratings for "having comprehensive knowledge about fire extinguishers", and ratings for "theoretical training is important". Also, there was a significant correlation ( $r = 0.497$ ,  $P = 0.008$ ) between the ratings for "having comprehensive knowledge about fire extinguishers", and ratings for "having hands-on experience". This can be understood as those who had hands-on experience with fire extinguishers also had good knowledge about how it works, indicating that theoretical training is important, and favored the new apparatus.

Similarly, those who preferred the new training apparatus to the traditional method, liked the training extinguisher, thought that simulated flames reacted as real fire, and that is good for developing necessary skills.

**Table 6.** Correlations of questionnaire items that had at least one statistically significant correlation

	Experience	Knowledge of theory	Theory importance	Hands-on importance	Traditional better	Developing skill	Fire real behavior
Knowledge of theory	<b>0.497</b> <b>0.008</b>						
Theory importance	0.708 0.075	<b>0.864</b> <b>0.035</b>					
Hands-on importance	<b>0.511</b> <b>0.006</b>	0.276 0.164	0.171 0.393				
Traditional better	-0.128 0.562	-0.355 0.097	<b>-0.440</b> <b>0.036</b>	0.139 0.526			
Developing skill	0.195 0.373	-0.077 0.728	-0.176 0.423	0.145 0.508	0.335 0.127		
Fire real behavior	0.158 0.460	-0.350 0.093	0.000 1.000	0.260 0.219	<b>-0.682</b> <b>0.000</b>	<b>0.430</b> <b>0.040</b>	
Operation of training extinguisher	0.251 0.236	0.022 0.919	0.219 0.304	0.204 0.339	0.198 0.365	0.354 0.097	<b>0.622</b> <b>0.00</b>

\* Cell Contents: Pearson correlation

P-Value

\*\* Bold numbers indicate statistically significant difference between Experts and Novices with  $P < 0.05$ .

Participants wrote many comments; the most frequent one was that water is not suitable extinguishing agent for propane. They also indicated the video was missing instructions in regards to standing upwind when fighting a fire, and to shake the extinguisher prior to use. Others wrote that they favored the fire pan since it was closest to a real fire scenario, commenting that the actual smoke and fire make it superior to any simulated fire. Two, suggested adding smoke to the fire simulator as an improvement. Many comments praised animations in the movie, and that it contained segments of all types of fire extinguishers being properly used. Also, few wrote positive comments about including a segment of females using fire extinguishers. There was a comment praising the movie for including male and female, as well as young and old people.

After completing the study, there were casual discussions with participants and administrators at the academy. Several comments were noted, mainly concerning the design of the fire simulator, and the suitability of water for extinguishing gas fires.

#### 4. Discussion

The ultimate goal of fire extinguisher training is to enable trainees to react in a manner that would reduce the overall risk of loss of life, injury, and/or property damages in real emergency situations. Therefore, evaluating the effectiveness of any fire extinguisher training program is limited, because it is not practical to create repeatable real emergency situations for testing. In the present study, measuring the effectiveness of the new program was done

through subjective assessments of the study participants. Their feedback was in reference to what they knew and/or believed in. No participant mentioned any other movie, nor indicated that they knew of other types of fire simulators. On the contrary, there were comments that explicitly mentioned the lack of training movies in Arabic, and that the fire pan was the method they always used. Basically, participants compared the video training to expert-instructions in a classroom setup, and compared the new apparatus to the fire pan. Also, trainers in the present study were not directly responsible for the cost of training; therefore cost was not a concern for them. In contrast, participant's comments indicated they were concerned about the impact of training on the environment. They reported that powder and foam make a substantial mess, and sometimes the use of powder extinguishers was problematic for trainees with pulmonary issues.

Almost for all questionnaire items, responses spanned over all the agreement scale. Responses indicated clear trends; however, variability was high. Causes for such variability include a negative disposition of some participants, caused by their strong belief that water is not suitable to put out gas fires in real situations. Although it was explained to participants that the fire simulator is designed in a specific way to produce flames that can be extinguished by the training extinguisher, some were doubtful about and not completely convinced in it. Another reason that may explain the high variability relates to the culture and norms within General directorate of Civil Defense in Jordan. Basically, Civil Defense in Jordan is a military organization and they pride themselves in their selfless and tireless efforts especially in dealing

with hazardous events and accidents. Quitting or backing up from danger is not an option for them. This was clear in the ratings of the video segment concerning the fight or evacuation decision. Many experts indicate that fleeing was not an option for them or for their trainees. Although such attitude is prideful, it indicates a distortion in the perception of the study objectives. The target of the study program was the general public and not professional firefighters.

Segment-2 presented the overall strategy for fire protection, and the role of fire extinguishers in it. It received a very good score for "importance to include", but much lesser score for "including comprehensive information". Actually, the intention was to include minimum information about fire prevention, automatic sprinkler systems, and emergency planning, and explain the role of portable fire extinguishers. It is not possible to include comprehensive information in a short video, but at the same time the intention was to explain that protecting against the hazards of fire requires a systematic approach.

There were differences between experts and novices in regards to the importance of the different video segments. For example, there were significant differences in the ratings of the fifth video segment; novices appreciated it more than experts. It was short and contained an introduction to the hands-on training: How the fire extinguisher should be carried, and instructions for safe backup if fire did not go out. Also, there were significant differences concerning the importance and completeness of the fourth segment. These differences highlight the need to consider how students learn, and maybe more than what the teachers think is important. Failing to address the needs of students would result in ineffective teaching.

Participants' comments indicated that the video did not include instructions to stand upwind when fighting a fire and it is true. Such instructions were discussed at the beginning of the hands-on training. However, the video might be used without the hands-on training segments, and then these instructions are lacking from the video. Ultimately, this will be fixed in future versions of the video. For the short-term, written instructions can be combined with the video to resolve this issue.

Participants also commented that instructions should include shaking the extinguisher before use; however, this is not within standard procedure. On the one hand, shaking a dry chemical fire extinguisher may help prevent the powder inside from settling or packing, but shaking is not always recommended by manufactures. On the other hand, lifting, turning upside down, and shaking the extinguisher require a significant strength and effort. Weaker people, such as the elderly and women, may shy away from attempting to use the extinguisher if the required effort is excessive for them. In general, firefighters have more strength than the average person and are experienced in the extinguisher-operating methods; hence, shaking the extinguisher for them maybe beneficial and would not cause harm. An NFPA standard does not include any requirements for shaking the extinguisher before use, and it is rarely recommended by extinguisher manufactures. Therefore, if shaking the extinguisher is recommended by the manufacturer, it should be done during monthly inspection and not before use.

Few participants from both groups raised the issue that the hands-on training was being carried out without (PPE). This also indicates that some participants had a distorted perception about the study objectives. While it is a requirement for firefighters to wear PPEs, it is not practical to impose the same requirement on the general public, employees and students. This distortion in the perception of few participants may make them undervalue the new apparatus.

The suitability for training of each of the video segments received a high score from novices (4.29 to 4.66), and positive scores from experts (3.46 to 3.92). Also, twenty-five out of the twenty-seven participants agreed or strongly agreed that the video was suitable for training employees and students. These scores indicate somewhat strong endorsement from both experts and novices.

Videos have been effectively used in trainings covering topics ranging from instructions for surgical procedures to vocational training [1, 8, 12]. Videos allow trainees to view the study material according to their own schedule and for as many times as they may need. For some topics, the use of animations and illustrations make videos superior to other methods of presentations. For example, the training video subject of the present study included clips of water, foam, powder, and CO<sub>2</sub> extinguishers being used. Some clips were shown from two different camera angles, and one was shown at slow speed allowing trainees to see comprehensive and detailed views. Creating the same effect through expert-instructions in a classroom setup might be impossible, or, at best, very time consuming and expensive. Therefore, the video is an effective and efficient presentation method to train the general public on the principles of fire extinguishers.

The need for training, in both theory and practice, was clear; experts indicated that a theoretical training was important with a score of 4.92, and hands-on training was important with a perfect score of 5. Also, after they practiced with the new apparatus, experts disagreed that hands-on training would eliminate the need for theoretical training. Novices' indications were similar to those of the experts'.

As mentioned earlier, there were few participants who had a strong disposition to undervalue the new apparatus because of their strong belief that water should not be used to extinguish gas fires. These participants voiced their doubts few times, which most likely affected the scores of other participants. Four to eight of the participants adopted the midpoint of the scale neither agreed nor disagreed on every issue. One way for reading rating scores is to exclude those neither agreed nor disagreed to determine trends. For example, there were 19 participants who agreed or strongly agreed that the operation of the training extinguisher was the same as regular ones; only 3 disagreed. Similarly, 15 agreed to 6 disagreed that training fire reacted to extinguishment in the same way like in real situation, and 20 agreed and one disagreed that using this hands-on training method will develop trainees' skills essential to put out a fire in a real emergency. Overall, the new apparatus received good ratings and it was favored over the traditional method by a ratio of 13 to 5. Given the obvious benefits in regards to low cost and low

environmental impact of the new apparatus, use of such should be encouraged.

**5. Conclusions**

Expert and novice firefighters indicated that both theoretical and hands-on fire extinguisher training are important. They also indicated that hands-on training does not cancel the need for theoretical training.

The training video, the subject of the present research study, includes important, comprehensive, and well-presented information on the fundamentals of fire extinguisher use. Expert and novice firefighters indicated its suitability in its current version for the training of employees and school students.

The combination of propane fire simulator and the training air-pressurized water extinguisher provides acceptable means for hands-on training; it has a relatively low cost, and has no, or very low, impact on the environment. The training apparatus, the subject of the present study, provides an effective means for hands-on training, as indicated by expert and novice firefighters.

**Limitations and Future Studies**

Findings and conclusions of the present study are important for establishing effective fire extinguisher programs. The study is important specifically for Jordan. The involvement and endorsement of civil defense in Jordan is essential for the people of Jordan as they consider it as the technical and ethical authority on fire protection. However, the present study was limited because it did not include the targeted audience: employees and students. Also, it was not possible to increase the number of participants because it included all expert trainers and students at the college of the Jordanian Civil Defense.

There were no established and verified standards for fire extinguisher training; thus, the standard achievement test is also lacking. In order to carry out future studies, that involve students and employees, an educational rubric must be established.

**Table 3.** Frequencies and averages of responses to questionnaire items for all segments of the training video

	Expert / Novice	Video Segment 1 Characteristics of fire					Video Segment 2 Comprehensive strategy for fire protection.					Video Segment 3 Portable fire extinguishers					Video Segment 4 Fight or flight					Video Segment 5 Introduction to hands on training						
		Strongly Disagree	Disagree	Neither Agree nor Disagree	Agree	Strongly Agree	Average	Strongly Disagree	Disagree	Neither Agree nor Disagree	Agree	Strongly Agree	Average	Strongly Disagree	Disagree	Neither Agree nor Disagree	Agree	Strongly Agree	Average	Strongly Disagree	Disagree	Neither Agree nor Disagree	Agree	Strongly Agree	Average			
Containing important information	E			1	6	6	4.38	1	2	8	3	4.00	1	1	7	4	4.08	1	3	7	2	3.77	3	4	5	1	<b>3.31</b>	
	N				5	9	4.64		2	9	3	4.07		1	6	7	4.43		1	10	3	4.14		1	9	4	<b>4.21</b>	
Presentation is clear and acceptable	E				5	8	4.62	1	3	7	2	3.77	1	1	8	3	4.00	1	5	6	1	3.54	4	3	5	1	<b>3.23</b>	
	N				9	5	4.36	2	1	8	3	3.86	1		8	5	4.21	1	2	8	3	3.86		3	9	2	<b>3.93</b>	
Containing comprehensive information	E		1	4	6	2	3.69	4	5	3	1	3.08	3	4	4	2	3.38	5	3	5		<b>3.00</b>	5	6	2	<b>2.77</b>		
	N		1	4	6	3	3.79	2	6	5	1	3.36	1	2	7	2	4.60		4	7	1	<b>4.50</b>		3	7	3	<b>4.33</b>	
Containing unnecessary information that can be taken out to reduce the video time	E	3	6	2	1		2.08	2	7	3	1	2.23	2	7	3	1	2.23	1	5	5	2		2.62	1	3	6	3	3.08
	N	3	2	6	1	1	2.50	3	7	1		2.50	3	7	2		2.30	2	8	3		2.45	3	5	3	2	2.50	
In general the video is suitable for training employees and student	E	1		2	7	3	3.85	2	1	9	1	3.69	2	2	4	5	3.92	1	5	4	3	3.69	4	3	2	4	3.46	
	N			1	7	6	4.36		3	4	7	4.29		1	6	7	4.43		2	5	6	4.66	1	1	5	7	4.29	

Bold average numbers indicate statistically significant difference between Experts and Novice with P<0.05.  
 Italic average numbers indicate statistically significant difference between Experts and Novice with P<0.10

## References

- [1] Anna Maria Giannini, Fabio Ferlazzo, Roberto Sgalla, Pierluigi Cordellieri, Francesca Baralla, Silvia Pepe. (2013) the use of videos in road safety training: Cognitive and emotional effects. *Accident Analysis & Prevention* 52.
- [2] Blackburn *et al.*, Flameless fire extinguisher training methods and apparatus, United States Patent 7748983, July 6, 2010.
- [3] BullexITS User Reference Guide, 2012. (Provided by the manufacturer with Bullex Intelligent System fir simulators).
- [4] Darois *et al.*, Training device for extinguishing fires, method and system of use thereof, United States Patent 7175439, February 13, 2007.
- [5] Deshoux *et al.*, Teaching installation for learning and practicing the use of fire-fighting equipment, United States Patent 6129552, 2000.
- [6] Hoglund, R.W., Firefighter's training simulator, United States Patent Application 233289, October 20, 2005.
- [7] Hughes Associates, Inc., Measuring the Impact of Fire Extinguisher Agents on Cultural Resource Materials. Report prepared for the National Fire Protection Association - Fire Protection Research Foundation. Hughes Associates, Baltimore, MD, 2010.
- [8] Isiaka, B. (2007, October 30). Effectiveness of video as an instructional medium in teaching rural children agricultural and environmental sciences. *International Journal of Education and Development using ICT* [Online], 3(3) Available: <http://ijedict.dec.uwi.edu/viewarticle.php?id=363>.
- [9] Joynt *et al.*, Portable firefighter training system for fire extinguishing training, United States Patent 5447437, September 5, 1995.
- [10] Moore, W.T., Electronically simulated flame, United States Patent 6688752, February 10, 2004.
- [11] National Fire Protection Association (NFPA), Standard for Portable Fire Extinguishers, NFPA 10, 2007 Edition, Quincy, MA, 2007.
- [12] Nousiainen, Markku *et al.* "Comparison of expert instruction and computer-based video training in teaching fundamental surgical skills to medical students." *Surgery* 143.4 (2008): 539-544.
- [13] Occupational Safety and Health Administration. "Fire Protection, 1910.157, Portable Fire Extinguishers", U.S. Department of Labor, OSHA Web. 18 Nov. 2013.
- [14] Oviedo-Trespalacios, O., R. Manjarres, and R. PeñabaenaNiebles. "The Learning Curve Applied to Fire Extinguisher Training: A Comparison Among Different Type of Fires." 22nd International Conference on Production Research (ICPR 22) 2013.
- [15] Poole, B. Ordinary People and Effective Operation of Fire Extinguishers. Unpublished dissertation, Eastern Kentucky University, 2012.
- [16] Williamson *et al.*, Dispersion burner for firefighter training, United States Patent 7744373, June 29, 2010

# Nonlinear Natural Frequencies and Frequency Veering of a Beam with an Arbitrary Initial Rise Supported by Flexible Ends and Resting on Elastic Foundation

Mutasim S. Abdeljaber

*Department of Civil Engineering, The University of Jordan, Amman 11942, Jordan,*

*Received Feb 26,2017*

*Accepted May 5,2017*

## Abstract

The present study reports results for the effect of support flexibility on nonlinear natural frequencies and frequency veering phenomenon of an elastic Euler-Bernoulli beam resting on Winkler elastic foundation with an initial arbitrary rise. Also, it extends the analysis presented for the linear vibration analysis [1], to account for the effects of beam's ends flexibility and rise shape on; veering zones, and nonlinear natural frequencies.

The beam is supported by translational and rotational springs at each end. The effect of the induced force due to mid-plane stretching is accounted for due to its importance and significance on the nonlinear dynamic and vibrational behavior of the beam, as it was proved and presented in earlier investigations and studies.

The governing integro-partial differential equation is discretized using the assumed mode method "Galerkin's single mode approach" and the resulting nonlinear temporal equation was solved using the harmonic balance method to obtain results for the nonlinear natural frequencies. The results are presented for the nonlinear natural frequencies of the first three modes of vibration, for a selected range of physical parameters, like rotational and translational springs at both ends of the beam, elastic foundation stiffness and initial rise shape and level

© 2017 Jordan Journal of Mechanical and Industrial Engineering. All rights reserved

**Keywords:** *Non-Linear Frequency Veering, Rise Shape, Elastic Foundation, Flexible Supports.*

## 1. Introduction

Many civil structures, bridges, space structures and space frames can be modeled as beam like structures. In many cases and due to errors and defects in manufacturing, such beams may take the shape of a shallow arc which can be modeled as a beam with a half sine shape rise. Also, deformed pipe lines or pipes with geometrical imperfections can be modeled as a beam with a half sine / full sine rise resting on elastic foundation. Practically and in order to simulate the flexibility present in joints and fixing plates at the ends of the beam, the end supports of a given beam like structure are represented by translational and rotational springs.

The significance of the considered model lies in the varieties of engineering applications that it can model, such as soil-structure interaction problems, buried pipes, civil engineering structures and shafts in machinery, as well as the importance of studying and predicting the dynamic behavior of such systems needed for design, analysis, operation and evaluation. The model of an imperfect elastic beam element resting on elastic foundation, which can exhibit frequency curve veering, is used to study the dynamic behavior of a wide range of engineering systems found in, for example, foundation and structural engineering, fluid-structural interaction

problems, micro-switches, and sensing devices in Micro-Electro-Mechanical Systems (MEMS).

The free and forced responses of such beam models, and other structures having similar frequency veering behavior, with various boundary conditions, vertical and axial loading conditions, types of elastic foundations, initial imperfections, and different assumptions about the effect of mid-plane stretching, have been the subject of numerous theoretical, numerical and experimental studies over the years, [2-9]. A review of the relevant literature related to beams with initial rise/imperfection can be found in [7-9].

The present work extends a previous study [1], which investigated the effect of supports flexibility on frequency veering in imperfect beams resting on elastic foundation based on linear analysis only. The extension includes the derivation of the mathematical model to account for the mid-plane stretching from which the nonlinearities are introduced to the governing integro-partial differential equation of motion. Also, the extension includes a thorough study of the effect of the beam flexible ends and the initial rise shape/level on the nonlinear natural frequencies and frequency veering phenomenon.

The derivation of the mathematical model is similar to that followed in [7-9], but the nonlinear analysis for the natural frequencies and the initial rise shape are introduced in the present paper.

\* Corresponding author e-mail: m.abdeljaber@ju.edu.jo.

**2. System Description and Problem Formulation**

A schematic of the two beam systems under consideration, initial 1/2 -sine rise and full sine rise, are shown in Figure (1). The beam is assumed to be uniform with length  $l$  and cross sectional area  $A$ . It has mass per unit length  $m$ , flexural rigidity  $EI$ , resting on a linear Winkler type elastic foundation of stiffness  $K_f$ . It is assumed that the beam is supported by two translational springs at the right and left ends ( $K_{TR}$  and  $K_{TL}$ ) and two rotational springs at the right and left ends ( $K_{RR}$ ,  $K_{RL}$ ), respectively. The beam's initial rise shape "initial imperfection", regardless its form, is assumed to extended over the beam span. The moderately large vibrations  $\hat{w}$  of the beam about the imperfect rest configuration  $\hat{w}_0$ , are governed in dimensional form, by the following non-linear integro-partial partial differential equation [1, 7-9]:

$$m \frac{\partial^2 \hat{w}}{\partial t^2} + EI \frac{\partial^4 \hat{w}}{\partial x^4} - \frac{EA}{l} \left[ \int_0^l \left( \frac{1}{2} \left( \frac{\partial \hat{w}}{\partial x} \right)^2 + \frac{\partial \hat{w}}{\partial x} \frac{\partial \hat{w}_0}{\partial x} \right) dx \right] \left( \frac{\partial^2 \hat{w}}{\partial x^2} + \frac{\partial^2 \hat{w}_0}{\partial x^2} \right) + K_f \hat{w} = 0 \tag{2.1}$$

Introducing the following non-dimensional parameters:  $w = \hat{w}/r$ ,  $\xi = \hat{x}/l$ ,  $w_0 = \hat{w}_0/r$  and  $t = \hat{t} \sqrt{\frac{EI}{ml^4}}$ , where  $r$  is the beam's radius of gyration  $r = \sqrt{I/A}$ , equation (2.1) can be re-written in the following form:

$$\frac{\partial^2 w}{\partial t^2} + \frac{\partial^4 w}{\partial \xi^4} - \left[ \int_0^l \left( \frac{1}{2} \left( \frac{\partial w}{\partial \xi} \right)^2 + \frac{\partial w}{\partial \xi} \frac{\partial w_0}{\partial \xi} \right) d\xi \right] \left( \frac{\partial^2 w}{\partial \xi^2} + \frac{\partial^2 w_0}{\partial \xi^2} \right) + K_f^* w = 0 \tag{2.2}$$

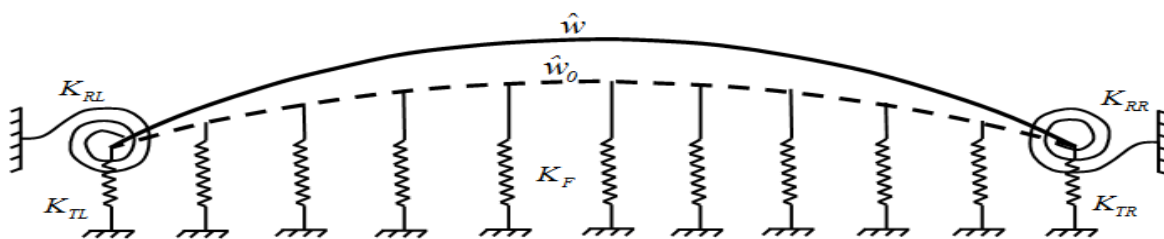
where  $K_f^* = K_f l^4 / EI$ . The boundary conditions in non-dimensional form for the considered beam with initial rise for instance, are:

$$\begin{aligned} w'' + K_{TL}^* w &= 0 \text{ at } \xi = 0, \text{ translational spring at the left end} \\ w'' - K_{RL}^* w' &= 0 \text{ at } \xi = 0, \text{ rotational spring at the left end} \\ w'' - K_{TR}^* w &= 0 \text{ at } \xi = 1, \text{ translational spring at the right end} \\ w'' + K_{RR}^* w' &= 0 \text{ at } \xi = 1, \text{ rotational spring at the right end} \end{aligned} \tag{2.3}$$

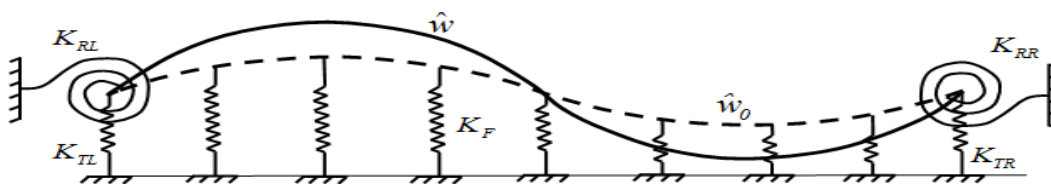
where  $K_{TL}^* = K_{TL} l^3 / EI$ ,  $K_{TR}^* = K_{TR} l^3 / EI$ ,  $K_{RR}^* = K_{RR} l / EI$  and  $K_{RL}^* = K_{RL} l / EI$ . The initial rise or imperfection is assumed to take the form:

$$w_0 = R \sin(n\pi\xi) \tag{2.4}$$

where  $R$  is a non-dimensional rise amplitude equals to the actual rise  $\hat{R}$  divided by the radius of gyration, *i.e.*  $R = \hat{R}/r$ ,  $n$  is the number of half -waves in the sinusoid. For a beam with a 1/2 -sine initial  $n = 1$  and  $n = 2$  for a beam with full sine rise.



(a) Beam with half sine rise/imperfection over the beam span



(b) Beam with full sine rise/imperfection

**Figure 1.** The schematic of beam resting on Winkler foundation with 1/2 and full sine rise

### 3. Analysis and Solutions

#### 3.1. Non-Linear Temporal Model

The nonlinear integro-partial differential equation (2.2) can be discretized by assuming:

$$w = \sum_{i=1,2}^{\infty} \phi_i(\xi) q_i(t) \tag{3.1}$$

where  $\phi_i(\xi)$  is the normalized, self-similar (i.e., independent of the motion amplitude) assumed mode shape of the beam and  $q_i(t)$  is the generalized coordinates and it is the unknown time modulation of the assumed deflection mode  $\phi_i(\xi)$ . In the present work, Galerkin's method is used, whereby  $\phi_i(\xi)$  is the eigenfunction of the  $i$ -th mode of the beam.

Using a simplified single mode approach, i.e.,  $w = \phi(\xi) q(t)$  and substituting  $w_0$  from equation (2.4) into equation (2.2), multiplying by  $\phi(\xi)$  integrating from 0 to 1, and for convenience using the abbreviations  $\phi(\xi) = \phi$ ,  $q(t) = q$  one obtains the following reduced single-mode nonlinear temporal equation:

$$\int_0^1 \phi \phi'''' q d\xi + \int_0^1 \phi^2 \ddot{q} d\xi - \left\{ \int_0^1 \phi \left[ \int_0^1 \frac{1}{2} \phi'^2 q^2 d\xi \right] (\phi'' q) d\xi \right\} - \left\{ \int_0^1 \phi \left[ \int_{\xi_a}^{\xi_b} \phi' q \frac{dw_0}{d\xi} d\xi \right] \left( \frac{d^2 w_0}{d\xi^2} \right) d\xi \right\} + K_f \int_0^1 \phi^2 q d\xi = 0 \tag{3.2}$$

Equation (3.2) can be re-arranged and written in the form:

$$\beta_0 \ddot{q} + \beta_1 q + \beta_2 q^2 + \beta_3 q^3 = 0 \tag{3.3}$$

Where

$$\beta_0 = \int_0^1 \phi^2 d\xi$$

$$\beta_1 = \int_0^1 \phi \phi'''' d\xi -$$

$$\int_0^1 \left\{ \left[ \int_{\xi_a}^{\xi_b} \phi \frac{dw_0}{d\xi} d\xi \right] \phi \frac{d^2 w_0}{d\xi^2} \right\} d\xi + K_f \int_0^1 \phi^2 d\xi$$

$$\beta_2 = - \int_0^1 \left( \int_0^1 \left( \frac{1}{2} \phi'^2 \right) d\xi \right) \phi \frac{d^2 w_0}{d\xi^2} d\xi$$

$$- \int_0^1 \left( \int_0^1 \phi' \frac{dw_0}{d\xi} d\xi \right) \phi \phi'' d\xi$$

$$\beta_3 = - \int_0^1 \left( \int_0^1 \left( \frac{1}{2} \phi'^2 \right) d\xi \right) \phi \phi'' d\xi \tag{3.4}$$

#### 3.2. Linear Model Mode Shapes and Natural Frequencies

The mode shapes and the associated natural frequencies can be obtained from the linearized version of the nonlinear integro-partial differential equation (2.2), which takes the form:

$$\frac{\partial^2 w}{\partial t^2} + \frac{\partial^4 w}{\partial \xi^4} - \frac{\partial^2 w_0}{\partial \xi^2} \left\{ \int_0^1 \frac{\partial w}{\partial \xi} \frac{\partial w_0}{\partial \xi} d\xi \right\} + \tag{3.5}$$

$$K_f^* w = 0$$

By substituting  $w(\xi, t) = \phi A \sin(\omega t)$ , where  $\omega$  is unknown natural frequency, into equation (3.5) and using the expression given by equation (2.4) for  $w_0(\xi)$ , equation (3.5) will have the following boundary value problem:

$$\phi'''' - (\omega^2 - K_f) \phi = - R^2 (n\pi)^3 \sin(n\pi\xi) \int_0^1 \phi' \cos(n\pi\xi) d\xi \tag{3.6}$$

The associated modes shape  $\phi$  can be obtained by solving the non-homogeneous, boundary value ordinary differential equation (3.6), i.e., by combining the homogenous and particular solutions, such that  $\phi = \phi_h + \phi_p$ . The homogenous solution, after substituting  $\phi_h = e^{s\xi}$ , is given by:

$$\phi_h = A_1 \sin \alpha \xi + A_2 \cos \alpha \xi + A_3 \sinh \alpha \xi + A_4 \cosh \alpha \xi \tag{3.7}$$

where  $\alpha = \omega^2 - K_f^*$ ,  $A_1$ ,  $A_2$ ,  $A_3$  and  $A_4$  are arbitrary constants to be determined from the following boundary conditions:

$$\phi'''(0) + K_{TL}^* \phi(0) = 0$$

$$\phi''(0) - K_{RL}^* \phi'(0) = 0$$

$$\phi'''(1) - K_{TR}^* \phi(1) = 0$$

$$\phi''(1) + K_{RR}^* \phi'(1) = 0 \tag{3.8}$$

The particular  $\phi_p$  to equation (3.6) takes the form:

$$\phi_p = D \sin(n\pi\xi) \tag{3.9}$$

Substituting equation (3.9) into equation (3.6), one obtains:

$$D = \frac{(n\pi)^3 R^2 \int_0^1 \phi' \cos(n\pi\xi) d\xi}{\alpha^4 - (n\pi)^4} \tag{3.10}$$

The total solution  $\phi = \phi_h + \phi_p$  is, thus, given by:

$$\phi = A_1 \sin \alpha\xi + A_2 \cos \alpha\xi + A_3 \sinh \alpha\xi + A_4 \cosh \alpha\xi + D \sin(n\pi\xi) \tag{3.11}$$

Substituting the derivative of equation (3.11), i.e., the sum of the homogenous and particular solutions, into equation (3.10) one obtains:

$$D = \frac{(n\pi)^3 R^2}{\alpha^4 - (n\pi)^4} \left\{ \int_0^1 \left( \begin{array}{l} \alpha A_1 \cos \alpha\xi - \\ \alpha A_2 \sin \alpha\xi + \\ \alpha A_3 \cosh \alpha\xi + \\ \alpha A_4 \sinh \alpha\xi + \\ (n\pi)D \cos(n\pi\xi) \end{array} \right) \cos(n\pi\xi) d\xi \right\} \tag{3.12}$$

Now the constant  $D$  can be obtained and calculated from the following expression, after some mathematical manipulations, which takes the form:

$$D = \left( \frac{a_5}{a_d} A_1 + \frac{a_6}{a_d} A_2 + \frac{a_7}{a_d} A_3 + \frac{a_8}{a_d} A_4 \right) \tag{3.13}$$

Where

$$\begin{aligned} a_5 &= \left\{ \frac{R^2(n\pi)^3}{\alpha^4 - (n\pi)^4} \alpha \right\} \int_0^1 \cos(\alpha\xi) \cos(n\pi\xi) d\xi \\ a_6 &= - \left\{ \frac{R^2(n\pi)^3}{\alpha^4 - (n\pi)^4} \alpha \right\} \int_0^1 \sin(\alpha\xi) \cos(n\pi\xi) d\xi \\ a_7 &= \left\{ \frac{R^2(n\pi)^3}{\alpha^4 - (n\pi)^4} \alpha \right\} \int_0^1 \cosh(\alpha\xi) \cos(n\pi\xi) d\xi \\ a_8 &= \left\{ \frac{R^2(n\pi)^3}{\alpha^4 - (n\pi)^4} \alpha \right\} \int_0^1 \sinh(\alpha\xi) \cos(n\pi\xi) d\xi \\ a_D &= \left\{ \frac{R^2(n\pi)^4}{\alpha^4 - (n\pi)^4} \alpha \right\} \int_0^1 (\cos(n\pi\xi))^2 d\xi \end{aligned} \tag{3.14}$$

Applying the four boundary conditions given in (3.8) yields a system of equations for the four arbitrary constants  $A_i$ ,  $i = 1, 2, 3, 4$ , which is a homogeneous matrix equation and from its determinant the system

natural frequency can be obtained and calculated by equating the determinant of the coefficient matrix to zero.

The procedure to obtain the natural frequency and the associated modshape is repeated here to show how the parameters  $\beta_i$ ,  $i = 1, 2, 3, 4$  of the nonlinear temporal equation, given in (3.3), can be calculated and evaluated. These parameters include all the system's physical parameters;  $K_f^*$ ,  $K_{TL}^*$ ,  $K_{TR}^*$ ,  $K_{RR}^*$ ,  $K_{RL}^*$  and initial rise shape  $R$  and  $n$ .

### 3.3. Non-Linear Natural Frequencies

The expressions of  $\beta_i$ , given in equation (3.3), were calculated numerically for a given value or combination of the physical system parameters. To simplify the analysis, and for convenience, equation (3.3) can be scaled and rewritten in the following non-dimensional form:

$$\ddot{q} + q + \varepsilon_2 q^2 + \varepsilon_3 q^3 = 0 \tag{3.15}$$

where a dot denotes a derivative with respect to  $T = (\beta_1/\beta_0)^{1/2} t$ , and  $\varepsilon_2$  and  $\varepsilon_3$  are dimensionless coefficients defined as  $\varepsilon_2 = \beta_2/\beta_1$  and  $\varepsilon_3 = \beta_3/\beta_1$ . It is noted from the definitions of  $\varepsilon_2$  and  $\varepsilon_3$  that they are functions of all of beam system physical parameters " $R$ ,  $K_f^*$ ,  $K_{TL}^*$ ,  $K_{TR}^*$ ,  $K_{RR}^*$ ,  $K_{RL}^*$  and  $n$ ".

In the present study, the nonlinear natural frequencies of the nonlinear equation of motion of the beam systems, shown in Figure (1) and given in equation (3.15) are obtained using the method of Harmonic Balance (HB). Since the oscillator includes asymmetric nonlinearity "quadratic term  $q^2$ ", the assumed solution should contain a constant bias, i.e., the approximate two terms- HB takes the form:

$$q(t) = A_0 + A_1 \cos(\omega t) \tag{3.16}$$

where  $\omega$  is the non dimensional nonlinear natural frequency. The initial conditions are taken to be  $q(0) = A_0 + A_1 = A$  and  $\dot{q}(0) = 0$ , where  $A$  is the amplitude of the motion.

Substituting equation (3.16) and its derivatives into equation (3.15) and balancing coefficients of different harmonics one obtains:

$$A_0 \left( 1 + \varepsilon_2 A_0 + \varepsilon_3 A_0^2 + \frac{3}{2} A_1^2 \right) + \frac{\varepsilon_2}{2} A_1^2 = 0 \tag{3.17}$$

$$A_1 \left( 1 + 2\varepsilon_2 A_0 + 3\varepsilon_3 A_0^2 - \omega^2 \right) + \frac{3\varepsilon_3}{4} A_1^3 = 0 \tag{3.18}$$

The above two coupled nonlinear algebraic equations were, for given physical parameters and amplitude of motion  $A$ , solved numerically to obtain results for the nonlinear natural frequency  $\omega$  of a given mode of vibration. In addition to the above HB solution, results for the nonlinear natural frequencies can be obtained also using the method of multiple scales MMS, Nayfeh [10].

It was shown in previous studies [7, 8] that the HB and MMS methods can predict the dynamics of the beams with asinificant accuracy and both can capture the vibratory behavior of the nonlinear oscillator given in [10].

Here, in the present study, the HB method is used to obtain results for the nonlinear natural frequencies versus the amplitude, for given values of the system physical parameters and will be presented and discussed in the next section.

#### 4. Results And Discussion

Dynamic behaviors of the beam systems, shown in Figure (1), were analyzed for some selected values of the system physical parameters: beam elastic foundation  $K_f^*$ , translational and torsional springs at the beam ends  $K_{TL}^*$ ,  $K_{TR}^*$ ,  $K_{RR}^*$ ,  $K_{RL}^*$ , initial rise amplitude  $R$  and rise type parameter  $n$ .

Figures (2) – (4) display results for the variation of nondimensional linear natural frequencies  $\omega$  versus the beam rise  $R$  for different physical parameters.

Figure (2) shows the results for a beam fixed at both ends, i.e.,  $K_{TL}^* = K_{TR}^* = K_{RR}^* = K_{RL}^* = \infty$ , but for  $K_f^* = 0$  and  $n = 1$  "1/2 sine rise". As can be seen from Figure (2), two veering zones are present. The first veering occur between the 1<sup>st</sup> and 2<sup>nd</sup> natural frequencies at  $R \approx 8.74$ , and second veering occur between the 2<sup>nd</sup> and 3<sup>rd</sup> natural frequencies at a rise of  $R \approx 16.7$ . At these two zones, the two natural frequencies approach each other and then veer away. Here, it is worth mentioning that a drastic change in mode shapes occurred also, as it was presented by [1].

Other results are obtained and presented in Figures (3) – (4) for beams with some flexibility at the two ends. In Figure (3), the same trend is obtained for  $K_{TL}^* = K_{TR}^* = 10^5$ ,  $K_{RR}^* = K_{RL}^* = 50$ ,  $K_f^* = 0$  and  $n = 1$ . From Figure (3), the qualitative behavior is the same, i.e., two veering zones between the first three natural frequencies but with some differences in natural frequencies as one may expect due to the flexibility of the beam supports. In Figure (4), the nondimensional linear natural frequencies  $\omega$  versus the beam rise  $R$  are obtained for the same parameters of Figure (3), expect initial rise shape, i.e.,  $n = 2$ . As it can be seen from Figure (4), due to the change in rise shape, an increase in natural frequencies can be noticed as well as a shift in the veering zones. For instance, the first veering zone between the 1<sup>st</sup> and 2<sup>nd</sup> natural frequencies at  $R \approx 3.5$  compared to  $R \approx 7.7$  for the case of  $n = 1$ , while the second veering occurs between the 2<sup>nd</sup> and 3<sup>rd</sup> natural frequencies at a rise of  $R \approx 6.4$  for  $n = 2$ . From the results presented in Figures (3) and (4), it is demonstrated that the rise shape, whether it is 1/2 sine or full sine, has a significant role in the dynamical behavior as of the beam, as well as the other physical parameters, like elastic

foundation stiffness  $K_f^*$ , translational and torsional springs at the beam ends  $K_{TL}^*$ ,  $K_{TR}^*$ ,  $K_{RR}^*$ ,  $K_{RL}^*$ .

Results presented in Figures (2) – (4) are obtained from using the linearized version of the mathematical model. To have an idea about the nonlinear interaction between the modes of vibration and natural frequencies, the nonlinear derived mathematical model given in [6], will be analyzed and the nonlinear natural frequencies will be calculated, as mentioned in the previous section. This is due to the fact that the effect of vibration amplitude on natural frequency cannot be captured using the linear analysis. In addition, the frequency veering phenomenon is associated with drastic change in mode shapes and might have crossover instabilities between modes.

$$K_r = 5, K_f = 0.5$$

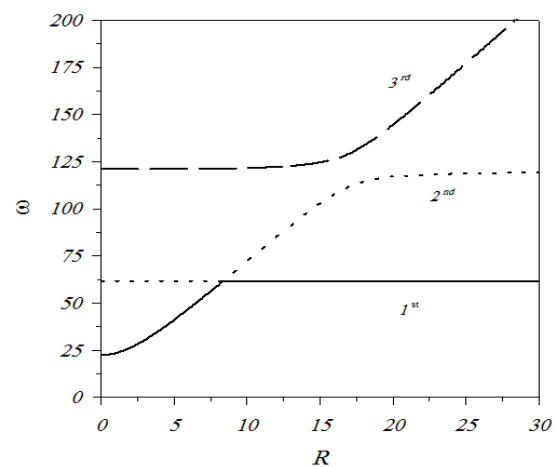


**Figure 2.** Variation of the non-dimensional linear natural frequencies  $\omega$  with the non-dimensional rise  $R$  for  $K_{TL}^* = K_{TR}^* = K_{RR}^* = K_{RL}^* = \infty$ ,  $K_f^* = 0$  and  $n = 1$  "1/2 sine rise"

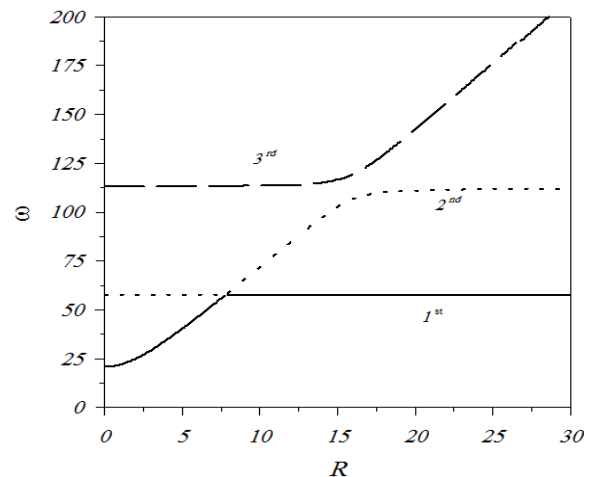


**Figure 3.** Variation of the non-dimensional linear natural frequencies  $\omega$  with the non-dimensional rise  $R$  for  $K_{TL}^* = K_{TR}^* = 10^5$ ,  $K_{RR}^* = K_{RL}^* = 50$ ,  $K_f^* = 0$  and  $n = 1$

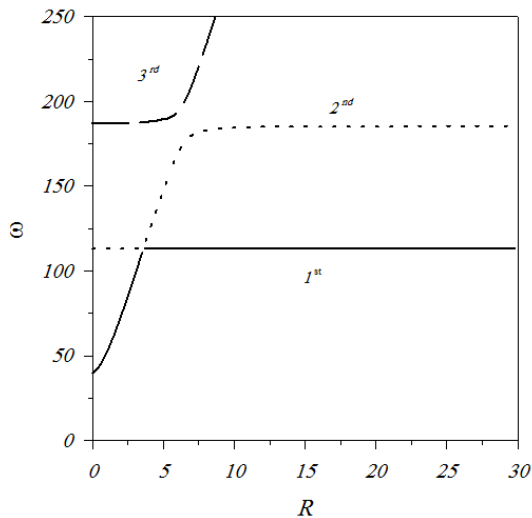


**Figure 4.** Variation of the non-dimensional linear natural frequencies  $\omega$  with the non-dimensional rise  $R$  for  $K_{TL}^* = K_{TR}^* = 10^5$ ,  $K_{RR}^* = K_{RL}^* = 50$ ,  $K_f^* = 0$  and  $n = 2$

To have a clear picture about the interaction between modes and natural frequencies near or at the veering zones, Figures (5) – (8) display results for the nonlinear natural frequencies obtained for  $K_{TL}^* = K_{TR}^* = 10^5$ ,  $K_{RR}^* = K_{RL}^* = 100$ ,  $K_f^* = 1$  and  $n = 1$ , for which the first veering zone between the 1<sup>st</sup> and 2<sup>nd</sup> natural frequencies occurs at  $R \approx 8.1$ .

Results in these Figures are presented as the variation of the nonlinear natural frequencies of the first three modes versus the amplitude of vibrational motion at a given beam rise  $R$ , near the veering zone.

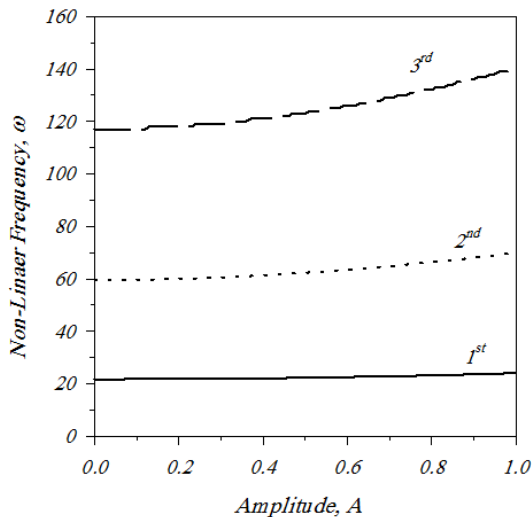


**Figure 5.** Variation of the non-linear natural frequencies  $\omega$  with the Amplitude  $A$  for  $K_{TL}^* = K_{TR}^* = 10^5$ ,  $K_{RR}^* = K_{RL}^* = 100$ ,  $K_f^* = 1$ ,  $n = 1$  and  $R = 0$

As it can be seen from Figure (5) that the three modes of vibration exhibit a hardening behavior, i.e., the natural frequency increases as the amplitude of motion increases, for the case of initial rise  $R = 0$ . On the other hand, as

the values of the initial rise increase, the first natural frequency exhibits a softening behavior, i.e., the natural frequency decreases as the amplitude of motion increases, till it reaches a zero value which represents an unstable vibratory motion. This behavior, for the first natural frequency, is obvious in Figures (6) and (7), while the behavior of the second and third natural frequencies is of hardening type, regardless the beam rise. This behavior is due to the two competing nonlinearities of the beam system, i.e.,  $\mathcal{E}_2$  and  $\mathcal{E}_3$  whether they are of softening or hardening type. As mentioned before,  $\mathcal{E}_2$  and  $\mathcal{E}_3$  contain all the system's physical parameters.

In addition, another phenomenon, like cross over, occurred between the second and third natural frequencies, as shown in Figure (8), for the case presented in Figure (2), near the second veering zone, between the second and third natural frequencies.

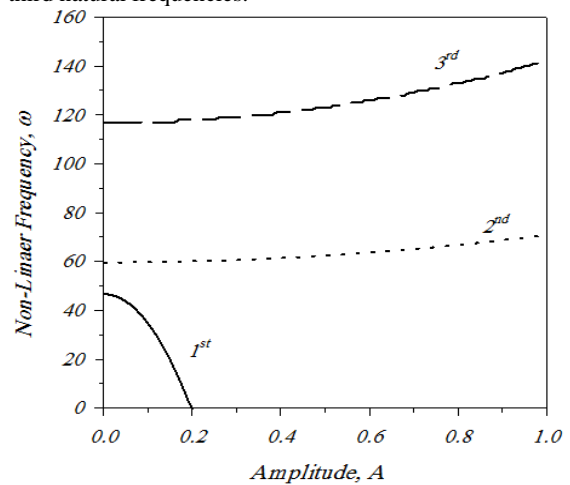


**Figure 6.** Variation of the non-linear natural frequencies  $\omega$  with the Amplitude  $A$  for  $K_{TL}^* = K_{TR}^* = 10^5$ ,  $K_{RR}^* = K_{RL}^* = 100$ ,  $K_f^* = 1$ ,  $n = 1$  and  $R = 6$

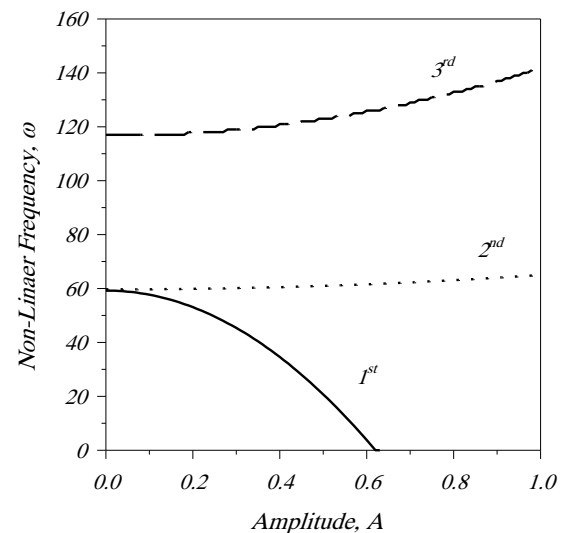


**Figure 7.** Variation of the non-linear natural frequencies  $\omega$  with the Amplitude  $A$  for  $K_{TL}^* = K_{TR}^* = 10^5$ ,  $K_{RR}^* = K_{RL}^* = 100$ ,  $K_f^* = 1$ ,  $n = 1$  and  $R = 8$

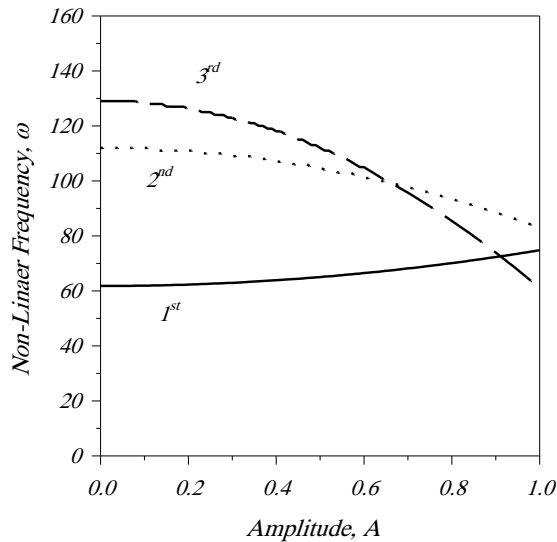


**Figure 8.** Variation of the non-linear natural frequencies  $\omega$  with the Amplitude  $A$  for  $K_{TL}^* = K_{TR}^* = K_{RR}^* = K_{RL}^* = \infty$ ,  $K_f^* = 0$   $n = 1$  and  $R = 17$

## 5. Conclusions

The present analyses of the nonlinear free vibration of a beam element, with flexible ends resting on elastic foundation with different rise shapes, show that the nonlinear natural frequency curves of the first three modes can exhibit a complex dynamic behavior which cannot be observed using the linear analysis. In addition to frequency veering phenomenon, these beam-like structures and, depending on system parameters, can exhibit crossover instabilities.

The obtained results indicate that the dynamic behavior is complicated enough and it needs a further and thorough analysis like the forced vibration and stability, which is beyond the scope of the present paper.

## References

- [1] M. S. Abdeljaber and A. A. Al-Qaisia, "Effect of Supports Flexibility on Frequency Veering in Imperfect Beams Resting on Elastic Foundation", Proceedings of the Fourteenth International Conference on Civil, Structural and Environmental Engineering Computing, **paper 237**, 2013.
- [2] E. Mettler, in: W. Flugge (Ed.), "Dynamic Buckling in Handbook of Engineering Mechanics", McGraw-Hill, New York, 1962.
- [3] J. S. Chen and Li Yuon-Tai, "Effects of elastic foundation on the snap-through buckling of a shallow arch under a moving point load", *International Journal of Solids and Structures*, **43**, p.p. 4220–4237, 2006.
- [4] M. O. Hassen and M. I. Younis, "Natural Frequencies and Mode Shapes of Initially Curved Carbon Nanotube Resonators Under Electric Excitation", *Journal of Sound and Vibration*, **330**, p.p. 3182-3195, 2011.
- [5] W. Lacarbonara, H. Arafat, and A. Nayfeh, "Large non-linear interactions in imperfect beams at veering", *International Journal of Non-Linear mechanics*, **40** (7), p.p. 987-1003, 2005.
- [6] R. H. Plaut, and E. R. Johnson, "The effect of initial thrust and elastic foundation on the vibration frequencies of a shallow arch", *Journal of sound and vibration*, **78** (4), p.p. 565-571, 1981.
- [7] A. A. Al- Qaisia and M. N. Hamdan, "Primary Resonance Response of a Beam with a Differential Edge Settlement Attached to an Elastic Foundation". *Journal of Vibration and Control*, Vol. **16** (6), p.p. 853-877, 2010.
- [8] A. A. Al- Qaisia and M. N. Hamdan, "Non-Linear Frequency Veering in a Beam Resting on Elastic Foundation". *Journal of Vibration and Control*. Vol. **15** (11), p.p. 1627-1647, 2009.
- [9] A. A. Al- Qaisia and M. N. Hamdan, "On Nonlinear Frequency Veering and Mode Localization of a Beam with Geometric Imperfection Resting on Elastic Foundation". *Journal of Sound and Vibration*. Vol. **332** (15), p.p 4641-4655, 2013.
- [10] A. H. Nayfeh and D. T. Mook, *Nonlinear Oscillations*, Wiley-Interscience, New York, 1979.



# Experimental Studies the Effect of Flap Peening Process on Aluminum Alloys

K. N. Abushgair

*Al-Balqa Applied University, Faculty of Engineering Technology, Amman, Jordan.*

*Received Dec 14,2016*

*Accepted March 23,2017*

## Abstract

The effects of flap peening on surface characteristics of aluminum alloy (7075-T6) is used in a wide range in airframes and structured; it has high ability for corrosion, since the corrosion resistance for this type of metal is relatively small. Flap peening is a process applied to add residual compression stresses in metallic surfaces with the intent of improving the material when exposed to corrosion due to stress and fatigue. Some studies about the effect of the flap peening process, on the fatigue resistance, bending fatigue behavior and residual surface stress in the aluminum alloys, have been performed. However, the effect of the flap peening process parameters on the corrosion and oxidation resistance of the aluminum alloys is not well known. In the present study, the influence of flap peening treatment on hardness and corrosion behavior of aluminum alloy (7075-T6) is investigated, compared with sand blasting process. In addition, the effect of the flap peening process parameters on the corrosion and oxidation resistance of the aluminum alloys is investigated. The obtained results show that the aluminum alloy (7075-T6) samples, treated with flap peening, presented a significant modification on the surface morphology, as seen by Scanning Electron Microscopy (SEM) photos. According to the hardness measurement results, the shot peening treatment increases the surface hardness and an important decrease of oxidation and corrosion resistance was noted, evidencing that the flap peening process compromises the chemical and physical properties of the surface.

© 2017 Jordan Journal of Mechanical and Industrial Engineering. All rights reserved

**Keywords:** ...

## 1. Introduction

Aircraft manufacturers have implemented many key design improvements over the past 30 years, ranging from the use of more corrosion-resistant materials, to improved adhesive bonding processes, to the use of sealants in fastener holes and on faying surfaces, to the control of spillage of galley and lavatory fluids as a result the design service life of new generation aircraft was moved from 20 to 40 years [1]. Despite of these improvement, aluminum alloys 7075-T6 and 2024-T3 which are corrosion- and stress corrosion cracking-prone alloys; but they are still widely used in aircraft industry [1, 2].

Flap peening, also known as "flapper peening" or "roto peening", employs 1 mm tungsten carbide balls bonded to a flexible polymeric flap. As seen in Figure (1), flap peening is a cold working process in which the surface of a part is bombarded with small spherical media called shot. Each piece of shot striking the material acts as a tiny peening hammer, imparting to the surface a small indentation or dimple. [3-6] In order for the dimple to be created, the surface fibers of the material must be yielded in tension. Below the surface, the fibers try to restore the surface to its original shape, thereby producing below the dimple, a hemisphere of cold-worked material highly stressed in compression. Overlapping dimples develop an even layer of metal in residual compressive stress.

Maximum compressive residual stress, produced at or under the surface of a part by flap peening, is at least as great as half the yield strength of the material being peened. Many materials will also increase in surface hardness due to the cold working effect of flap peening [5, 12].

Benefits obtained by flap peening are the result of the effect of the compressive stress and the cold working induced. Compressive stresses are beneficial in increasing resistance to fatigue failures, corrosion fatigue, stress by corrosion cracking, hydrogen assisted cracking, fretting, galling and erosion caused by cavitations. Benefits obtained due to cold working include work hardening, inter granular corrosion resistance, surface texturing, closing of porosity and testing the bond of coatings. Both compressive stresses and cold-worked effects are used in the application of flap peening in forming metal parts.

The effectiveness of peening depends in large measure on the flap peening intensity. The latter is a function of numerous variables, including work piece material, flap material, flap size, type of flap peening machine, and time of peening. Sizes and types of flap, to be selected for a certain peening application, depend on the material to be peened, desired peening intensity, fillet size, hole size, etc., for most peening applications. [4, 8, 9, 10, 11, 12]

On the other hand, sand blasting is the use of sand material to clean or textures a material, such as metal or masonry. Sand is the most widely used for blasting. Metal

is sand blasted to remove corrosion and sharp edges or as away to enhance adhesion of coatings and adhesives. The sand material used in the process is aluminum oxide (alumina  $Al_2O_3$ ) with a diameter of 250  $\mu m$ , the air pressure used in the process is 4 bar, sand hardness is 1440kg/mm<sup>2</sup>.

In the present work, we apply flap peening and sand blasting procedures on selected work specimens to study their effects on the material properties on rising the mechanical properties of the material, i.e., hardness, microstructure and investigate if the sand blasting process can compensate flap peening process since it is less expensive. Also, we study the effects of the rotational speed and the flap standoff distance for flap peening on the material properties, mainly hardness and microstructure.

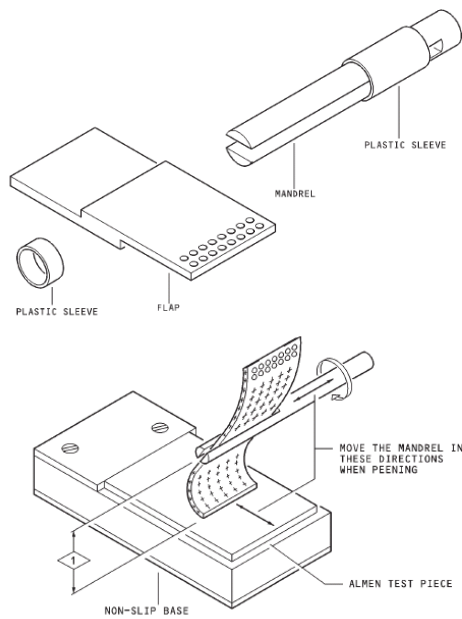


Figure 1. Flap peening process's main parts

## Experiment

### Specimens

The specimens selected for the present study are from aluminum alloy type (7075-T6) because this type of alloy is used in a wide range in airframes and it has a high ability for corrosion, since the corrosion resistance for this type of metal is relatively small.

Two groups of specimens were selected in the present work; the first group was for the comparison between flap peening procedure and sand blasting procedure; the second group, however, was selected to study flap peening process's main parameters, namely the effects of the rotational speed and the flap standoff distance on the material properties.

#### Group no. 1

18 specimens were prepared for this group; these specimens were taken from AIRBUS (A340-200/-300) aircraft from forward passenger cabin compartment (upper floor panel structure).

The thickness of the specimens was 2mm, as shown in Figure (17). Three types of these specimens were selected

for this process: Type (A) new parts, Type (B) used parts and Type (C) badly corroded parts.



Figure 2. Specimens of the first group

Tables (1), (2) and (3) show the preparation work done on these three types of specimens. The specimens were tested before and after work for hardness and microstructure. A grinding process is used to remove the primer and corrosion off the specimens using the corrosion disk. The flap peening process is done on this specimens group using the small flap and with a specified rotational speed and standoff distance which is recommended by the manufacturer (12.5 mm). Also, a paint remover is used to remove the paint and primer from the surface of the metal without making any effects on the metal; this material does not remove the corrosion on the metal.

Table 1: Specimens type A (new parts)

No	Type of work done on the specimens
A1	Grinding using the corrosion disk
A2	Grinding + flap peening
A3	Sand blasting
A4	Removing primer using paint remover
A5	Removing primer + flap peening
A6	Removing primer + Sand blasting

Table 2: Specimens type B (used parts)

No	Type of work done on the specimens
B1	Grinding using the corrosion disk
B2	Grinding + flap peening
B3	Sand blasting
B4	Removing primer using paint remover
B5	Removing primer + flap peening
B6	Removing primer + Sand blasting

Table 3: Specimens type C (badly corroded parts)

No	Type of work done on the specimens
C1	Grinding using the corrosion disk
C2	Grinding + flap peening
C3	Sand blasting
C4	Removing primer using paint remover
C5	Removing primer + flap peening
C6	Removing primer + Sand blasting

**Group no. 2**

16 new sheets specimens (3x5 cm and 2 mm thickness) were prepared for this group, as seen in Figure (3). The large flap was used on this group and with 4 speeds and 4 standoff distances worked out on this group. Table (4) shows the values of these parameters. To ensure that the standoff distances are steady throughout the work, stands between the mandrel and the specimens were used. The specimens were tested for hardness and microstructure.

**Table 4.** Samples values of the parameters

Specimen no	Rotational speed (rpm)	Flap standoff distance mm
F1	3000	14
F2	3000	12
F3	3000	10
F4	3000	8
F5	6000	14
F6	6000	12
F7	6000	10
F8	6000	8
F9	9000	14
F10	9000	12
F11	9000	10
F12	9000	8
F13	12000	14
F14	12000	12
F15	12000	10
F16	12000	8



**Figure 3.** Specimens of the second group



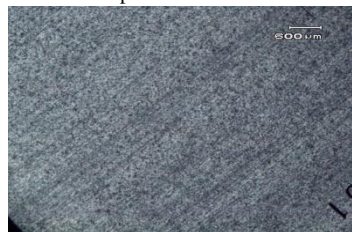
specimen no A1



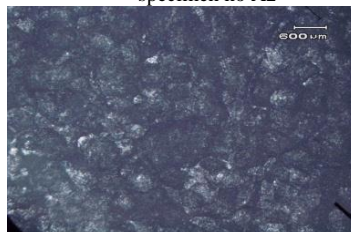
specimen no A2



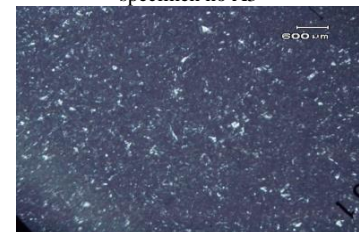
specimen no A3



specimen no A4



specimen no A5



specimen no A6

**Figure 4:** Scanning electron microscope images of different samples in group A

**Hardness Test**

Hardness test was carried out on the two groups of specimens to see the effect of these parameters on the metal hardness. Rockwell (C) hardness test was used due to the thickness of the specimens. 3 different places were tested for the hardness, and the average of these values were calculated. Table (5) shows the hardness values of the first group specimens. Table (6) shows the minimum and maximum values of the two variables and the specimen hardness of the second group.

**Table 5.** Hardness values in (HRC) of the first group specimens

Specimen no	Hardness test (1)	Hardness test (2)	Hardness test (3)	Average Hardness
A1	18	18.5	17.5	18
A2	21	20.5	22	21.16
A3	15	16	15.5	15.5
A4	23.5	25	30	26.16
A5	17.5	19	18.5	18.33
A6	14	17	17.5	16.16
B1	19	20	19.5	19.5
B2	20.5	21.5	23	21.66
B3	14	16	17	15.66
B4	15.5	15	17	15.83
B5	20	21.5	22	21.16
B6	18	17	17.5	17.5
C1	15	16	16	15.66
C2	17	16.5	18	17.16
C3	13	12.5	13	12.83
C4	17	14.5	18	16.5
C5	21.5	16.5	20	19.33
C6	11.5	14	10.5	12

**Microstructure Test**

Microstructure test was carried out on the two groups of specimens to see the effect of these parameters on the metal surface. Figures (4) through (6) show the SEM pictures of the first group specimens. Figures (7) through (10) show the images of the second group.

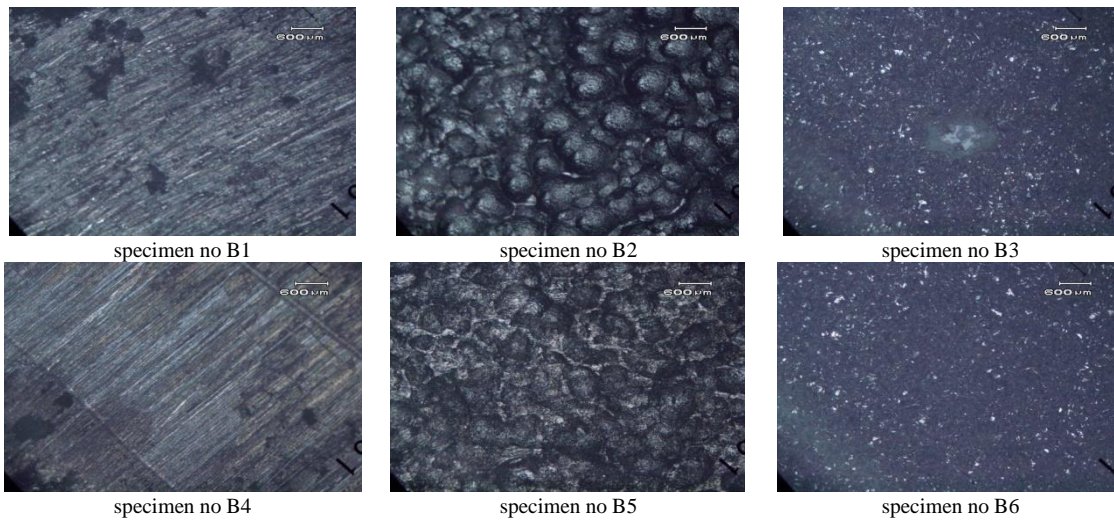


**Figure 5.** Scanning electron microscope images of different samples in group B

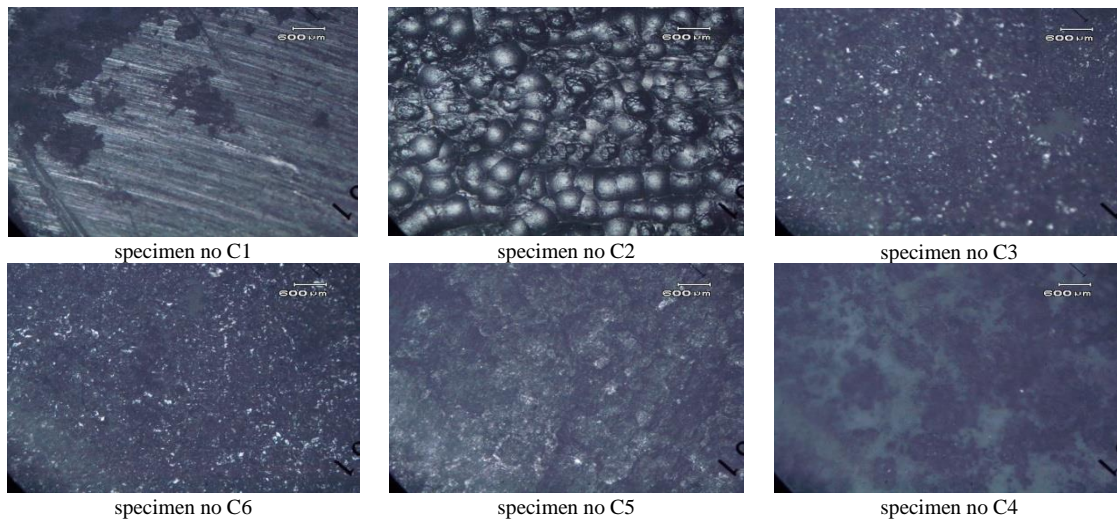


**Figure 6.** Scanning electron microscope images of different samples in group C

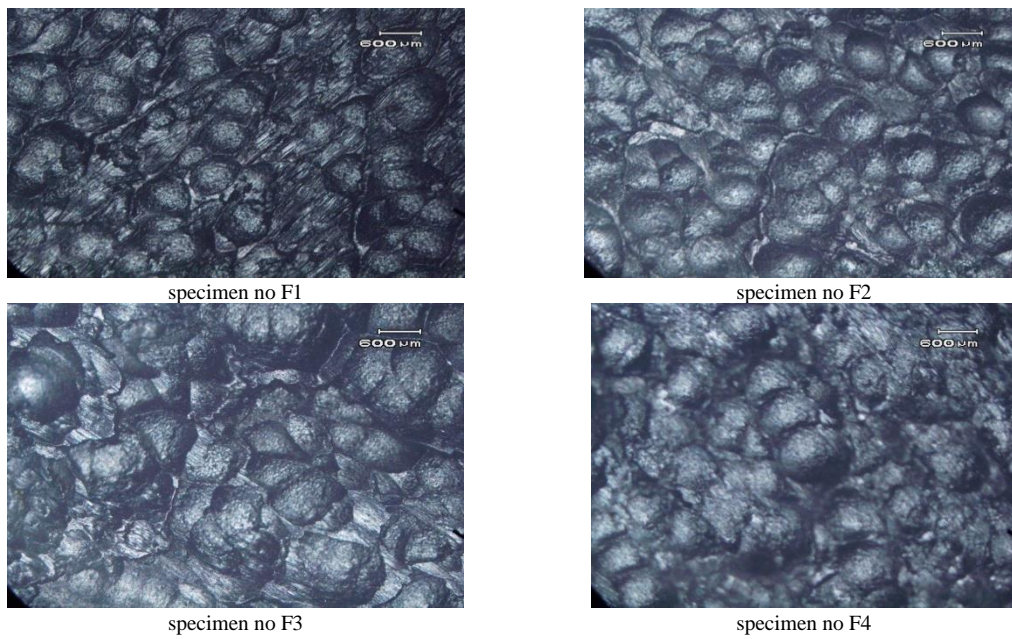


**Figure 7.** SEM images of different samples With Rotational speed 3000 rpm

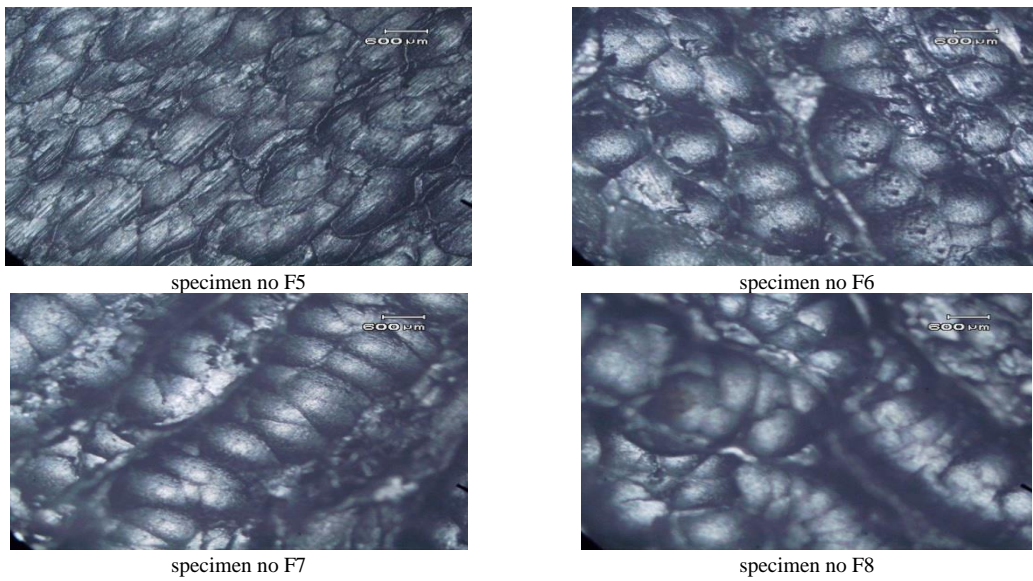


**Figure 8.** SEM images of different samples With Rotational speed 6000 rpm

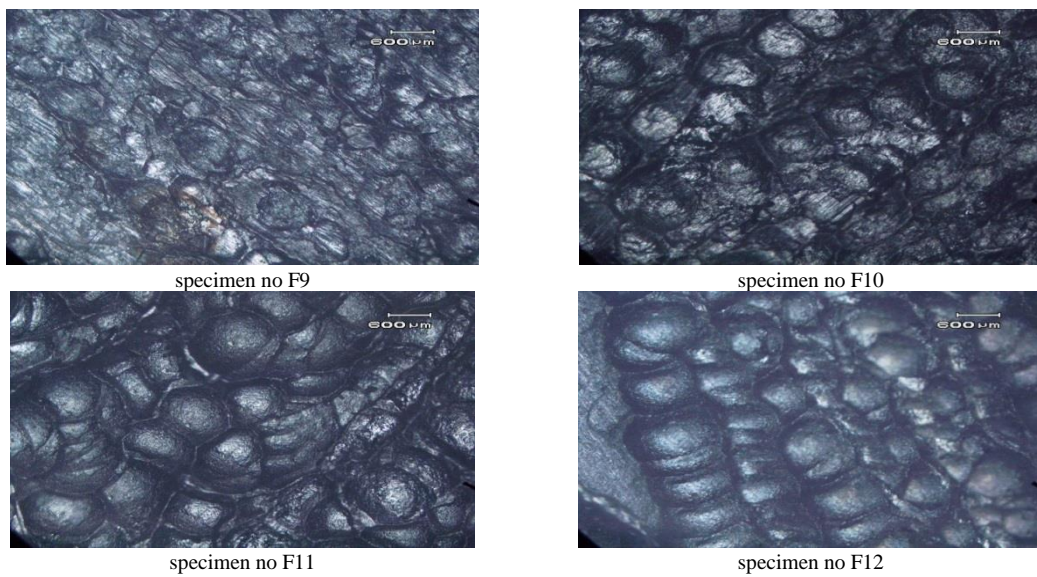


**Figure 9.** SEM images of different samples With Rotational speed 9000 rpm

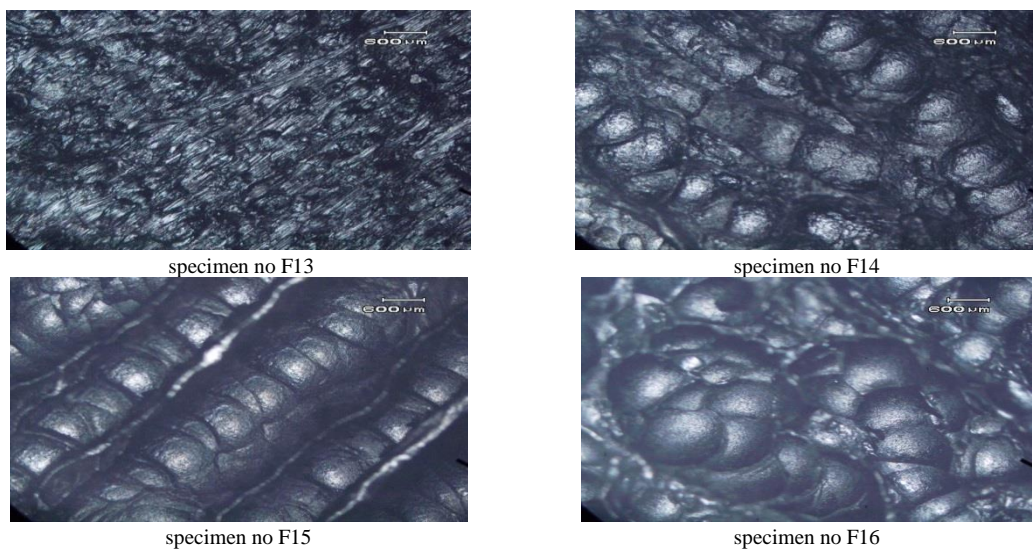


**Figure 10.** SEM images of different samples With Rotational speed 12000 rpm

## Results and Discussion

### Group no. 1

#### (A) Microstructure Test

Refer to Figures (4) to (6) for the microstructure test. Comparing between specimen (A1), which reveals the surface of the specimen after the grinding process, and specimen (A4), which reveals the surface of the specimen after removing the primer using the paint remover, shows that the paint remover does not remove the anodized layer on the surface of the specimen (A4). So, the grinding process is used to remove the anodized layer. Same results can be noted between samples (C1) and (C4).

Specimens (A1), (B1) and (C1) were grinded while specimens (A2), (B2) and (C2) were flap peening; the overlapping dimples that develop the compressive stresses, induced by flap peening, were noted, which in turn provides a considerable increase in parts fatigue life.

Comparing the intensity of specimens (A2), (B2) and (C2) surface, after the flap peening process, it is noticed that specimen (C2) has a bigger intensity and specimen (A2) the smallest; this shows that specimen (C2) has accepted the biggest intensity of compressive stresses because it has the lowest hardness among the other two, which means that the peening time under a specified speed and standoff distance is constant.

Specimens (A5), (B5) and (C5) show the surface after the flap peening process (without the grinding process), the flap peening process cannot remove the anodized layer or corrosion from the surface of the metal.

Comparing specimens (A4), (B4) and (C4), which reveal the anodized layer and corrosion on the surface of the specimen after removing the primer using the paint remover, with specimens (A3), (A6), (B3), (B6), (C3), and (C6), which show the surface of the specimens after the sand blasting process, we can see that the sand blasting process can remove the anodized layer and corrosion from the surface of the metal; it also shows that the abrasive particles or the sand penetrates the surface of the metal, which, in turn, causes a decrease in the parts hardness, which, in turn, decreases the fatigue life of the parts.

#### (B) Hardness Test

Table (5) shows the hardness values (HRC) of the first group specimens. The average hardness of the specimens before the work is (18 HRC) for type (A), (19.5 HRC) for type (B) and (15.66 HRC) for type (C). Therefore, the hardness of specimens type (B) is more than that of specimens type (A) because they are used parts so they have been work hardened due to operation. For specimens type (C), however, their average hardness was reduced to a value less than that of specimens type (A) because of the high fatigues and stress corrosions on them. This shows, however, that the selection of the specimens was good. Figure (11) shows the increasing and decreasing on the average hardness for the three types of specimens before the work.

After the flap peening procedure was done on specimens number (A2), (B2) and (C2), the values of their average hardness were (21.16 HRC), (21.66 HRC) and (17.16 HRC), respectively. This means that the hardness of the specimens increases after flap peening, and this, in turn, causes the fatigue life of the specimens to increase. Figure (12) shows the increase on the average hardness for the three types of specimens.

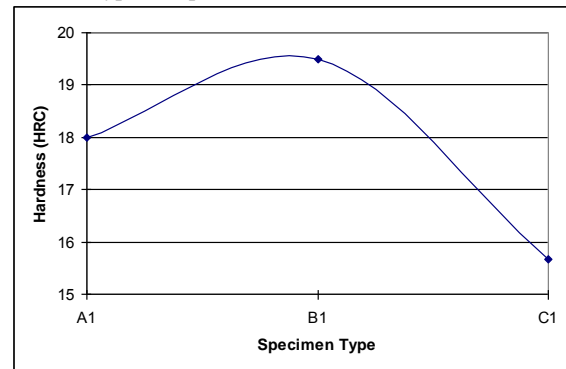


Figure 11. Average hardness for the three types of specimens before test

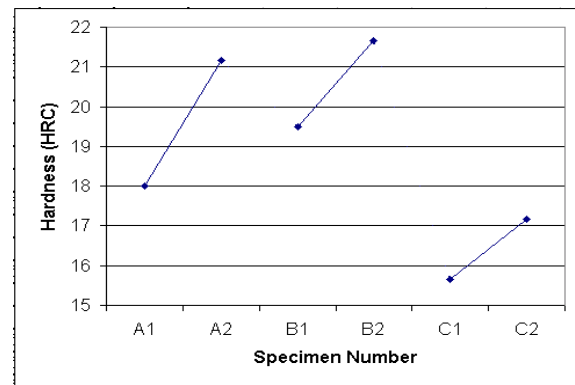


Figure 12. Average hardness for the three types of specimens after flap peening

After the sand blasting procedure was done on specimens number (A3), (B3) and (C3), the values of the average hardness on them were (15.5 HRC), (15.66 HRC) and (12.83 HRC), respectively. This means that the hardness of the specimens decreases after sand blasting, and this, in turn, causes the fatigue life of the specimens to decrease. Figure (13) shows the decrease on the average hardness for the three types of specimens.

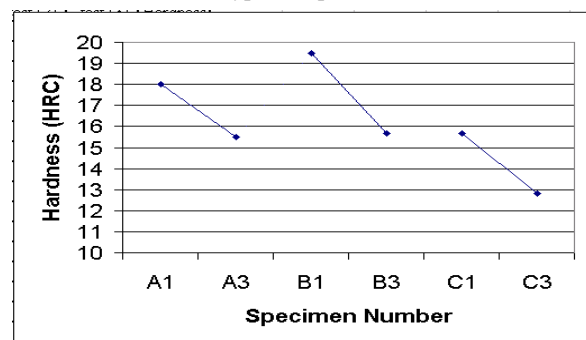


Figure 13. Average hardness for the three types of specimens after sand blasting

**Group no. 2**

**(A) Hardness Test**

Two plots are introduced for the mandrel speed (rpm), the flap standoff distance and the hardness, as a result of using such values for the two variables. The average hardness of each specimen, before the flap peening test, was 18 HRC. Table (6) shows the hardness values before and after the flap peening. The maximum hardness of 13 HRC was at speed of 12000 rpm and a flap standoff distance of 8 mm. The minimum hardness of 2 HRC was at speed of 3000 rpm and a flap standoff distance of 14 mm.

Figures (14) and (15) are a plot for the flap peening test with the two variables and the average hardness.

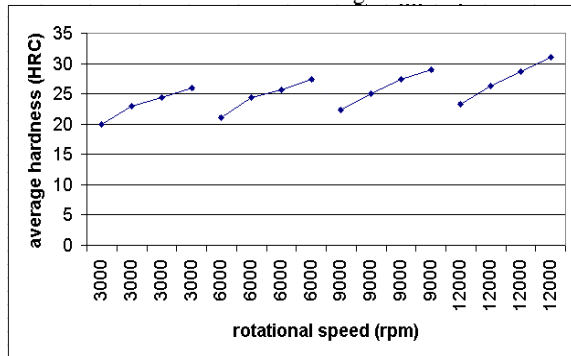


**Figure 14.** Flap peening test with the rotational speed variables and the average hardness

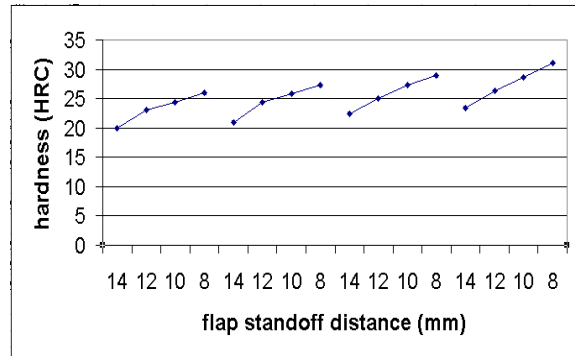


**Figure 15.** Flap peening test with the flap stand off distance and the average hardness

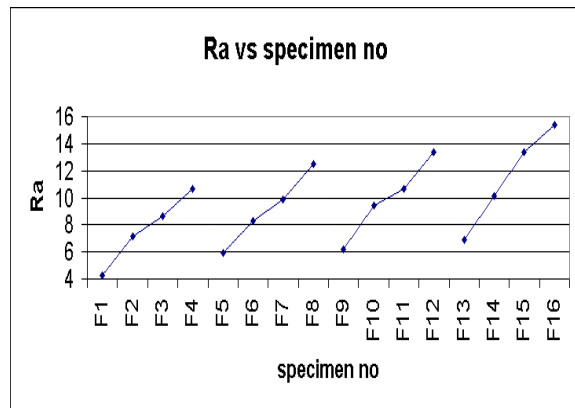


**Figure 16.** Surface roughness for flap peening test samples

**Table 6.** Samples with hardness before and after the flap peening

Specimen no	Rotational speed (rpm)	Flap standoff distance mm	Hardness test (1)	Hardness test (2)	Hardness test (3)	average Hardness (HRC)	difference in hardness (HRC)	Ra (µm)
F1	3000	14	20	19.5	20.5	20	2	4.3
F2	3000	12	22	23.5	23.5	23	5	7.13
F3	3000	10	25	24	24	24.33	6.33	8.62
F4	3000	8	27	24	27	26	8	10.68
F5	6000	14	20	22	21	21	3	5.93
F6	6000	12	23	25	25	24.33	6.33	8.26
F7	6000	10	23	27	25	25	7	9.84
F8	6000	8	28	27	27	27.33	9.33	12.51
F9	9000	14	24	20	23	22.33	4.33	6.22
F10	9000	12	24.5	25.5	25	25	7	9.43
F11	9000	10	26	25	29	27.33	9.33	10.64
F12	9000	8	30	29.5	27.5	29	11	13.39
F13	12000	14	22	25	23	23.33	5.33	6.93
F14	12000	12	26	27	26	26.33	8.33	10.13
F15	12000	10	27	28	31	28.66	10.66	13.35
F16	12000	8	32	30	31	31	13	15.41

### (B) Microstructure Test

Figures (7) to (10) show the differences in intensity between the tested specimens; the maximum intensity occurs in specimen no (F16), which has the maximum hardness; the minimum intensity occurs in specimen no (F1), which has the minimum hardness. This means that the highest hardness occurs at the highest intensity.

Figure (16) shows the surface roughness for the different samples where we can note that sample (F16) has the higher Ra value.

### Conclusions

#### Group no. 1

From the above results, we can conclude the following points:

- Flap peening process increases the hardness of surface of the metal; so, this, in turn, causes the fatigue life of the metal to increase.
- Sand blasting process reduces the hardness of surface of the metal; so, this, in turn, causes the fatigue life of the metal to decrease, and this is due to the small particle size of the sand material which penetrates the surface of the metal.

#### Group no. 2

- In the first group, the maximum hardness on the new parts (specimens type A), accomplished by the flap peening process under the recommended speed and standoff distance, was 21.16 HRC. But after entering variable speeds and standoff distances on the second group, the maximum hardness accomplished was 31 HRC. So, a difference in hardness of approximately 10 HRC was increased after entering those variables on the second group. This, in turn, gives more rising in the fatigue life of the metal.
- Rotational speed of the tool and standoff distance, controlled by operator, are the major variables of intensity control. The type of rotary tool used has a major effect on controlling the flap speed and, hence, intensity. Standoff distance has a significant effect on intensity control. It is concluded that the maximum hardness increases when the maximum mandrel speed

and an 8 mm standoff distance is used. The minimum was at 3000 rpm of mandrel speed and a distance of 14 mm.

- The increase in hardness is directly proportional with the increase in intensity.

### References

- [1] R.L. Cook, A.W. Myers and J. E. Elliott. "Chromate Free On Demand Releasable Corrosion Inhibitors for Aluminum Alloys", APPENDIX P, AIRCRAFT. 2005.
- [2] Structural Repair Manual, AIRBUS INDUSTRIE (A340-200/-300) Chapter (51-22-00 and 51-29-11).
- [3] Roto Peen Flap Assemblies manuals. 3M Surface conditioning Industries .2003.
- [4] J. E. Campbell, "metals and ceramics information center, Materials Information ", Division Battella Columbus, Ohio, 1971.
- [5] B. Baldwin, "Methods of Dust-Free Abrasive Blast Clearing, Plant Engineering", 32(4), February 16, 1978.
- [6] V. Azar, B. Hashemi, Mahboobeh Rezaee Yazdi. "The effect of shot peening on fatigue and corrosion behavior of 316L stainless steel in Ringer's solution." Surface and Coatings Technology, Volume 204, Issues 21–22, 15 August 2010, Pages 3546-3551.
- [7] Wencai Liu, Jie Dong, Ping Zhang, Chunquan Zhai and Wenjiang Ding1. "Effect of shot peening on surface characteristics and fatigue properties of T5-treated ZK60 alloy". Materials Transactions, Vol. 50, No. 4 (2009) pp. 791 to 798.
- [8] J. Peltza, L. Beltrami<sup>a</sup>, S. Kunst<sup>b</sup>. "Effect of the Shot Peening Process on the Corrosion and Oxidation Resistance of AISI430 Stainless Steel". Materials Research. 2015; 18(3): 538-545.
- [9] Xiang ZD and Datta PK.; Scripta Materialia. "Shot peening effect on aluminide diffusion coating formation on alloy steels at low temperatures". 2006; 55(12):1151-1154.
- [10] Ebrahimifar H and Zandrahimi M. "Oxidation and electrical behavior of AISI 430 coated with cobalt spinels for SOFC interconnect applications". Surface and Coatings Technology. 2011; 206(1):75-81.
- [11] Ezhil Vannan, Paul Vizhian, "Corrosion Characteristics of Basalt Short Fiber Reinforced with Al-7075 Metal Matrix Composites". JJMIE, Volume 9 Number 2, April.2015 Pages 121 – 128.
- [12] Nabeel Alshabatat , Safwan Al-qawabah," Effect of 4%wt. Cu Addition on the Mechanical Characteristics and Fatigue Life of Commercially Pure Aluminum" . JJMIE,Volume 9 Number 4, August.2015Pages 297- 301.

# Solar Thermal Hybrid Heating System

Ahmad Al aboushi

Faculty of Engineering and Technology, Department of Mechanical Engineering- Al Zaytoonah University of Jordan

Received Feb 10,2017

Accepted June 15,2017

## Abstract

In the present work, a solar hybrid system is used to heat up a swimming pool to maintain it at around 30 °C around the year. The solar energy is collected using evacuated tubes collectors, within which water is heated up as it flows inside the tubes, before it is introduced into a heat exchanger located inside a large well-insulated storage tank, where it cools down as it loses heat to water in the tank. In winter, during cloudy days, an auxiliary system (in addition to the solar thermal system) was used to provide the required heating load. Three types of auxiliary systems were used, namely natural gas, electrical power and diesel powered boiler. In addition, an energy management system is used to optimize the percentage of the heating load to be supplied by each auxiliary heating system.

It was found that during summer season, the heating load may be completely provided by the solar system, while during the rest of the year an auxiliary system is required to maintain the pool temperature at the desired value. Furthermore, it was found and based on current costs of electrical power, diesel fuel and natural gas in Jordan, that natural gas is the most economical source of energy to be used as an auxiliary system.

© 2017 Jordan Journal of Mechanical and Industrial Engineering. All rights reserved

**Keywords:** Hybrid solar thermal system, evacuated solar collectors, thermal solar fraction, auxiliary system.

## 1. Introduction

Nowadays, the growing concern due to continuous escalation of the energy cost, environmental pollution caused by the conventional fossil-based fuels and the realization that they are non-renewable have led to the search for more environmental-friendly and renewable sources of energy. Among the various options investigated is solar energy, which has been recognized as a strong contender for the reduction in emissions emitted during the combustion of conventional fuels and for the reduction of the national energy bill.

Photovoltaic solar energy (PV) is considered one of the renewable sources of energy. Hybrid photovoltaic/thermal system in the other hand is the continuity of the photovoltaic solar energy system, it combined both systems into one system known as Hybrid photovoltaic/thermal (PV/T or PVT) solar system [1]. As reported by Zondag [2], and again by Prakash [3], the system can be segregated into two parts; the photovoltaic technology which derived from solar cell technology and convert into electricity, and thermal solar technology which derived from the thermal collector and convert the solar energy into heat. Bhargava *et al.* [4] mentioned that the hybrid system is operated solely by the solar radiation. However, and in spite of their advantages, the applicability PVT system is limited due to some drawbacks, such as:

1. Non uniform cooling;
2. Low efficiency;
3. High cost;

4. Not suitable for integration with present roof system; and
5. Needs a larger space for separate systems.

As an alternative to PVT systems, the solar hybrid heating system, which uses a conventional source of energy to provide a heating load for certain applications, such as swimming pool heating, where the heating load in addition to the collected solar energy is supplied by auxiliary system, such as anconventional diesel fuel, whose cost is continuously increasing in addition to its severe impact on the environment due to the emission of different pollutants when it is burned. Consequently, it is necessary to select the most economical auxiliary system to use it alongside with the solar system to achieve the desired thermal comfort.

Evacuated Tube Collector (ETC) has been used as a tool to make use of solar energy. Excellent presentation for ETC, together with its various applications, such as space heating, domestic hot water, solar cooling, solar desalination, cooking, is presented in Ref. [5].

The thermal performance of a prototype solar cooker based on an evacuated tube solar collector with Phase Change Material (PCM) storage unit was investigated [6]. The design has separate parts for energy collection and cooking coupled by a phase change material (PCM) storage unit. Solar energy is stored in the PCM storage unit during sunshine hours and is utilized for cooking in late evening/night time. Noon and evening cooking experiments were conducted with different loads and loading times. Cooking experiments and PCM storage processes were carried out simultaneously. It was found

\* Corresponding author e-mail: A.aboushi@zuj.edu.jo.

that noon cooking did not affect the evening cooking, and evening cooking using PCM heat storage was found to be faster than noon cooking.

Experimental and numerical works on evaluating the performance of the two common types of evacuated tube solar water heaters for domestic hot-water applications was conducted by Chow *et al.* [7]. They used the single-phase open thermosyphon system and the two-phase closed thermosyphon system. It was shown that the daily and annual thermal performance of the two-phase closed thermosyphon solar collector is slightly better than the single-phase open thermosyphon design. However, the payback periods of the two are relatively the same because of the higher initial costs of the two-phase closed thermosyphon collector system. In addition, they concluded that although economically they are less attractive than the flat-plate type collector system, they are suitable for applications in advanced systems with higher temperature demands.

A year round energy performance monitoring results of two solar water heaters with 4m<sup>2</sup> flat plate and 3 m<sup>2</sup> heat pipe evacuated tube collectors (ETCs) operating under the same weather conditions in Dublin, Ireland, was conducted by Ayompe [8]. The annual average collector efficiencies were 46.1% and 60.7% while the system efficiencies were 37.9% and 50.3% for the FPC and ETC, respectively. Economic analysis showed that both Solar Water Heating (SWH) systems are not economically viable while Simple Payback Periods (SPPs) varied between 13 years and 48.5 years.

Mazarrón *et al.* [9] analyzed how the required tank water temperature affects the useful energy that the system is capable of delivering, and consequently its profitability. The results show how the energy that is collected and delivered to the tank decreases with increasing the required temperature due to a lower performance of the collector and losses in the pipes. The annual system efficiency reaches average values of 66%, 64%, 61%, 56%, and 55% for required temperatures of 40 °C, 50 °C, 60 °C, 70 °C, and 80 °C. As a result, profitability decreases as temperature increases.

A heat pipe evacuated tube solar collector has been investigated by Farzad *et al.* [10], both theoretically and experimentally. The results showed a good agreement between the experiment and theory. Using the theoretical model, the effect of different parameters on the collector's energy and exergy efficiency has been investigated. It is concluded that inlet water temperature, inlet water mass flow rate, the transmittance of tubes and absorptance of the absorber surface have a direct effect on the energy and exergy efficiency of the heat pipe evacuated tube solar collector. Increasing water inlet temperature in heat pipe evacuated solar collectors leads to a decrease in heat transfer rate between the heat pipe's condenser and water.

Jordan is an energy importing country; about 96% of its needs supplied from abroad as crude oil and refined products. The special situation of Jordan and other countries in the Middle East and the present world oil price suggest that renewable energy sources, such as solar energy, can be adapted much better to the needs of the country. Solar energy is considered the largest domestic energy source and it is very attractive because it is reliable, and pollution-free. Currently, the most common fuel used

for heating is heating oil, which recently has witnessed a dramatic cost increase. This necessitated researches to look for alternative sources of energy for heating purposes.

The main objective of the present work is to design, install and to test a solar heating system that may be used to heat up a swimming pool, this system may be used as a standalone or operates with an auxiliary system (hybrid system). In the case of the latter option, a control system will be used to act as an energy management system, which will optimize the contribution of auxiliary system to provide the required heating of a swimming pool.

## 2. Experimental Work

The main components of the experimental setup are shown in Figure (1); as indicated, the following instrumentations were used to conduct the present work:

1. Evacuated tube collectors with a total number of 85 tube, these collectors are installed on the roof of the house where the swimming pool is located. This number of the tube was selected based on initial calculations such that the collected solar heat will cover the total required heating load to maintain the pool at 30 °C during summer season;
2. Kipp and Zonen CAM Albedo meter, which is used to measure the solar incident radiation in W/m<sup>2</sup>.
3. A national Instrument DataLogger, that is used to record and store the collected hourly solar radiation and the hourly pool temperature;
4. 30 kW.hr locally made Electric heater;
5. 30 kW.hr gas boiler (Lamborghini);
6. 50 000 Kcal Chapeeand diesel boilers, fitted with Lamborghini burner.

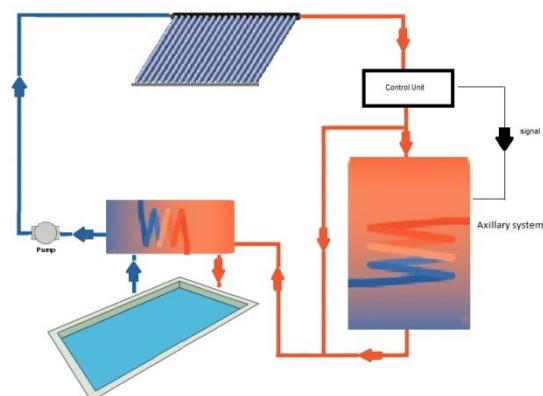


Figure 1. Experiment setup

After the installation of the above instrumentations at the site, experimental work was conducted during the summer season, including the measurements of solar incident hourly solar radiation using the albedo meter and swimming pool temperature at five different locations using thermocouples, with the measured data recorded and stored in the data acquisition system. In addition, water inlets and outlets temperatures were recorded. All temperatures measurements were conducted using K-type thermocouples, which are connected to the data acquisition system. Preliminary conducted work during summer season indicated that the total heating load required to maintain the pool at a temperature of 30 °C was provided

by the collected solar energy and hence no auxiliary system was required.

Further work was conducted in Fall and winter seasons; this is to cover a year round measurements (taking into account that both spring and fall measurements are almost similar to each other). In addition to the heating load provided by solar energy, work was conducted to find out most economical auxiliary heating system (diesel fuel, electrical power and natural gas) to maintain the pool at the desired temperature all year round.

In order to optimize the percentage of the heating load to be supplied by each heating auxiliary system, a temperature controlled Energy Management System (EMS) was designed installed and used. This EMS was installed in a way to sense the evacuated tube collector outlet water temperature, such that if this value of the water outlet temperature drops below 60 °C (this corresponds to an average pool temperature of 30 °C), the auxiliary system is triggered by a signal from the energy control system in order to increase the pool water temperature to a value of 30 °C.

It is to be noted that, for each auxiliary system in operation, the experimental data collected were:

1. The hourly incident radiation;
2. the average pool temperature;
3. the energy consumed by the auxiliary system;
4. the ambient temperature;
5. the water outlet temperature from pool, which was found almost identical to the average pool temperature;
6. the inlet water temperature to the pool, which was noticed to be almost constant due the operation of the auxiliary system to maintain the pool temperature at a constant value;
7. the water inlet temperature to solar collector, which was almost of the same value of the water outlet temperature from the pool. This is due to the fact that the pipes are well insulated; and
8. the water outlet temperature from the collector, if this value drops below 60 °C, the control system triggers the auxiliary system.

The data above were collected over three days during which metrological data were almost identical and, then, average results were estimated this to ensure the repeatability of the obtained data. It is to be noted that the measurements of the above data were conducted on a daily basis during the year. Not all data will be presented here; instead, selected data will be presented and discussed in detail.

### 3. Results and Discussion

Hourly data were collected, stored and, then, analyzed. These data were obtained around the whole year, starting in the summer of the year of 2013 to the end of spring of the year 2014. For simplicity, only two cases will be presented and discussed in the present paper. The first one is during the summer season (the day 21<sup>st</sup> of June was selected), while the second case is selected during the winter season (17<sup>th</sup> of February). These two cases

represent the hottest and the coldest days in Amman during the period of the experimental work.

### 4. Summer Measurements

Figure (2) shows typical hourly solar radiation data during the day of 21<sup>st</sup> of June. As indicated, the incident solar radiation increases in the morning to a maximum value during the day, beyond which it starts to decrease with time in the afternoon. The pool temperatures measurements during the months of June through September were found to slightly exceed the desired required temperature, which is 30 °C. Consequently, the solar radiation collected by the collectors was sufficient to completely heat up the swimming pool and to maintain its high temperature; no auxiliary systems were required to heat up the swimming pool during summer season.

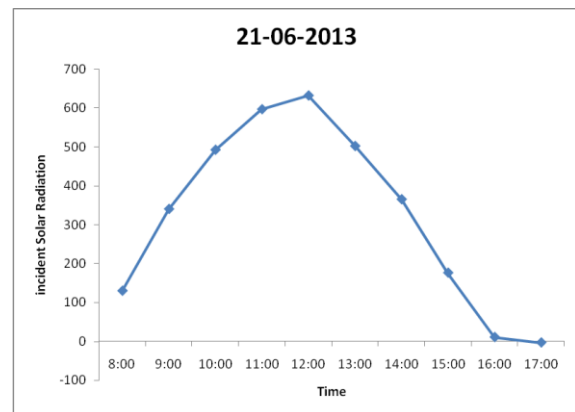


Figure 2. Hourly Solar Radiation at 21<sup>st</sup> /6/2013

### 5. Winter Measurements

Typical measurements for the hourly solar radiation and the temperature distribution within the pool during the day of 17<sup>th</sup>/02/2014 are shown in Figures (3) and (4), respectively. An auxiliary heating system were used to maintain the pool temperature at a desirable temperature of 30 deg. Furthermore, it was found that the total heat required to heat up the pool from 20.4 °C up to 30 °C was 2090 MJ, and the solar contribution to this heat was 197 MJ. While the auxiliary system provided 9%.

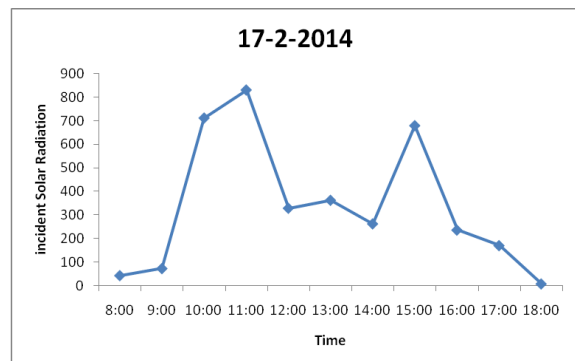
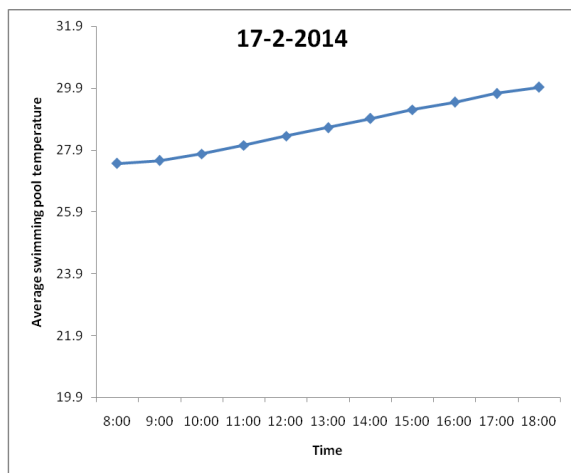


Figure 3. Hourly solar radiation on 17<sup>th</sup>/02/2014 (auxiliary system powered by natural gas)



**Figure 4.** Temperature distribution within the pool during the day of 17<sup>th</sup>/02/2014 (auxiliary systems powered by natural gas)

## 6. Conclusion

Solar hybrid system was designed, installed and tested using a swimming pool. Three types of auxiliary systems were used, in addition to the solar system, namely Liquefied Petroleum Gas (LPG), electrical boiler and diesel boiler. From the present work, the following may be concluded:

1. During summer, the heating required to maintain the pool at a desirable temperature was completely covered by the solar system alone with no need to operate an auxiliary system;
2. during fall, spring and winter, an auxiliary system was required to maintain the pool at the desirable temperature which the solar system provided; and
3. based on Jordanian current energy cost, LPG was found to be the most economical auxiliary system to be used with the solar system.

## Acknowledgement

The author would like to thank the Deanship of Research at Al Zaytoonah University of Jordan for financing and funding the present research work.

## References

- [1] Tripanagnostopoulos Y. Aspects and improvements of hybrid photovoltaic/ thermal solar energy systems. *Solar Energy* 2007; 81(9):1117–31.
- [2] Zondag HA. Flat-plate PV-thermal collectors and systems: a review. *Renewable and Sustainable Energy Reviews* 2008; 12:891–959.
- [3] Prakash J. Transient analysis of a photovoltaic-thermal solar collector for cogeneration of electricity & hot air/water. *Energy Conversion Management* 1994; 35(11):967–72.
- [4] Bhargava AK, Garg HP, Agarwal RK. Study of a hybrid solar system—solar air heater combined with solar cells. *Energy Conversion and Management* 1991; 31:471–9.
- [5] Soteris A. Kalogirou. Solar thermal collectors and applications. *Progress in Energy and Combustion Science* 30 (2004) 231–295.
- [6] Sharma, S. D. *et al.* an evacuated tube solar collector with a PCM storage unit. *Solar Energy*, 2005, 78, (3), 416-426.
- [7] -Tai Chow, Zhaoting Dong, Lok-Shun Chan, Kwong-Fai Fong, Yu Bai. Performance evaluation of evacuated tube solar domestic hot water systems in Hong Kong Tin. *Energy and Buildings* 43 (2011) 3467–3474.
- [8] L.M. Ayompea\*, A. Duffy a\*, M. Mc Keeverc, M. Conlon c, S.J. McCormack. Comparative field performance study of flat plate and heat pipe evacuated tube collectors (ETCs) for domestic water heating systems in a temperate climate. *Energy* 36 (2011), pp. 3370-3378.
- [9] Fernando R. Mazarrón, Carlos Javier Porras-Priet, José Luis García , Rosa María Benavente. Feasibility of active solar water heating systems with evacuated tube collector at different operational water temperatures. *Energy Conversion and Management* Volume 113, 1 April 2016, Pages 16–26.
- [10] Jafarkazemi Farzad, Ahmadifard Emad, Abdi Hossein. Energy and exergy efficiency of heat pipe evacuated tube solar collectors. *Thermal Science* 2016 Volume 20, Issue 1, Pages: 327-335.

# A Comparative Study of Single Phase Grid Connected Phase Looked Loop Algorithms

Ashraf Samarah\*

\* *Electrical Energy Department, Faculty of Engineering, Al-Balqa Applied University, Jordan*

*Received Nov 16, 2016*

*Accepted June 15, 2017*

## Abstract

A Phase-Locked Loop (PLL) is a vital part of power inverters for achieving synchronization with the utility grid. Throughout the phase angle of the grid voltage, a reference signal is generated in order to synchronize the operation condition of the renewable energy generation systems with the utility grid. The present paper presents a comparative study of the enhancement for conventional phase-locked loop using four different filters, including adaptive notch filter, second order adaptive notch filter, generalized integrator filter and second order generalized integrator filter. A comparison among these four studied improvements was conducted under normal operation condition. On the other hand, the performance of these filters was tested under two abnormal scenarios; voltage sag and phase jump. The results showed that the second order generalized integrator based PLL has superior performance over the other filters based PLL under both normal and fault operation conditions. In contrast, the adaptive notch based filter based PLL has the lowest response under both operation conditions.

© 2017 Jordan Journal of Mechanical and Industrial Engineering. All rights reserved

**Keywords:** *Phase-Locked Loop; Adaptive Notch filter; Generalized Integrator; SOGI; enhanced Phase-Locked Loop.*

## 1. Introduction

Worldwide, electric power systems have experienced a rapid change due to the integration of new technologies, such as photovoltaic, wind generation and/or fuel cells generation systems. These comprehensive transformations into new generation technologies became a result of the depletion in the conventional fossil fuel resources, increasing the concerns regarding the environment. Power electronics have been used to interface these generation technologies with the conventional power system [1]. However, this interface creates inevitable new challenges for efficient and reliable operating and controlling the utility power grid.

For grid-connected inverters, phase angle is a vital piece of information for an accurate and efficient synchronization. Thus, a phase-locked technique is required to achieve this synchronization. In this research, a specific type of phase-locked loop technology is studied based on four different filter structures. Then, the performance of the four studied filters based Phase-Locked Loop (PLL) is compared under normal and fault operation conditions.

Voltage source inverters enable the new generation technologies to be utilized as a dynamic voltage regulator through dynamic controlling of the voltage at the point of common coupling. However, they have more controlled variables compared with the conventional generation

technologies [2]. The fundamental phase angle of the utility voltage, for example, is a critical controlled variable for the grid synchronization. This angle is used to generate a reference signal in order to synchronize the operation condition of the distributed generation systems with the utility grid. As a result, an accurate phase tracking method is needed to achieve the phase angle information of the grid. Various phase tracking methods were developed which can be classified into two approaches. These are an open loop tracking approach (such as low pass filters, Kalman method, and space vector method) and a closed loop approach, such as a Phase-Locked Loop (PLL) [3].

The PLL approach has been widely used in different systems, such as communication, motor control and other industrial applications. In power system fields, this technique has been adopted to provide fast and accurate synchronization between the generation side and the utility [4, 5, 6]. It should have a high immunity to disturbances, such as harmonics, noises, sags, unbalances and other distortions.

The PLL technique can be divided according to its structure into Stationary Reference (SR) frame-based PLL, Synchronously Rotating Reference frame (SRF), or Zero Crossing Detection (ZCD)-based PLL. The ZCD-based PLL method is sensitive to frequency transient and distortion notch [7]. SR frame and SRF-based PLLs do not work accurately during unbalance condition [8, 9]. Thus, the Enhanced PLL (EPLL) has been adopted as it has a

\* Corresponding author e-mail: samarah@bau.edu.jo.

high degree of immunity to harmonic and unbalance conditions over conventional PLLs [5], [10, 11].

The operation principle of the conventional PLL is accomplished through a Phase Detector (PD), where the fundamental phase component is estimated [13]. Therefore, the output signal of the PD is filtered by a Loop Filter (LF) before entering a Voltage Controlled Oscillator (VCO), where it is synchronized with the input signal as shown in Figure (1)

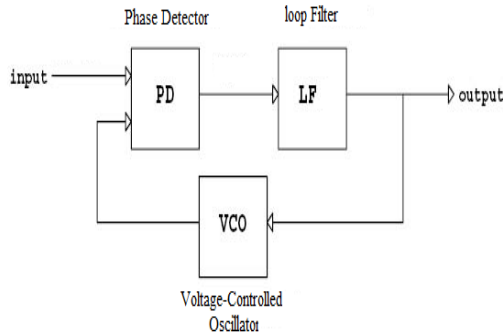


Figure 1. Block diagram of a basic phase locked loop

An Adaptive Filter (AF) works on the concept of the Adaptive Noise Cancelling (ANC) concept, at which its own parameters are automatically adjusted. An Adaptive Notch Filter (ANF) technique is used in PLL to attenuate specific range of frequencies of the input signal to enhance the performance of the PD of the conventional PLL. Figure (2) illustrates the main concept of ANF where the output of the VOC is applied to the PD as a reference signal.

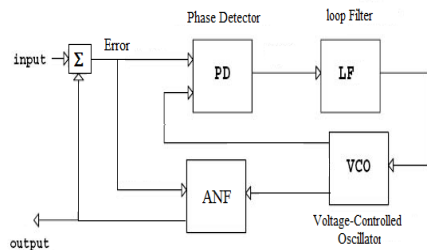


Figure 2. Block diagram of an enhanced phase locked loop with adaptive notch filter

PD causes a phase shift by 90° between the input phase signal and the reference phase signal. Yet, ANF generates zero-signal for the PD as the PLL locked to the input signal. The design of a PLL can be optimized more by introducing a second order ANF which is built based on the ANC where the reference signal need to be filtered. However, the amplitude integrator in the second order ANF does not act ideally for the sinusoidal input signal with the center frequency of the VCO but depends on of the input signal, and its output contains a steady-state error [9].

In order to cancel this error, the Generalized Integrator (GI) adaptive filter is adopted. In this technique, the error is cancelled at a resonance frequency. However, as the GI based filter is a function of feed-forward frequency which restricts its applications in a variable-frequency environment. Thus, the Second Order Generalized Integrator based filter (SOGI) has been introduced as a good technique for variable frequency application, since it

is a function of the gain only [14, 15]. Figure (3) shows the structure of the four studied filters.

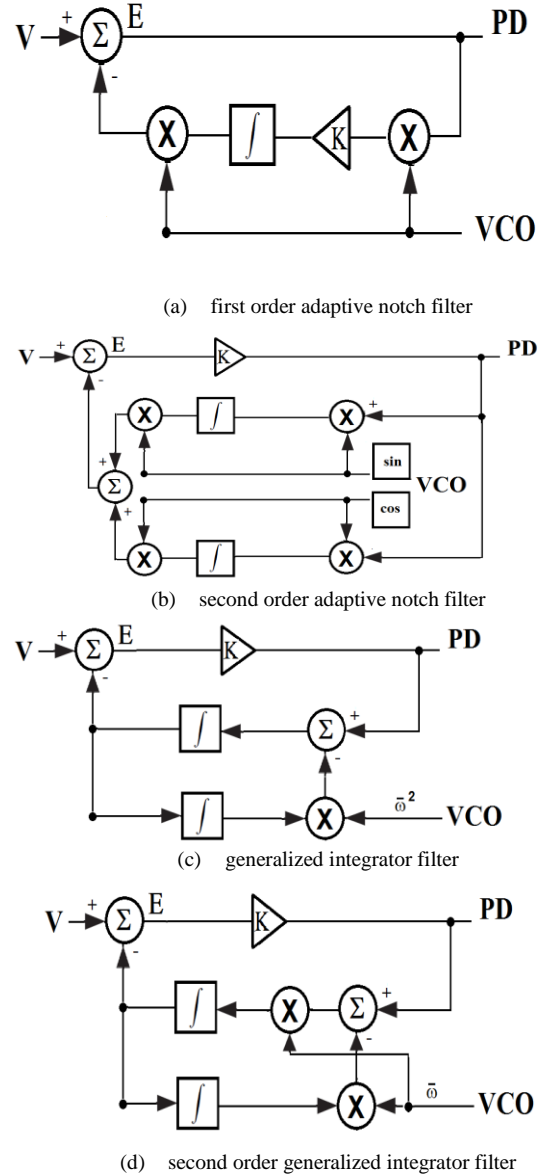


Figure 3. Structure of four filters based phase locked loop

The aim behind the present work is to design the phase-locked loop with conventional adaptive notch filter, second order adaptive notch filter, generalized integrator filter and second order generalized integrator. Then, the performance of the enhanced phase-locked loop algorithms are simulated and analyzed in the Matlab/Simulink computer environment under normal operation condition and then during fault scenarios

2. Methodology

The mathematical modeling of a PLL is adopted based on the system in [9- 11, 13], where the Phase Detector (PD) finds the difference between the input signal applied to the system and the output signal generated by VCO, which is known as the error. The output of PD has the double frequency ripple which can be partially removed using a loop filter. As a result, the LP bandwidth needs to

be small in order to remove the double frequency ripple and other distortions but not too small that affects the system response. Finally, the VCO changes its operating frequency when the error is not zero in order to generate the output signal at center frequency.

After the parameters of the design were calculated, the four studied PLLs were tested under a normal operation condition in Matlab environment. During normal operation condition, a single phase voltage 1 per unit was applied to the four filters based PLLs as an input with 50 Hz frequency, where the performance of the PLLs is compared. After that, a comparison of the PLLs is done under two fault scenarios: voltage sag and phase jump.

Voltage sag is defined as reductions in the grid voltage, lasting from a cycle to seconds, which are caused by unexpected increases in loads such as faults, or by sudden increases in source impedance. In this scenario, voltage amplitude of input signal is reduced by 70% from its value, during the second half of sample period, which gives a rise to high short circuit currents. Finally, during the phase jump scenario the phase is jump after one minute of simulation period.

The PLL can mathematically be interpreted as in equations (1), (2) and (3):

$$e(t) = V_{in}(t) - V_{out}(t) \quad (1)$$

$$V_{in}(t) = V \sin(\omega t - \varphi_{in}) \quad (2)$$

$$V_{out}(t) = V \sin(\omega t - \varphi_{out}) \quad (3)$$

where  $e(t)$  is the output signal of the PD, which is known as error signal,  $V_{in}(t)$ , is the input signal of EPLL, and  $V_{out}(t)$  is the output signal of the PLL. Clearly, that the error is a multivariable function of voltage magnitude, frequency and phase angle. As a result, this error cost function needs to be minimized in the sense of the linear least square, as shown in equation (4).

$$E(V, \omega, \varphi) = \|V_{in} - V_{out}\|^2 \quad (4)$$

By using the method of steepest descent, the following three differential equations can be obtained:

$$\dot{v}(t) = K e(t) \sin(\varphi_{out}) \quad (5)$$

$$\Delta \dot{\omega}(t) = K_i e(t) \cos(\varphi_{out}) \quad (6)$$

$$\dot{\varphi}_{out}(t) = (\omega_0 + \omega_{out}) K_p e(t) \cos(\varphi_{out}) \quad (7)$$

where  $K, K_i$ , and  $K_p$  are step size. By using linear analysis [12], equations (5), (6) and (7) can be expanded to:

$$\dot{V} \approx \frac{K}{2} (V_{in} - V_{out}) \quad (8)$$

$$\dot{\omega}(t) = \frac{K_i}{2} V_{in} (\varphi_{in} - \varphi_{out}) \quad (9)$$

$$\dot{\varphi}(t) = (\omega_{out} - \omega_{in}) + \frac{K_p}{2} V_{in} (\varphi_{in} - \varphi_{out}) \quad (10)$$

where  $\bar{\omega} = \omega_{out} - \omega_{in}$  is the estimated angular frequency and  $\bar{\varphi} = \varphi_{out} - \varphi_{in}$  is the estimated phase. From these equations the approximated transfer function of the closed-loop system gives:

$$\frac{K_p V_{in}}{2} = 2\zeta\omega_n \quad (12)$$

$$\frac{K_i V_{in}}{2} = \omega_n^2 \quad (13)$$

$$K = \frac{2}{\tau} \quad (14)$$

The design parameters are shown in Table (1), where  $\zeta$  is damping ratio, which controls how fast the filter reaches its settle point and how much overshoot can have. In general, most of the control systems, except for robotic control systems, are designed with damping factor  $\zeta < 1$  to achieve a high response speed consistent [16]. Thus, damping factor  $\zeta = 0.7$  is chosen where, at this value, the system converges reasonably fast. Note that feed-forward frequency is;  $\omega_0 = 100\pi$  rad/s, at which the output of the regulator is zero once the regulator has tracked the phase.

The design parameters are shown in Table (1), where  $\zeta$  is damping ratio, which controls how fast the filter reaches its settle point and how much overshoot can have. In general, most of the control systems, except for robotic control systems, are designed with damping factor  $\zeta < 1$  to achieve a high response speed consistent [16]. Thus, damping factor  $\zeta = 0.7$  is chosen where, at this value, the system converges reasonably fast. Note that feed-forward frequency is  $\omega_0 = 100\pi$  rad/s, at which the output of the regulator is zero once the regulator has tracked the phase.

**Table 1.** Design Parameters

Parameters	Values
$\zeta$	0.7
$\tau$	2ms
$\omega_0$	314rad/s
K	500
Kp	10,000
Ki	200
F	50Hz

To do a comparison between control systems, two indices are considered: the integration for the square of the error (ISE) and the integration for the absolute magnitude of the error (IAE) are given by:

$$ISE = \int_0^{\infty} e(t)^2 dt \quad (15)$$

$$IAE = \int_0^{\infty} |e(t)| dt \quad (16)$$

where the system with the minimum indices is considered the best control system.

### 3. Results and Discussions

To test the performance of a fast and accurate synchronization of PLL, it has been simulated in MATLAB under normal and grid fault conditions. During different fault scenarios, the single phase voltage experience transients due to the appearance of voltage sags and frequency jump.

3.1. The PLL Response under Normal Operation Condition

The second order generalized integrator based PLL has the fastest and the most efficient response, as depicted in Figure (4-d), compared with other filters based PLLs. This result shows the ability of SOGI filter based PLL of

tracking the input signal without delay due to its resonance at the fundamental frequency [17]. GI-based PLL has the second best response, as illustrated in Figure (4-c), where it locked the reference signal during the first cycle. While the ANF-based PLL tracking the input signal, after about 70 ms, makes it the slowest tracking technique among the four filters.

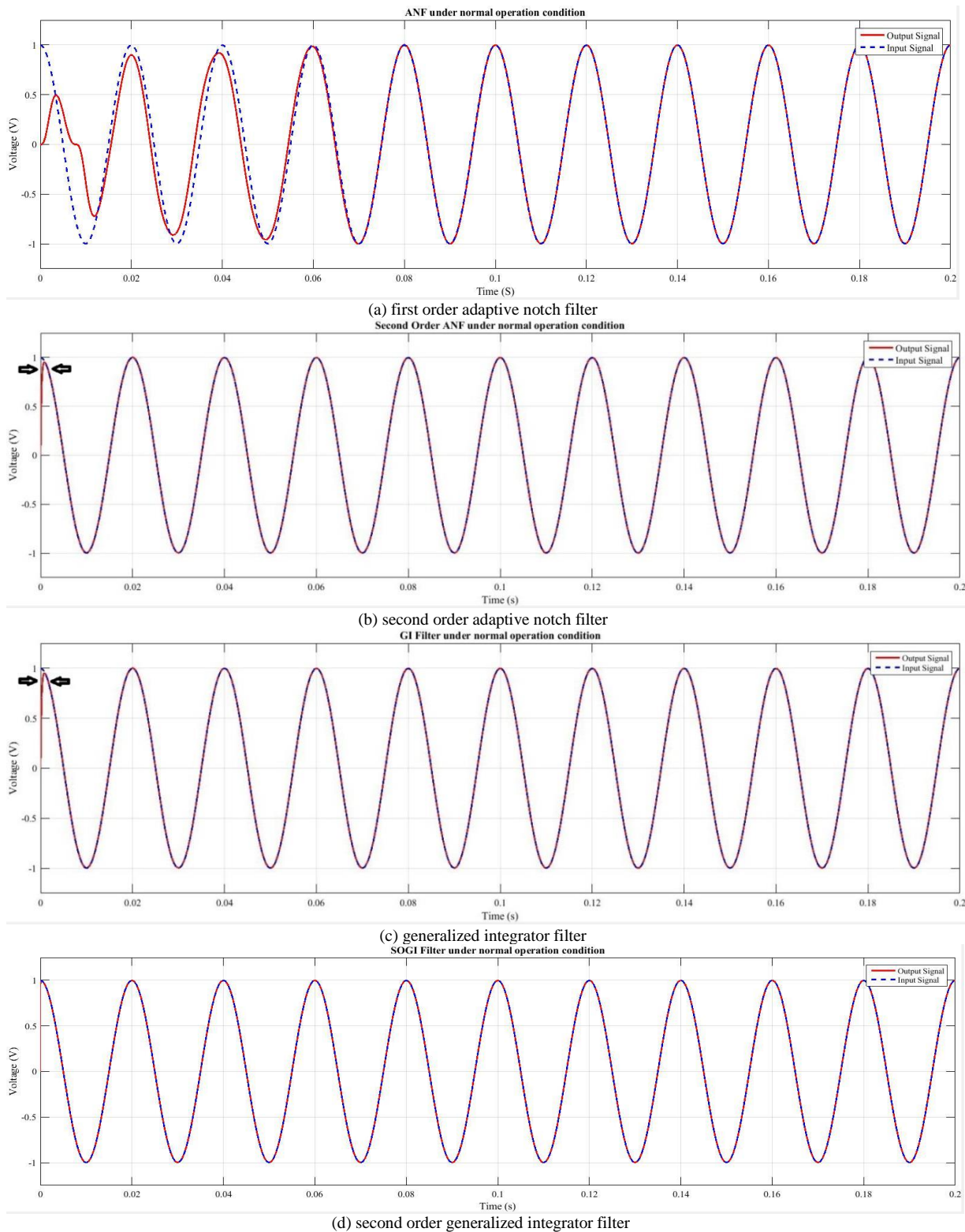


Figure 4. the PLL response during normal operation condition

Moreover, Figure (5) illustrates the error signal of the four proposed techniques. Clearly, the SOGI filter-based PLL has zero error signal faster than the other three filter-based PLLs. In addition, the error signal of GI filter and second order ANF-based PLL have almost the same response. The amplitude integrator in the second order ANF and GI filter do not act ideally for the sinusoidal input signal, as mentioned [9]. Moreover, the error signal of SOGI filter-based PLL reaches zero steady state much faster than other filters.

The integration error values for the four filters based PLL are depicted in Table (2). It is obvious that SOGI filter-based PLL has the lowest ISE and IAE values, which indicates that SOGI has the best response, compared with the other three filters under normal operation condition. In comparison, ANF has the highest ISE and IAE, which shows that ANF-based PLL has the worst phase locking characteristics among the four proposed filters.

**Table 2:** The ISE and IAE for the Four Proposed Filters Based PLLs under Normal Operation Condition

Error Signal	ANF	Second Order ANF	GI Filter	SOGI Filter
ISE	5.602mV	99.68μV	99.72μV	3.175μV
IAE	14.22mV	0.4111mV	0.422mV	15.61μV

3.2. The PLL Response under Different Fault Conditions

Now, the performance of the four filters based PLL are simulated for two different fault scenarios. The following is a detailed presentation of these scenarios.

3.2.1. Scenario 1: Voltage Sag

During this scenario, as depicted in Figure (6), the ANF-based PLL output signal was able to lock with the input signal after about two cycles from fault, despite of its ability for providing an output signal locked to the fundamental component of the input signal in its amplitude and frequency [3], while the SOGI-based PLL keeps tracking the input signal even during fault. In contrast, both second order ANF and GI filter-based PLL show acceptable level of immunity against voltage sag.

Further, Figure (7) depicts that once the SOGI-based PLL has the lowest zero error signal during fault condition, while the ANF-based PLL error signal experiences the oscillations after the fault occurs. This oscillation in error signal resulted experimentally in [18]. As its output, signal locked to the fundamental component of the input signal in its amplitude and frequency results in a high steady state error.

Clearly, the SOGI filter-based PLL has the lowest error indices among other filter-based PLLs, as shown in Table (3). In addition, the ANF-based PLL has the highest indices due to its operation principle as discussed before.

**Table 3:** The ISE and IAE for the Four Proposed Filters Based PLLs under Voltage

Error Signal	ANF	Second Order ANF	GI Filter	SOGI Filter
ISE	1.123mV	0.1379mV	0.1034mV	0.274μV
IAE	5.244mV	3.61mV	3.209mV	0.3172mV

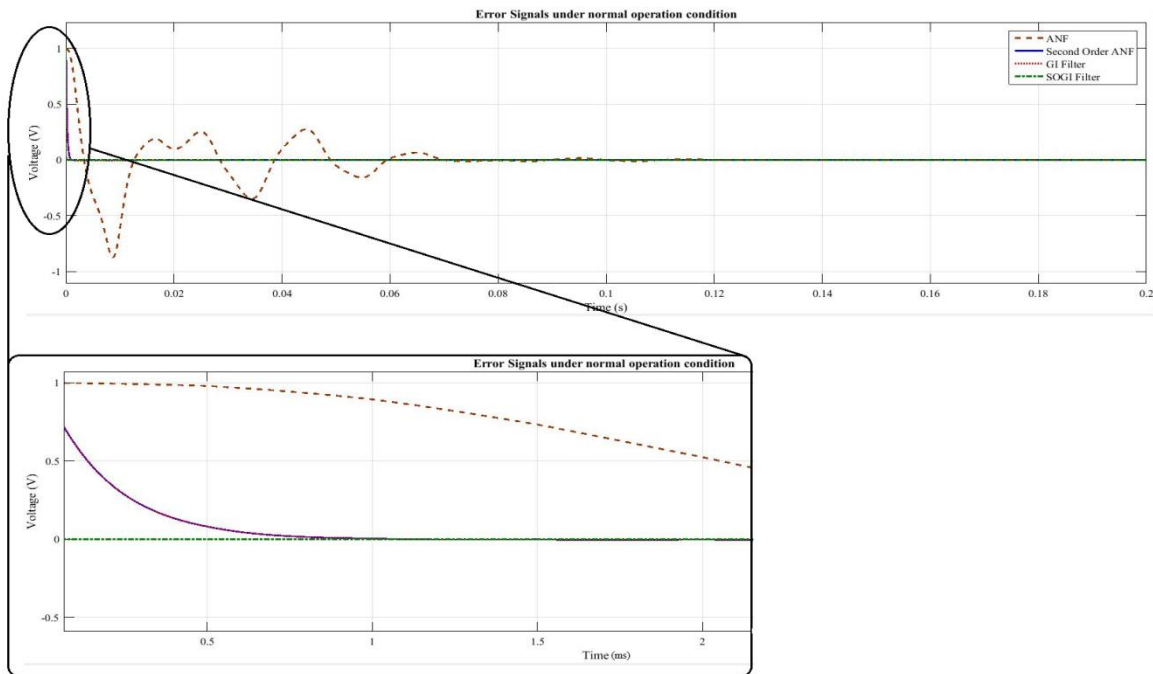


**Figure 5.** Error signal under normal operation condition

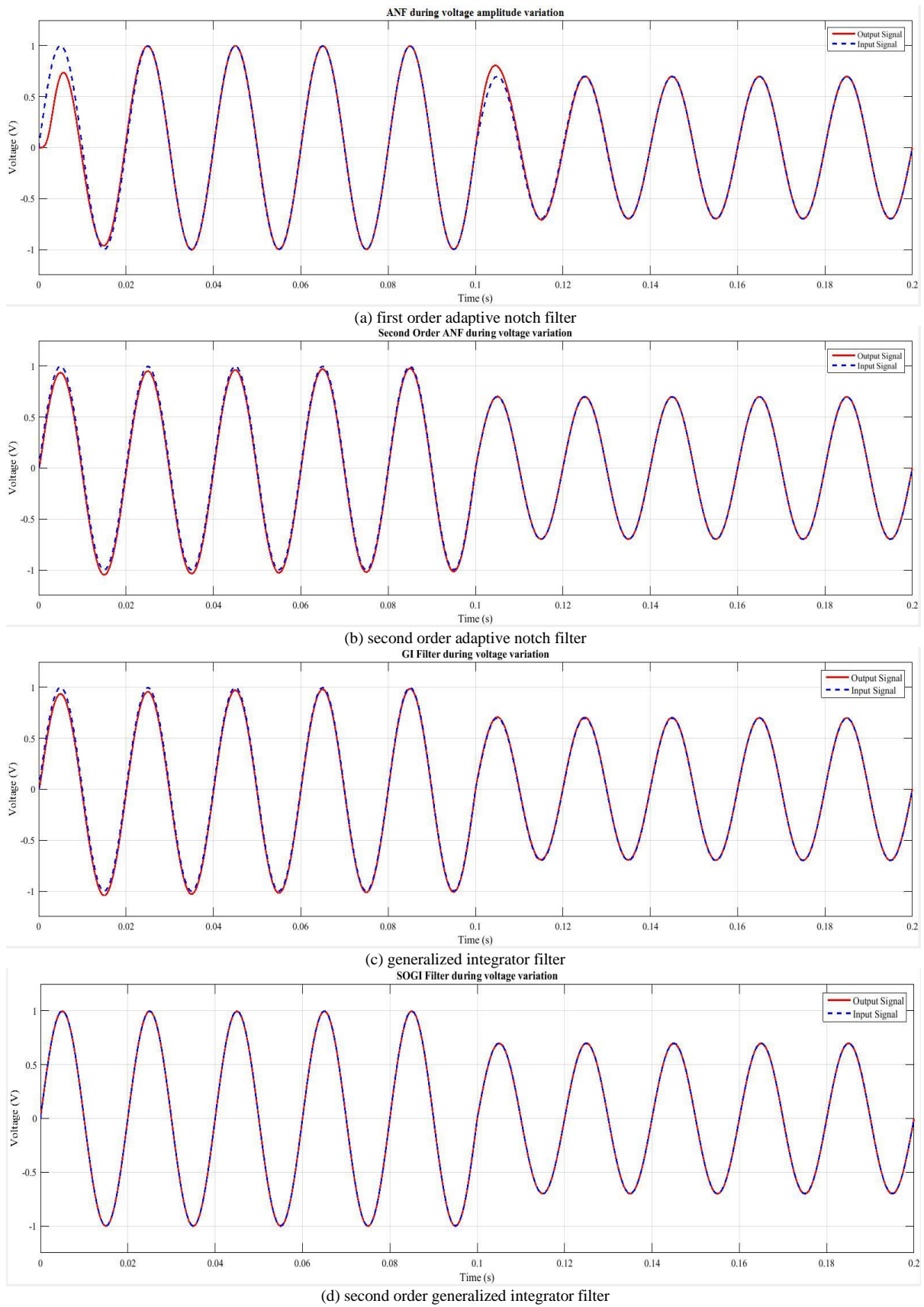


Figure 6. the PLL response during voltage sag

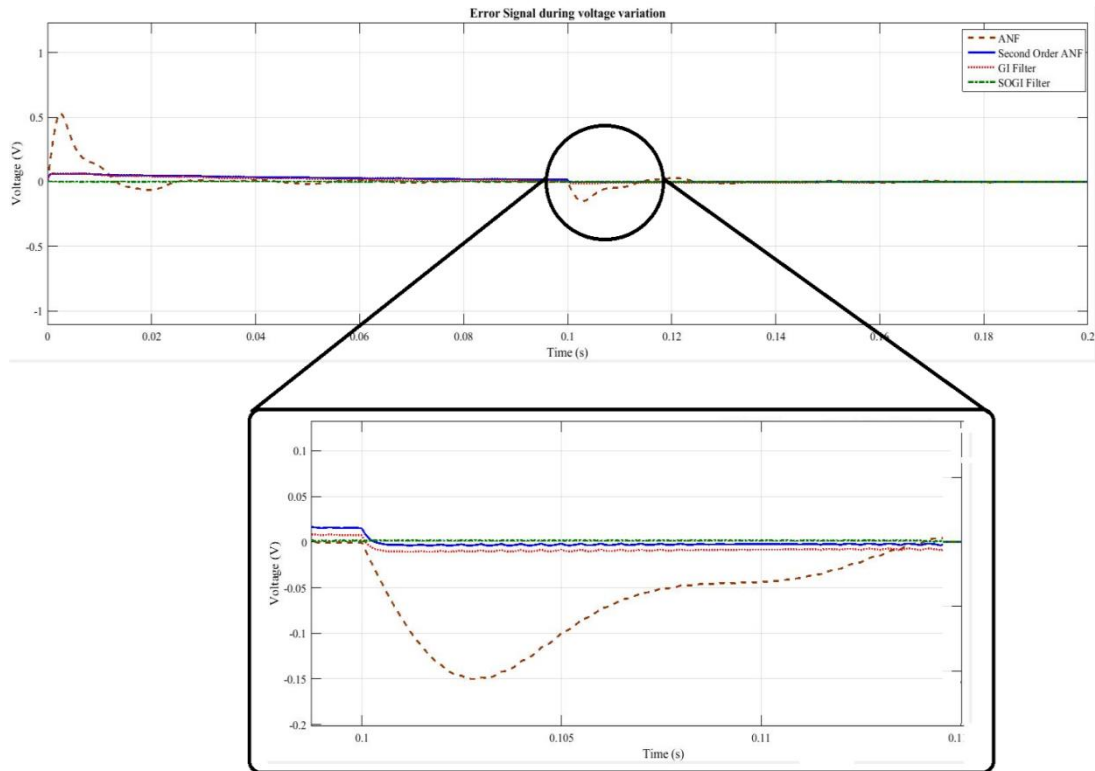


Figure 7. Error signal under voltage sag condition

3.2.2. Scenario 2: Phase Jump

During this scenario, a phase jump occurs after about 86ms. As illustrated in Figure (8), the ANF-based PLL mistraces the input signal for about three cycles after the faults occur. This result shows that the ANF-based PLL is highly effected by phase jump, in comparison with the other three filters, which are able to keep locked with the input signal even after the phase jump take place. However, the SOGI-based PLL has the lowest error response during phase jump, as shown in Figure (9), while ANF-based PLL error signal experiences a high oscillation once the fault takes place. The same result was reported by [18] experimentally during phase. This severe response is attributed to the fact that ANF-based PLL output signal is locked to the fundamental component of the input signal in

its amplitude and frequency which reflects in a high oscillation error once any distortion affect the input signal. Finally, the errors of the proposed filter-based PLLs are also tested using ISE and IAE indices, as shown in Table (4). It is obvious that SOGI-based filter has the lowest ISE and IAE, while the ANF-based PLL has the highest ones.

Table 4: The ISE and IAE for the four proposed filters based PLLs under phase jump condition

Error Signal	ANF	Second Order ANF	GI Filter	SOGI Filter
ISE	11.43mV	0.2834mV	0.2583mV	0.4411mV
IAE	23.23mV	3.598mV	3.321mV	0.2939mV

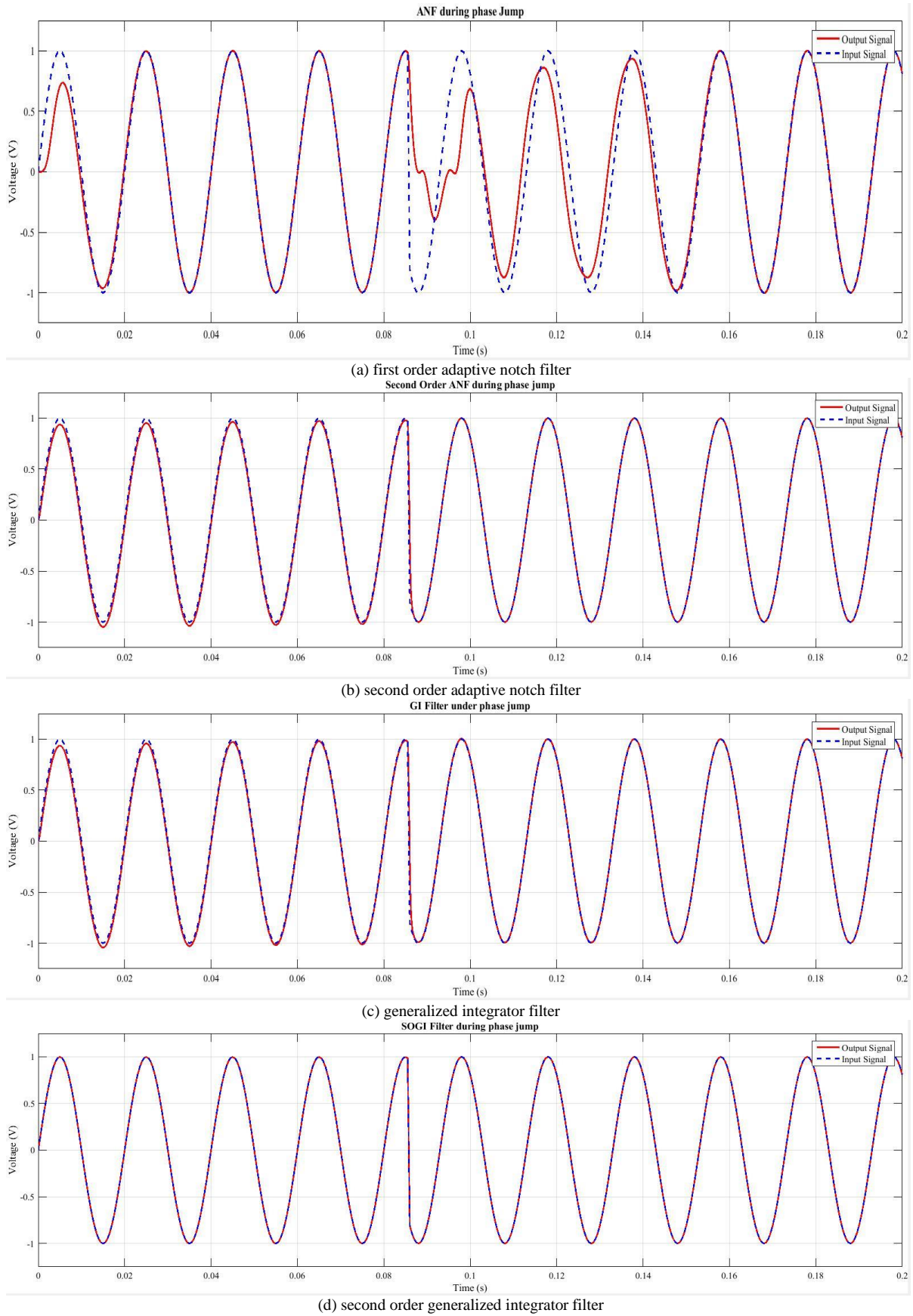
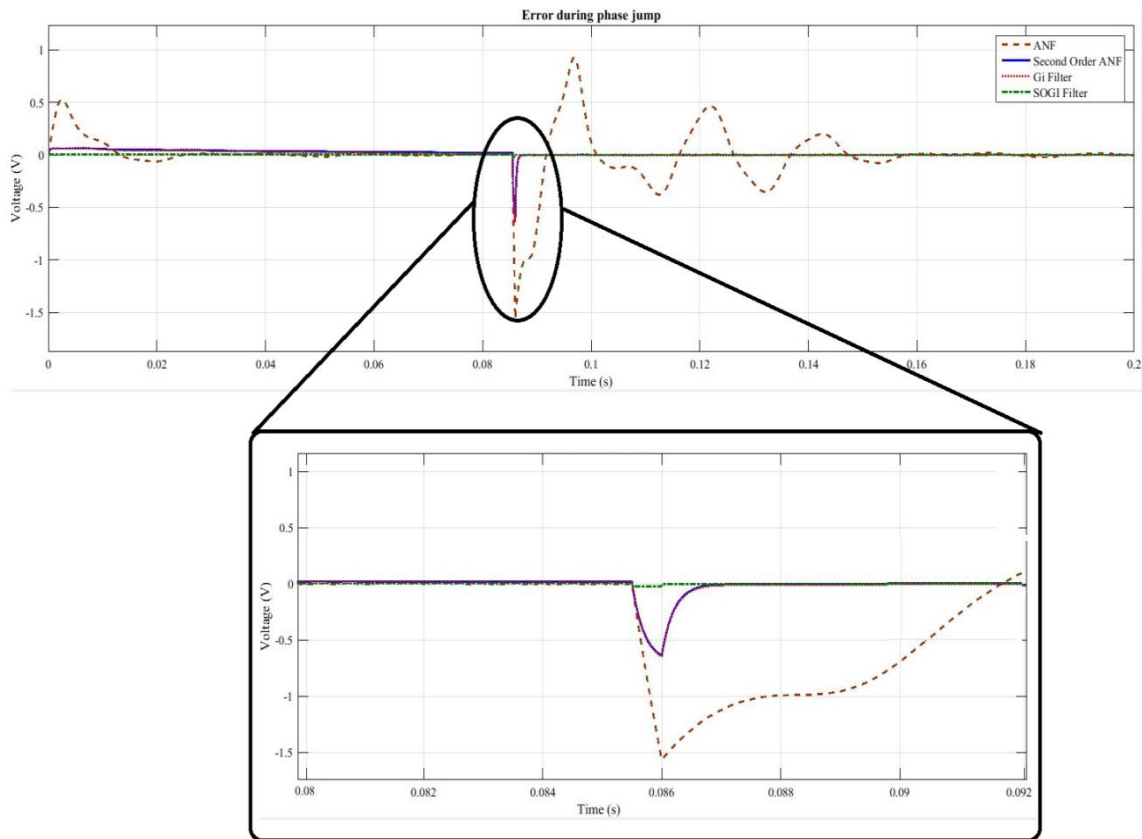


Figure 8. the PLL response during phase jump



**Figure 9.** Error signal under phase jump condition

#### 4. Conclusion

In order to achieve synchronization with the utility grid, a phase locked loop is used. It generates a reference signal to synchronize the operation condition of the inverter side with the utility grid. In the present study, an enhancement for a conventional phase locked loop using four different filters, including adaptive notch filter, second order adaptive notch filter, generalized integrator filter and second order generalized integrator filter, were investigated. Then a comparison between these four proposed improvements was conducted under normal and two abnormal operation condition scenarios: voltage sag and phase jump.

The results show that the second order generalized integrator based PLL has a superior performance over other filters-based PLL under both normal and fault operation conditions. During normal condition, the SOGI based PLL locked the input signal very fast and accurate. Moreover, it kept tracking the input signal even after the occurrence of a fault condition, such as a phase jump or voltage sag.

The ANF-based PLL had a sluggish response to reach zero steady state error signal during normal operation condition as well as during voltage sag. In addition, its error signal experienced a high oscillation during phase jump at which the output signal of this PLL missed the input signal and relock back again after three cycles.

In comparison with the second order ANF-based PLL, the GI-based PLL has a negligible enhancement over the former under both normal and abnormal operation condition.

In general, the four different filter techniques have an acceptable performance during the proposed operation conditions. The preferability of any of these filters-based PLL depends on its application in power system environment.

#### References

- [1] F. Blaabjerg, Z. Chen and S. B. Kjaer, "Power Electronics as Efficient Interface in Dispersed Power Generation Systems", *Trans. on Power Electronics* Vol. 19, No.5, 2004, 1184-1194
- [2] K. T. Tan, P. L. So and Y. C. Chu, "Control of parallel inverter-interfaced distributed generation systems in microgrid for islanded operation", *IEEE 11th International Conference on Probabilistic Methods Applied to Power Systems (PMAPS)*, Singapore, 2010, 1-5
- [3] M. Karimi-Ghatemani and M. R. Iravani, "A Method for Synchronization of Power Electronic Converters in Polluted and Variable-Frequency Environments", *IEEE Trans. on Power Systems*, Vo. 19, No.3, 2004, 1263-1270
- [4] G. C. Hsieh and J. C. Hung, "Phase-locked loop techniques—A survey", *IEEE Trans. Ind. Electron.*, Vol. 43, No.6, 1996, 609–615
- [5] S. K. Chung, A phase tracking system for three phase utility interface inverters, *IEEE Trans. on Power Electronics* Vol. 15, No.3, 2000, 431 – 438
- [6] L. N. Arruda, S. M. Silva, and B. Filho, "PLL structures for utility connected systems", in *Proc. IEEE-IAS Annu. Meeting*, Vol. 4, 2001, 2655–2660.
- [7] J. W. Choi, Y. K. Kim and H. G. Kim, "Digital PLL control for single-phase photovoltaic system", *IEE Proceedings - Electric Power Applications* Vol. 153, No. 1, 2006, 40 – 46
- [8] A. Timbus, M. Liserre, R. Teodorescu and F. Blaabjerg, "Synchronization methods for three phase distributed power generation systems - An overview and evaluation", *IEEE 36th Power Electronics Specialists Conference*, Recife, 2005, 2474 – 2481
- [9] M. Karimi-Ghartemani and M. R. Iravani, "A signal processing module for power system applications", *IEEE Trans. on Power Delivery* Vol. 18, No.4, 2003, 1118 – 1126
- [10] M. Karimi-Ghartemani and M. Reza Iravani, "Robust and Frequency-Adaptive Measurement of Peak Value", *IEEE Trans. on power delivery* Vol. 19, No. 2, 2004, 481-489
- [11] M. Karimi-Ghartemani, H. Mokhtari, M. R. Iravani, "A single Processing System for Extraction of Harmonics and Reactive Current of Single-Phase Systems", *IEEE Trans. on Power Delivery*, Vol. 19, No. 3, 2004
- [12] M. Bobrowska-Rafal, K. Rafal, M. Jasinski and M. P. Kaszmierkowski, "Grid synchronization and symmetrical components extraction with PLL algorithm for grid connected power electronic converters – a review", *Bulletin of The Polish Academy of Sciences Technical Sciences*, Vol. 59 No.4, 2011, 485-497
- [13] R. Teodorescu, Marco Liserre and Pedro Rodríguez, *Grid Converters for Photovoltaic and Wind Power Systems*, United Kingdom, John Wiley & Sons, Ltd., 2011
- [14] P. Rodriguez, R. Teodorescu, I. Candela, A.V. Timbus, M. Liserre, and F. Blaabjerg, "New Positive-sequence Voltage Detector for Grid Synchronization of Power Converters under Faulty Grid Conditions", in *Proc. IEEE Power Electron. Spec. Conf. (PESC'06)*, 2006, 1-7
- [15] M. Ciobotaru, R. Teodorescu, and F. Blaabjerg, "A New Single-Phase PLL Structure Based on Second Order Generalized Integrator", in *Proc. IEEE Power Electron. Spec. Conf. (PESC'06)*, 2006, 1-7
- [16] J. Nagrath and M. Gopal, *A Textbook of Control Systems Engineering*, Delhi, New Age International Publishers, 2008
- [17] M. Gao, B. Li, M. Chen, W. Yao and Z. Qian, "Analysis and Implementation of a PLL Structure for Single-Phase Grid-Connected Inverter System", *IEEE 6th International Power Electronics and Motion Control Conference (IPEMC '09)*, Wuhan, 2009, 716 – 719
- [18] S.A.O. Silva and V. D. Bacon, "An Adaptive Phase-Locked Loop Algorithm for Single-Phase Utility Connected System", *15th European Conference on Power Electronics and Applications (EPE)*, Lille, 2013, 1 – 10

# Optimal Batch Size Considering Partial Outsourcing Plan and Rework

Yuan-Shyi Peter Chiu <sup>a</sup>, Chen-Ju Liu <sup>b</sup>, Ming-Hon Hwang <sup>c\*</sup>

<sup>a</sup>Department of Industrial Engineering & Management, Chaoyang University of Technology, Taichung 413, Taiwan

<sup>b</sup>Department of Business Administration, Chaoyang University of Technology, Taichung 413, Taiwan

<sup>c</sup>Department of Marketing & Logistics Management, Chaoyang University of Technology, Taichung 413, Taiwan

Received Oct 30, 2016

Accepted April 15, 2017

## Abstract

Coping with the severe competition in the global markets and the limited in-house capacity, the management of present-day manufacturing firm always pursues possible alternatives to level production schedule by shortening production uptime, assure product quality, and reduce overall system cost in order to stay competitive. Inspired by this concept, the present study attempts to derive the optimal batch size for a fabrication system with outsourcing policy and rework. Mathematical modeling and optimization techniques are employed to explore the problem. As a result, a closed-form optimal batch size for the proposed system is determined. Besides, various critical system performance indicators, such as the breakeven points of unit outsourcing cost, in-house defective rate, and unit reworking cost, etc., can now be revealed for assisting diverse managerial decision-makings.

© 2017 Jordan Journal of Mechanical and Industrial Engineering. All rights reserved

**Keywords:** Production Batch Size, Outsourcing, Rework, Defective Items.

## Appendix A

K	= in-house production setup cost per cycle,
C	= unit fabrication cost,
h	= unit holding cost,
CR	= unit reworking cost,
$K\pi$	= fixed outsourcing cost per cycle,
$C\pi$	= unit outsourcing cost,
$\beta_1$	= the linking variable between $K\pi$ and K, where $K\pi = [(1 + \beta_1)K]$ and $-1 \leq \beta_1 \leq 0$ , where we assume that practically the in-house setup cost is relative higher than fixed outsourcing cost,
$\beta_2$	= the linking variable between $C\pi$ and C, where $C\pi = [(1 + \beta_2)C]$ and $\beta_2 \geq 0$ ,
Q	= batch size per cycle – the decision variable of the proposed system,
$T\pi$	= the replenishment cycle time,
H1	= the level of on-hand perfect quality inventory when in-house production finishes,
H2	= the level of on-hand perfect quality inventory when rework process ends,
H	= maximum level of on-hand perfect quality inventory when outsourcing items are received,
t1	= production uptime if $\pi = 0$ ,
t2	= reworking time if $\pi = 0$ ,
t3	= production down time if $\pi = 0$ ,
T	= cycle time if $\pi = 0$ ,
I(t)	= the level of on-hand perfect quality inventory at time t,
Id(t)	= the level of on-hand defective inventory at time t,
TC(Q)	= total operating cost per cycle,
E[TCU(Q)]	= the expected operating cost per unit time.

## 1. Introduction

The present study determines the optimal batch size for a fabrication system with outsourcing policy and rework, with the aim of leveling production schedule by shortening production uptime, assuring product quality, and reducing overall system cost. The classic economic production lot-size problem [1] assumed a perfect production process and solved by using mathematical model which balanced the setup and stock holding costs in order to derive the optimal lot-size that minimizes the long-run total system costs. In most real manufacturing environments, however, caused by various controllable/uncontrollable factors, production of defective products is inevitable [2-5]. Reworking of the imperfect quality items could be an alternative to lower overall production cost [6-7]. Chern and Yang [6] assumed that a work center produces good, rework-able, and scrap items, and it adopts a threshold control policy to handle regular process and rework job. Guidelines were established for the machine in work center to switch between regular and rework processes. Their objective was to simultaneously find the optimal threshold and lot-size that maximize the expected long-term profit. Grosfeld-Nir and Gerchak [7] studied multistage fabrication systems where defective products can be repeatedly reworked at every stage. Random yield in each stage is assumed; hence, multiple production runs may be needed to meet the desired demand of the product. They explored and discussed how the studied multistage fabrication systems can be turned into a single-bottleneck

\* Corresponding author e-mail: hwangmh@cyut.edu.tw.

system. Recursive algorithms were also developed for solving two- and three-stage systems. Studies related to various aspects of fabrication systems with reworking of nonconforming items can also be found elsewhere [8-13].

To cope with production capacity constraints, shortening production uptimes is often used by management as an alternative of leveling/smoothing production schedules/operations [14-18]. Coman and Ronen [14] proposed a linear programming model to study the outsourcing problem and identify relevant parameters and their relationships. They examined the model using both approaches of cost accounting and theory of constraints, and obtained various results to assist management in determining whether or not to outsource. With fewer computation requirements, they concluded that their model is simpler than other existing models. Amaral *et al.* [15] proposed various strategies for Original Equipment Manufacturers (OEMs) for deciding what activities to outsource and the ways to establish effective controls over the outsourcing procedure so that the business risks can be minimized. They pointed out that several renowned manufacturers had implemented these strategies. Kumar and Arbi [16] discussed how the implementation of right Information Technology (IT) systems and supply chain measures can help apparel manufacture reduce lead-times and total cost. Through a case study, they demonstrated that major components of customer lead-time (such as freight transportation time, order processing time and manufacturing time) can be minimized by an improved IT and logistics capabilities. Chiao *et al.* [17] developed a model to determine the outsource quantity decision for a single-manufacturer two-outsourcer system. Wherein, one outsourcer offers a lower unit outsourcing price, but whose supplies are of higher deteriorating rate; on the contrary, the other outsourcer's supplies are of lower deteriorating rate, but requires a higher outsourcing price. Through a case study by adopting the real production data from an ice cream company in Taiwan, they demonstrated that their model can assist manufacture in allocating the optimal quantity decision to each outsourcer in order to receive the highest profits. They also provided guidelines for allocation of outsourcing items to different outsourcers with different qualities and costs. Lee and Lan [18] examined an extended EPQ model with stochastic demand. To cope with uncertain demand rate and decrease the complexity of production planning, they assumed a fixed batch size policy along with an outsourcing of a secondary facility to supplement the fixed batch size policy. Shortage is permitted in their study, and the relevant cost parameters, including production setup cost, variable production cost, stock holding cost, backorder cost, and the outsourcing cost. Although global optimization on the batch size cannot be obtained, through extensive computational tests, they demonstrated that their model can significantly reduce the system cost as compared to that of classic lot-size policy. Studies related to various aspects of fabrication systems with outsourcing policy, manufacturing strategy and quality assurances can also be found elsewhere [19-29].

With the aim of shortening production uptime, assuring product quality, and reducing overall system cost, the present study proposes a decision model to

determine the optimal batch size for a fabrication system with outsourcing policy and rework. Because little attention has been paid to the area of proposing a decision model to study joint effects of outsourcing policy and rework on the optimal production lot-size, the present paper is intended to bridge the gap.

## 2. The Proposed System and Formulations

Assumptions of the present proposed study include: (i) It is a deterministic fabrication system with a partial outsourcing policy, wherein both annual demand and production rates are steady, (ii) a random defective rate exists in the in-house fabrication system and all defective products are assumed to be repairable thru a rework process in the same cycle with extra cost, and (iii) a portion of the batch in each cycle is outsourced and the schedule of receiving outsource products is predetermined (i.e., in the end of rework process) and these products are promised to be of perfect quality.

The description of the proposed system with rework and a partial outsourcing plan is as follows. Consider a specific product can be made at  $P$  units per year by a production system to meet a steady demand of  $\lambda$  units per year. An  $x$  portion of repairable defective products may be randomly produced during the fabrication at a rate of  $d$ , thus  $d = Px$ . In each production cycle, the reworking of defective items starts right after the end of regular fabrication process, at a reworking rate  $P_1$  units per year (see Figure 1). By not allowing shortage, we assume that  $P$  must be larger than the sum of  $\lambda$  and  $d$ , or  $P - d - \lambda > 0$ .

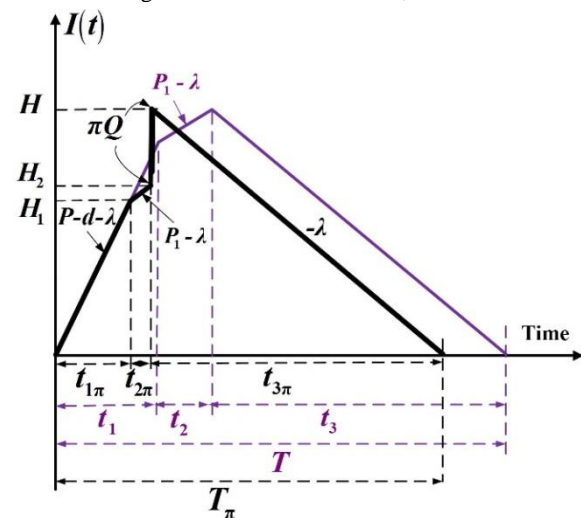


**Figure 1.** The level of on-hand perfect quality inventory in the proposed system (in black) compared to that of the same system without outsourcing plan (in purple)

Furthermore, a  $\pi$  portion (where  $0 < \pi < 1$ ) of the batch size  $Q$  is outsourced in the proposed system, and all outsourcing items are of perfect quality (i.e., guaranteed by the contractor) and are scheduled to be received in the end of rework time, prior to delivery (Figure 1). It is noted when  $\pi = 1$  the proposed system becomes a purchase system, and if  $\pi = 0$  the proposed system comes to be an in-house production system. Other notation used in the proposed system is listed in Appendix A. The level of on-hand defective products in production and reworking times of the proposed system is depicted in Figure (2).

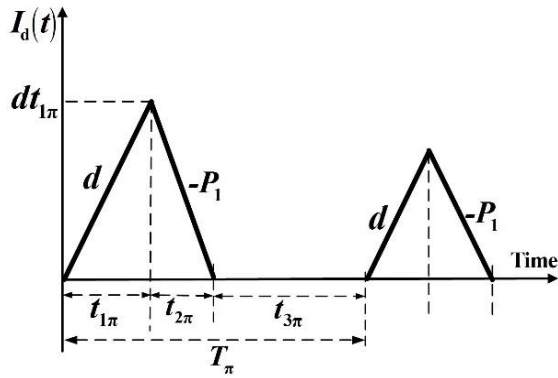


**Figure 2.** The level of on-hand defective products in production and reworking times of the proposed system

From Figures (1) and (2), the following formulas can be directly obtained:

$$H_1 = (P - d - \lambda)t_{1\pi} \tag{1}$$

$$H_2 = H_1 + (P_1 - \lambda)t_{2\pi} \tag{2}$$

$$H = H_2 + \pi Q = \lambda t_{3\pi} \tag{3}$$

$$t_{1\pi} = \frac{H_1}{P - d - \lambda} = \frac{(1 - \pi)Q}{P} \tag{4}$$

$$t_{2\pi} = \frac{x[(1 - \pi)Q]}{P_1} \tag{5}$$

$$t_{3\pi} = \frac{H}{\lambda} = \frac{H_2 + \pi Q}{\lambda} \tag{6}$$

$$T_\pi = t_{1\pi} + t_{2\pi} + t_{3\pi} = \frac{Q}{\lambda} \tag{7}$$

$$dt_{1\pi} = xPt_{1\pi} = x[(1 - \pi)Q] \tag{8}$$

Total operating cost per cycle for the proposed system,  $TC(Q)$ , consists of production setup cost, variable production cost, fixed outsourcing cost, variable outsourcing cost, reworking cost, holding cost for reworked items, holding cost for perfect quality and defective items in  $t_{1\pi}$ ,  $t_{2\pi}$ , and  $t_{3\pi}$ . Therefore,  $TC(Q)$  is as follows:

By substituting  $K\pi$  and  $C\pi$  in Equation (9), the operating cost per cycle for the proposed system  $TC(Q)$  becomes as follows:

We use the expected values of  $x$  in cost analysis to deal with randomness of defective rate  $x$ . By substituting all related parameters from equations (1) to (8) into equation (10) and with further derivations, the expected operating cost per unit time for the proposed system  $E[TCU(Q)]$  can be obtained as follows:

$$TC(Q) = K + C[(1 - \pi)Q] + K_\pi + C_\pi(\pi Q) + C_R x[(1 - \pi)Q] + h_1 \frac{dt_{1\pi}}{2}(t_{2\pi}) + h \left[ \frac{H_1 + dt_{1\pi}}{2}(t_{1\pi}) + \frac{H_1 + H_2}{2}(t_{2\pi}) + \frac{H}{2}(t_{3\pi}) \right] \tag{9}$$

$$TC(Q) = K + C[(1 - \pi)Q] + (1 + \beta_1)K + (1 + \beta_2)C(\pi Q) + C_R x[(1 - \pi)Q] + h_1 \frac{dt_{1\pi}}{2}(t_{2\pi}) + h \left[ \frac{H_1 + dt_{1\pi}}{2}(t_{1\pi}) + \frac{H_1 + H_2}{2}(t_{2\pi}) + \frac{H}{2}(t_{3\pi}) \right] \tag{10}$$

$$E[TCU(Q)] = \frac{E[TC(Q)]}{E[T]} = \frac{\lambda K}{Q} + \lambda(1 - \pi)C + \frac{\lambda[(1 + \beta_1)K]}{Q} + \lambda\pi[(1 + \beta_2)C] + \lambda(1 - \pi)E[x]C_R + \frac{Q(h_1 - h)}{2} \left( \frac{\lambda E[x]^2(1 - \pi)^2}{P_1} \right) + \frac{hQ}{2} \left[ 1 - \lambda \left( \frac{1 - \pi^2}{P} \right) + \frac{\lambda E[x](1 - \pi)}{P_1}(-2\pi) \right] \tag{11}$$

### 3. Determining Optimal Batch Size

Upon obtaining the expected operating cost per unit time  $E[TCU(Q)]$ , we apply the first and second derivatives of  $E[TCU(Q)]$  with respect to  $Q$  as follows:

$$\frac{dE[TCU(Q)]}{dQ} = -\frac{\lambda}{Q^2}K - \frac{\lambda}{Q^2}[(1+\beta_1)K] + \frac{(h_1-h)}{2} \left[ \frac{\lambda E[x]^2(1-\pi)^2}{P_1} \right] + \frac{h}{2} \left[ 1-\lambda \left( \frac{1-\pi^2}{P} \right) + \frac{\lambda E[x](1-\pi)(-2\pi)}{P_1} \right] \quad (12)$$

$$\frac{d^2E[TCU(Q)]}{dQ^2} = \frac{2\lambda}{Q^3} [K + (1+\beta_1)K] \quad (13)$$

Since  $\lambda, Q, (1+\beta_1)$ , and  $K$  are all positive, one confirms that equation (13) is positive. Hence,  $E[TCU(Q)]$  is a strictly convex function for all  $Q$  different from zero. It follows that to derive the optimal replenishment batch size  $Q$ , one can set first derivative of  $E[TCU(Q)]$  equal to zero, and with further derivation the optimal batch size  $Q^*$  can be obtained as follows:

$$Q^* = \sqrt{\frac{2\lambda K(2+\beta_1)}{(h_1-h) \left[ \frac{E[x]^2(1-\pi)^2\lambda}{P_1} \right] + h \left[ 1-\lambda \left( \frac{1-\pi^2}{P} \right) + \frac{\lambda E[x](1-\pi)(-2\pi)}{P_1} \right]}} \quad (14)$$

### 4. Numerical Example with Sensitivity Analysis

To show the applicability of the obtained result, a numerical example with sensitivity analysis is provided in this section for this purpose. Assume a fabrication system can produce a particular product at a rate of  $P = 20,000$  units per year to meet its steady demand rate of  $\lambda = 4,000$  units per year. A portion  $\pi = 0.4$  of the replenishment batch size is outsourced in each cycle to cope with the limited production capacity. The production setup cost  $K = \$5,000$  and unit fabrication cost  $C = \$100$ . For outsourcing fixed and variable costs, assuming the relating parameters  $\beta_1 = -0.7$  and  $\beta_2 = 0.2$ , or  $K_\pi = \$1,500$  and  $C_\pi = \$120$ . An  $x$  portion of repairable defective items may randomly produce, where  $x$  follows a uniform distribution over the range of  $[0, 0.2]$ . A rework process is adopted right after the end of regular production in each cycle, and it can repair the defective items at a rate of  $P_1 = 5,000$  units per year with unit rework cost  $C_R = \$60$ . Other system parameters also include holding cost  $h = \$30$  per unit per year and holding cost  $h_1 = \$40$  per reworked item per year.

Applying Equations (14) and (11), we obtain the optimal batch size  $Q^* = 1,477$  and the optimal operating cost per unit time for the proposed system  $E[TCU(Q^*)] = \$481,607$ . Applying Equation (11) with different values of  $Q$ , the behavior of  $E[TCU(Q)]$ , with respect to different replenishment batch size  $Q$ , can be obtained as displayed in Figure (3).

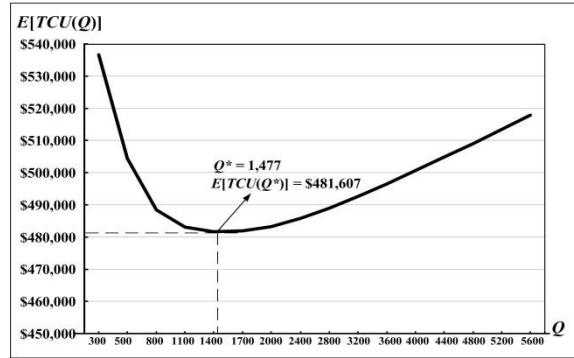


Figure 3. Behavior of  $E[TCU(Q)]$  with respect to  $Q$

Similarly, applying Equation (11) with different values of  $Q$ , different cost components of  $E[TCU(Q)]$  with respect to  $Q$  are shown in Figure (4). It is noted that as the batch size  $Q$  increases, the total holding cost of perfect quality and reworked items increase significantly, and the rework cost rises slightly; however, the production setup cost declines significantly.

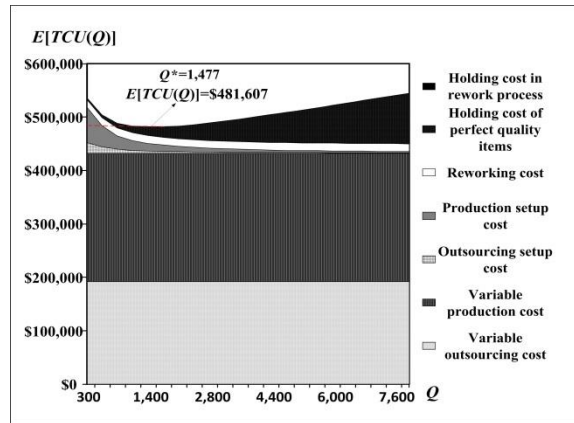


Figure 4. Different cost components of  $E[TCU(Q)]$  with respect to  $Q$

Applying Equation (11) with both  $\pi = 0$  and  $\pi = 1$ , and different values of  $x$ , the analytical result of the breakeven point of defective rate  $x$  in the proposed system can be found as depicted in Figure (5). It is noted that a breakeven point of  $x = 0.24$  is found for the 'make or buy' decision making. For instance, if the random defective rate is less than 0.24, then the decision of 'make' is in favor in terms of cost savings.

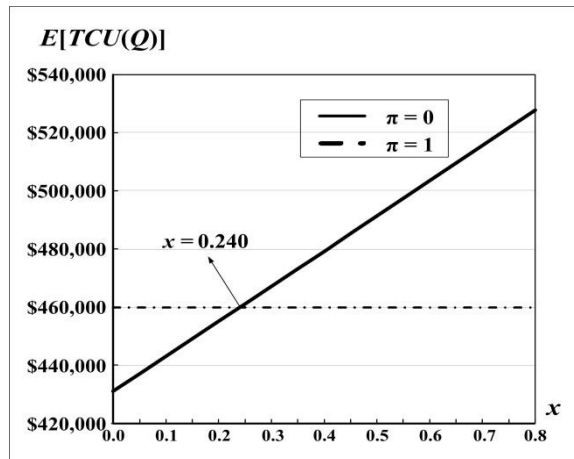


Figure 5. Analysis of the breakeven point of defective rate in the proposed system

Applying Equation (11) with both  $\pi = 0$  and  $\pi = 1$ , and different values of  $C_R$ , the analytical result of the breakeven point of ratio of rework cost  $C_R/C$  for  $\beta_2 = 0.1$  in the proposed system can be obtained, as shown in Figure (6). It is noted that a breakeven point of  $C_R/C = 0.722$  is obtained for the 'make or buy' decision making. For example, if the ratio of rework cost  $C_R/C$  is less than 0.722, then the decision of 'make' is in favor in terms of cost savings.

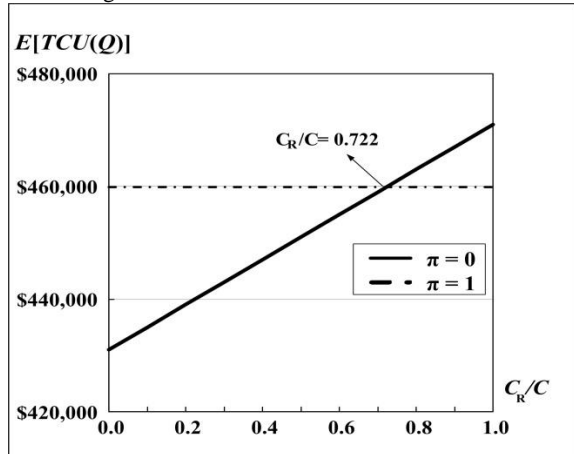


Figure 6. Analysis of the breakeven point of ratio of rework cost  $C_R/C$  for  $\beta_2 = 0.1$  in the proposed system

Applying Equation (11) with different values of  $\pi$  and  $\beta_2$ , the joint effects of different  $\pi$  and  $\beta_2$  on the expected system cost  $E[TCU(Q)]$  are found and displayed in Figure (7). It is noted that there is a breakeven point on  $\beta_2$  (i.e.,  $C_\pi/C - 1$ ), when  $\beta_2$  goes beyond the breakeven point, as  $\pi$  increases, the expected system cost  $E[TCU(Q)]$  rises significantly; and as  $\beta_2$  increases,  $E[TCU(Q)]$  also goes up significantly.

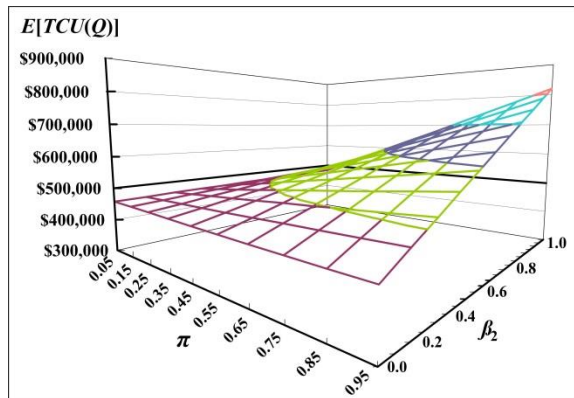


Figure 7. Joint effects of different ratios of  $\pi$  and  $\beta_2$  on the expected system cost  $E[TCU(Q)]$

Applying Equation (11) with both  $\pi = 0$  and  $\pi = 1$ , and different values  $\beta_2$ , the analytical result of the breakeven point of  $\beta_2$  in the proposed system is obtained and depicted in Figure (8). It is noted that a breakeven point of  $\beta_2 = 0.086$  is found for the 'make or buy' decision making. For instance, if  $\beta_2$  (i.e.,  $C_\pi/C - 1$ ) is less than 0.086; thus, the decision of 'buy' is in favor in terms of cost savings.

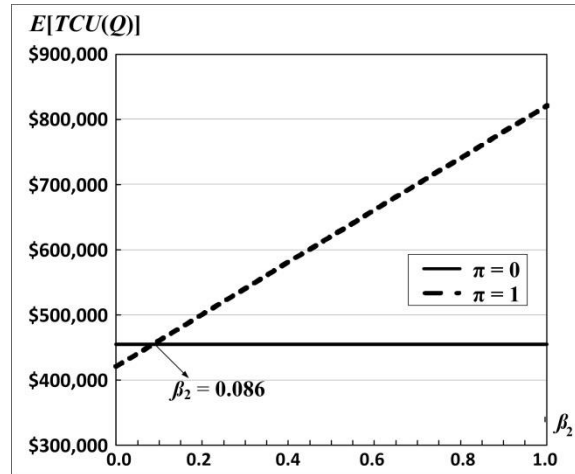


Figure 8. Analytical result of the breakeven point of  $\beta_2$  in the proposed system

### 5. Conclusions

The present study developed an exact model for solving a replenishment batch size problem considering rework and a partial outsourcing plan. We not only successfully achieved the goal of deriving the optimal batch size that minimizes overall production and outsourcing costs, but also provided a decision-support-system type of tools to help managerial decision makings (refer to Figures (4) to (8)). For instances, various critical system performance indicators, such as the breakeven points of unit outsourcing cost (see Figure (8)), in-house defective rate (refer to Figure (5)), and unit reworking cost (see Figure (6)), etc., can now be revealed for assisting diverse decision-makings. One interesting direction for future studies will be incorporating a stochastic product demand rate into the present system and examining its effect on the optimal batch size.

### Acknowledgements

Authors appreciate the Ministry of Science and Technology of Taiwan for sponsoring the present study under Grant No.: MOST 104-2410-H-324-008-MY2.

### References

- [1] E. W. Taft, "The most economical production lot". *Iron Age*, Vol.101, 1918, 1410-1412.
- [2] W. Shih, "Optimal inventory policies when stock-outs result from defective products". *International Journal of Production Research*, Vol. 18, No.6, 1980, 677-686.
- [3] M. Henig, Y. Gerchak, "Structure of periodic review policies in the presence of random yield". *Operations Research*, Vol. 38, No. 4, 1990, 634-643.
- [4] T. Boone, R. Ganeshan, Y. Guo, J.K. Ord, "The impact of imperfect processes on production run times". *Decision Sciences*, Vol. 31, No. 4, 2000, 773-785.
- [5] Y-S. P. Chiu, K-W. Chiang, S. W. Chiu, M-S. Song, "Simultaneous determination of production and shipment decisions for a multi-product inventory system with a rework process". *Advances in Production Engineering & Management*, Vol. 11, No. 2, 2016, 141-151.

- [6] C-C. Chern, P. Yang, "Determining a Threshold Control Policy for an Imperfect Production System with Rework Jobs". *Naval Research Logistics*, Vol. 46, No. 2-3, 1999, 273-301.
- [7] A. Grosfeld-Nir, Y. Gerchak, "Multistage production to order with rework capability". *Management Science*, Vol. 48, No. 5, 2002, 652-664.
- [8] B. J. Yum, E. D. McDowell, "Optimal Inspection Policies in a Serial Production System including scrap, rework and repair: An MILP approach". *International Journal of Production Research*, Vol. 25, No. 10, 1987, 1451-1464.
- [9] P. Biswas, B.R. Sarker, "Optimal batch quantity models for a lean production system with in-cycle rework and scrap". *International Journal of Production Research*, Vol. 46, No. 23, 2008, 6585-6610.
- [10] A. Coman, B. Ronen, "Production outsourcing: A linear programming model for the theory-of-constraints". *International Journal of Production Research*, Vol. 38, No. 7, 2000, 1631-1639.
- [11] S. W. Chiu, C-C. Huang, K-W. Chiang, M-F. Wu, "On intra-supply chain system with an improved distribution plan, multiple sales locations and quality assurance". *SpringerPlus*, Vol. 4, No. 1, 2015, Article No. 687.
- [12] Y-S. P. Chiu, P-C. Sung, S. W. Chiu, C-L. Chou, "Mathematical modeling of a multi-product EMQ model with an enhanced end items issuing policy and failures in rework". *SpringerPlus*, Vol. 4, No. 1, 2015, Article No. 679.
- [13] P. Jawla, S. R. Singh, "Multi-item economic production quantity model for imperfect items with multiple production setups and rework under the effect of preservation technology and learning environment". *International Journal of Industrial Engineering Computations*, Vol. 7, No. 4, 2016, 703-716.
- [14] A. Coman, B. Ronen, "Production outsourcing: A linear programming model for the theory-of-constraints". *International Journal of Production Research*, Vol. 38, No. 7, 2000, 1631-1639.
- [15] J. Amaral, C.A. Billington, A.A. Tsay, "Safeguarding the promise of production outsourcing". *Interfaces*, Vol. 36, No. 3, 2006, 220-233.
- [16] S. Kumar, A.S. Arbi, "Outsourcing strategies for apparel manufacture: A case study". *Journal of Manufacturing Technology Management*, Vol. 19, No. 1, 2008, 73-91.
- [17] H-E. Chiao, H-M. Wee, M.V. Padilan, "A model to outsource deteriorating items using two outsourcers with different deteriorating rates and costs". *International Journal of Computer Integrated Manufacturing*, Vol. 25, No. 6, 2012, 536-549.
- [18] S-D. Lee, S-C. Lan, "Production lot sizing with a secondary outsourcing facility". *International Journal of Production Economics*, Vol. 141, No. 1, 2013, 414-424.
- [19] B. Leavy, "Outsourcing strategy and a learning dilemma". *Production and Inventory Management Journal*, Vol. 37, No. 4, 1996, 50-54.
- [20] G.P. Cachon, P.T. Harker, "Competition and outsourcing with scale economies". *Management Science*, Vol. 48, No. 10, 2002, 1314-1333.
- [21] S. Narayanan, V. Jayaraman, Y. Luo, J.M. Swaminathan, "The antecedents of process integration in business process outsourcing and its effect on firm performance". *Journal of Operations Management*, Vol. 29, No. 1-2, 2011, 3-16.
- [22] K. R. Balachandran, H.W. Wang, S-H. Li, T. Wang, "In-house capability and supply chain decisions". *Omega*, Vol. 41, No. 2, 2013, 473-484.
- [23] R. Malhotra, G. Taneja, "Comparative study between a single unit system and a two-unit cold standby system with varying demand". *SpringerPlus*, Vol. 4, No. 1, 2015, article no. 705.
- [24] G.J. Hahn, T. Sens, CDecouttere, N.J. Vandaele, "A multi-criteria approach to robust outsourcing decision-making in stochastic manufacturing systems". *Computers & Industrial Engineering*, Vol. 98, 2016, 275-288.
- [25] J. Gómez, I. Salazar, P. Vargas, "Sources of information as determinants of product and process innovation". *PLoS ONE*, Vol. 11, No. 4, 2016, article no. e0152743.
- [26] C. Ma, X. Liu, H. Zhang, Y. Wu, "A green production strategies for carbon-sensitive products with a carbon cap policy". *Advances in Production Engineering & Management*, Vol. 11, No. 3, 2016, 216-226.
- [27] V.V.S. Prasad Patnaik, D.P. Patnaik, R.K. Srinivasa, "A Numerical Study on Deterministic Inventory Model for Deteriorating Items with Selling Price Dependent Demand and Variable Cycle Length". *Jordan Journal of Mechanical and Industrial Engineering*, Vol. 9, No. 3, 2015, 223-240.
- [28] L. Ocampo, E. Clark, "A Sustainable Manufacturing Strategy Decision Framework in the Context of Multi-Criteria Decision-Making". *Jordan Journal of Mechanical and Industrial Engineering*, Vol. 9, No. 3, 2015, 177-186.
- [29] H. Kaylani, A. Almuhtady, A. M. Atieh, "Novel approach to enhance the performance of production systems using lean tools". *Jordan Journal of Mechanical and Industrial Engineering*, Vol. 10, No. 3, 2016, 215-229.





الجامعة الهاشمية



المملكة الأردنية الهاشمية

المجلة الأردنية  
للمهندسة الميكانيكية والصناعية

JJMIE

مجلة علمية عالمية محكمة  
تصدر بدعم من صندوق البحث العلمي

<http://jjmie.hu.edu.jo/>

ISSN 1995-6665

# المجلة الأردنية للهندسة الميكانيكية والصناعية

## مجلة علمية عالمية محكمة

المجلة الأردنية للهندسة الميكانيكية والصناعية: مجلة علمية عالمية محكمة تصدر عن الجامعة الهاشمية بالتعاون مع صندوق دعم البحث العلمي في الأردن

### هيئة التحرير

#### رئيس التحرير

الأستاذ الدكتور أحمد الغندور.

قسم الهندسة الميكانيكية و الصناعية، الجامعة الهاشمية، الزرقاء، الأردن.

#### الأعضاء

الأستاذ الدكتور ناصر الحنيطي  
الجامعة الاردنية

الأستاذ الدكتور محمد أحمد حمدان  
الجامعة الاردنية

الأستاذ الدكتور محمد هياجنه.  
جامعة العلوم والتكنولوجيا الاردنية

الاستاذ الدكتور نسيم سواقد.  
جامعة مؤتة

الاستاذ الدكتور سهيل كيوان  
جامعة العلوم والتكنولوجيا الاردنية

الاستاذ الدكتور أمين الريدي.  
جامعة البلقاء التطبيقية

### فريق الدعم

#### تنفيذ وإخراج

م . علي أبو سليمة

#### المحرر اللغوي

الدكتور قصي الذبيان

ترسل البحوث إلى العنوان التالي

رئيس تحرير المجلة الأردنية للهندسة الميكانيكية والصناعية

الجامعة الهاشمية

كلية الهندسة

قسم الهندسة الميكانيكية

الزرقاء - الأردن

هاتف : 00962 5 3903333 فرعي 4537

Email: [jjmie@hu.edu.jo](mailto:jjmie@hu.edu.jo)

Website: [www.jjmie.hu.edu.jo](http://www.jjmie.hu.edu.jo)